IEEE Access
Multidisciplinary ⋮ Rapid Review ⋮ Open Access Journal

Received March 16, 2021, accepted April 4, 2021, date of publication April 9, 2021, date of current version April 19, 2021.

Digital Object Identifier 10.1109/ACCESS.2021.3072336

An Improved Tunicate Swarm Algorithm for Global Optimization and Image Segmentation

ESSAM H. HOUSSEIN[1], BAHAA EL-DIN HELMY[2], AHMED A. ELNGAR[2], DIAA SALAMA ABDELMINAAM[3], AND HASSAN SHABAN[1]
[1]Faculty of Computers and Information, Minia University, Minia 61519, Egypt
[2]Faculty of Computers and Artificial Intelligence, Beni-Suef University, Beni Suef 62619, Egypt
[3]Faculty of Computers and Artificial Intelligence, Benha University, Benha 12311, Egypt

Corresponding author: Essam H. Houssein (essam.halim@mu.edu.eg)

ABSTRACT This study integrates a tunicate swarm algorithm (TSA) with a local escaping operator (LEO) for overcoming the weaknesses of the original TSA. The LEO strategy in TSA–LEO prevents searching deflation in TSA and improves the convergence rate and local search efficiency of swarm agents. The efficiency of the proposed TSA–LEO was verified on the CEC'2017 test suite, and its performance was compared with seven metaheuristic algorithms (MAs). The comparisons revealed that LEO significantly helps TSA by improving the quality of its solutions and accelerating the convergence rate. TSA–LEO was further tested on a real-world problem, namely, segmentation based on the objective functions of Otsu and Kapur. A set of well-known evaluation metrics was used to validate the performance and segmentation quality of the proposed TSA–LEO. The proposed TSA-LEO outperforms other MA algorithms in terms of fitness, peak signal-to-noise ratio, structural similarity, feature similarity, and segmentation findings.

INDEX TERMS Metaheuristic algorithms, tunicate swarm algorithm (TSA), local escaping operator (LEO), multilevel thresholding, image segmentation, Kapur's entropy, Otsu method.

I. INTRODUCTION

Objective optimization problems, such as minimizing time consumption, energy, cost, and error or maximizing efficiency, performance, and quality of a process, are commonly encountered in real-world applications [1]. Recently, several researchers have embraced a new family of optimization algorithms called metaheuristic algorithms (MAs), and numerous optimizers have been developed for complex real-world problems. Such algorithms randomly search the feature space to obtain an optimal solution among various solutions, which are mainly inspired by nature. Among a large body of nature-inspired MAs, some are popular such as moth flame optimization (MFO) [2], whale optimization algorithm (WOA) [3], sine cosine optimization (SCA) [4], seagull optimization algorithm (SOA) [5], krill herd algorithm [6], and barnacles mating optimizer (BMO) [7], because they are simple, efficient, and robust in finding optimal solutions. Moreover, the No-Free Lunch Theorem [8] states that no specific optimization algorithm can accurately solve multiple optimization problems. Thus, several MAs have been developed for use in biomedicine [9], [10], bioinformatics [11], [12], cheminformatics [13], [14], feature selection [15], engineering problems [16]–[19], pattern recognition, text clustering [20], [21], and wireless sensor networks [22], [23]. However, all MAs need to balance exploration and exploitation stages; otherwise, solutions tend to become trapped in local optima or cannot properly converge [24], [25]. Randomization during the solution-finding process can cause such problems. Hybridization of multiple concepts from different scientific fields is mandatory, especially in human-aided systems. Hybridization can combine the advantages of different algorithms to produce enhanced versions with promising performance and accuracy.

For example, the authors in [26] improved the grey wolf optimization (GWO) algorithm for engineering design problems.The enhanced version, which is known as I-GWO, adopts a new movement strategy called dimension-learning hunting (DLH). DLH enhances the diversity of solutions to balance exploration and exploitation phases and avert local optima. Results confirmed the robustness of I-GWO on the CEC'2017 test suit functions. Moreover, the study in [27] boosted the WOA algorithm (one of the most well-known optimization algorithms) with two search strategies: chaotic

The associate editor coordinating the review of this manuscript and approving it for publication was Huaqing Li.

and Gaussian mutation. The two search strategies were expected to avoid local optima by balancing the exploration and exploitation phases. The algorithm achieved promising performance results compared with state-of-the-art methods. Moreover, the algorithm proposed a method that uses static single assignment (SSA) and particle swarm organization (PSO) to solve complex optimization problems. This method prevents local optima trapping and unbalanced exploitation in the original SSA. The proposed SSA–PSO outperformed competing methods in a comparison test on the CEC'2005 and CEC'2017 functions. The authors of [28]integrated SCA with PSO, which overcomes the drawbacks of SCA in the exploitation phase. The combined ASCA–PSO achieved good performance (high accuracy and low time complexity) on several benchmarks. The authors of [29] combined SCA with operator-based linearization (OBL), increasing the performance and improving solutions of SCA. The superiority of the proposed SCA–OBL was evaluated in several benchmark functions and engineering problems. Orthogonal learning strategy was hybridized with MFO to optimize its parameters [30]. This new MFO version avoids the searchability of the original MFO and enhances the diversity of solutions. The algorithm explores new regions in the search for an optimal agent with the best solution. The effectiveness of the enhanced MFO was verified on CEC'2014 test functions and several engineering problems. The proposed method outperformed other optimization algorithms as proven by the comparison result.

On the other hand, the development and application of vision systems have accelerated in the recent era [31]–[34]. Image processing without a vision system is ill-advised, and a proper pre-processing improves the accuracy of the results. Segmentation pre-processing facilitates the representation and analysis of images [35], and must be accurately performed in any vision application [36]. In particular, the image should be subdivided to extract only the regions carrying useful information. Segmentation methods can be parametric or non-parametric [37]. Parametric segmentation defines each class based on the probability density function; non-parametric segmentation uses specific standards, such as variance, entropy, or error rate, to obtain the optimal thresholds that effectively separate the image. One of the most popular and promising segmentation tools, i.e., thresholding, divides the image into multiple homogeneous segments. Thresholding is also adopted in image analysis and processing because it is easily understood and implemented [38].

Bi-level (BT) and multilevel (MT) thresholding techniques can be used to select the thresholds in a grayscale image [39]. The BT technique divides the entire image into two classes based on a single threshold state, whereas the MT technique segments the image into several classes based on two or more thresholds [40], [41]. Otsu's between-class variance [42], Kapur's entropy [43], and Tsallis entropy [44] are used to optimize the threshold(s). These methods have optimal thresholds that separate an image into multiple segments, but this can be considered a complex task, especially when the number of thresholds increases [45]–[47]. Several optimization methods have been blended with classical thresholding methods to operate with the complexities of multilevel thresholding problems. Tunicate swarm algorithm (TSA) is a new robust search method inspired by the strange behavior of tunicates (a marine invertebrate animal) during foraging [48].

Tunicates adopt two main strategies while searching for food: jet propulsion and swarm intelligence. Most optimization algorithms obtain new solutions based on the previous solution. Two strategies in the original TSA are used to dictate a new solution: jet propulsion and swarm intelligence. These strategies are randomly applied to the current solutions to obtain the best solution. in some optimization cases, the original TSA determines the optimal solution from subregions, which lowers the convergence rate and prevents full coverage of the search space (the latter problem leads to premature convergence of the TSA). These problems are common in most optimization algorithms, especially in complex and high-dimensional problems [49]. Local escaping operator (LEO) is, a new mathematical approach [50] that was developed as a local search used for generating an efficient solution aiming to visit the unseen search regions, and thus, escaping from the local optimal problem. Moreover, operators such as $p1$, $f1$ and $f2$ are used to balance between the exploration and exploitation phases, shown in Eqs. (9 and 8).

MOTIVATION AND CONTRIBUTIONS:

To mitigate TSA's problems, this paper hybridizes the original TSA with an efficient operator LEO to address the shortcoming that the standard TSA may exhibit, i.e. 1) evades trapping in local optima, 2) balances between exploration and exploitation, and 3) improves the convergence speed. The proposed method was validated on the CEC'2017 benchmark functions, and its performance was compared with those of seven established optimization algorithms namely MFO, WOA, SCA, SOA, BMO, chaotic TSA (CTSA), and the original TSA. Then it is applied to tackle multilevel thresholding image segmentation problems based on maximizing two objective functions namely Otsu and Kapur objective functions. Peak signal-to-noise ratio (PSNR), structural similarity (SSIM), and feature similarity (FSIM) are three quality metrics used to evaluate segmentation results in terms of fitness. Optimization and segmentation results revealed the robustness of the proposed TSA–LEO compared with a set of well-known optimization algorithms. In summary, the major contributions of the paper are summarized below:

- An efficient TSA based on LEO called TSA-LEO is presented.
- TSA-LEO is proposed for solving optimization and multilevel thresholding image segmentation.
- The effectiveness of TSA-LEO is assessed on the CEC'2020 suite.
- Two objective functions, Kapur and Otsu, are applied.

- The quality of segmentation is verified in terms of the PSNR, SSIM, FSIM.
- The proposed method is compared with state-of-the-art algorithms.
- Extensive results show the more stable performance of the proposed TSA-LEO.
- Significant threshold results are obtained.

The remainder of this paper is arranged as follows. Section IIdevices the problem; Section III introduces the proposed TSA–LEO and its main procedure; Section IV discusses and analyzes the benchmark results; and in Section V, TSA–LEO is applied to image segmentation-based thresholding. Conclusions and forthcoming works are represented in Section VI.

II. PRELIMINARIES

A. TUNICATE SWARM ALGORITHM (TSA)

Kaur *et al.* [48] proposed a bio-inspired optimization algorithm that simulates the natural foraging process of tunicates, marine invertebrates that emit bright bio-luminescence. The TSA was inspired by the strange behaviors of tunicates in oceans, in particular, the jet-drive and swarm intelligence of their foraging process. A mathematical model of jet propulsion is developed under three constraints: preventing conflict among the exploration agents, following the positions of the most qualified agents, and remaining near the optimal agents.

1) PREVENTING CONFLICTS AMONG THE AGENTS

To prevent inter-agent conflicts while searching for better positions, the new agent positions are calculated as:

$$\vec{A} = \frac{\vec{G}}{\vec{M}} \tag{1}$$

$$\vec{G} = c_2 + c_3 - \vec{F} \tag{2}$$

$$\vec{F} = c_1 \cdot \vec{F}. \tag{3}$$

where $\vec{A}$ is a vector of new agent positions, $\vec{G}$ is the gravity force, $\vec{F}$ represents the water flow in the deep ocean, and c_1, c_2 and c_3 are three random numbers. The social forces between agents are stored in a new vector $\vec{M}$, represented as follows:

$$\vec{M} = [P_{min} + c_1 \cdot P_{max} - P_{min}]. \tag{4}$$

Here $P_{min} = 1$ and $P_{max} = 4$ describe the first and second subordinates respectively, indicating the speeds of establishing social interactions.

2) FOLLOWING THE POSITIONS OF THE BEST AGENT

Following the current best agent is essential for reaching the optimal solution. Hence, after ensuring that no conflicts exist between neighboring agents in the swarm, the best position of the best agent is computed as,

$$\vec{PD} = |X_{best} - r_{rand} \cdot \vec{P_p(x)}| \tag{5}$$

where $\vec{PD}$ stores the length between the food origin and the optimal agent, X_{best} is the best position, r_{rand} is a stochastic value in the range [0, 1], and the vector $\vec{P_p(x)}$ contains the positions of the tunicates during iteration x.

3) KEEPING CLOSE TO THE OPTIMAL AGENTS

To ensure that search agents still close to the best agent, their positions are computed as follows:

$$\vec{P_p(x)} = \begin{cases} X_{best} + A \cdot \vec{PD}, & if\ r_{rand} \geq 0.5 \\ X_{best} - A \cdot \vec{PD}, & if\ r_{rand} < 0.5 \end{cases} \tag{6}$$

where $\vec{P_p(x)}$ contains the updated positions of the agents at iteration x relative to the best scored position X_{best}.

4) SWARMING BEHAVIOR

To model the swarming behavior of tunicates, the positions of the current agents are updated based on the positions of two agents:

$$P_p(\vec{x+1}) = \frac{\vec{P_p(x)} + P_p(\vec{x+1})}{2 + c_1} \tag{7}$$

To clarify the TSA, the main steps given below illustrate the flow of the original TSA in detail.

Step 1: Initialize the first population of tunicates $\vec{P_p}$.

Step 2: Set the original value for parameters and the highest number of iterations.

Step 3: Measure the fitness value of each exploration agent.

Step 4: After calculating the fitness, the best agent is investigated in the supplied search space.

Step 5: Update the positions of each exploration agent using Eq7.

Step 6: Return the new updated agents to its boundaries.

Step 7: Measure the fitness cost of the updated search agent. If there is a better solution than the past optimal solution, then update $\vec{P_p}$ and save the best solution in X_{best}.

Step 8: If the termination criterion is met, then the processes stop. Otherwise, iterate Steps 5–8.

Step 9: Declare the best optimal solution (X_{best}), which is achieved so far.

B. LOCAL ESCAPING OPERATOR (LEO)

The LEO proposed as a local search algorithm in [50] which is used to enhance the ability of an optimization algorithm namely Gradient-based optimizer (GBO) aiming to explore new regions which are desired in complex real-world problems. The LEO enhances the quality of solutions by updating their positions under some criteria. Specifically, it prevents the algorithm from trapping in local optima and improves its convergence behavior. LEO generates its alternative solutions ($\vec{P}_{LEO}$) with excellent performance by using several solutions such as the best position of tunicates X_{best}, two randomly generated solutions X^m_{r1} and X^m_{r2}, two randomly chosen solutions X^m_{r1} and X^m_{r2}, and a new randomly generated solution X^m_k. Hence, the solution $\vec{P}_{LEO}$ can be determined based on

Eqs. (8 and 9) which can be mathematically formulated as follows:

if rand < pr

if rand < 0.5

$$\vec{P}_{LEO}^{m} = \vec{P}_{n}^{m} + f_1 \times \left(u_1 \times X_{\text{best}} - u_2 \times X_k^m\right) + f_2 \times \rho_1 \times \left(u_3 \times \left(X2_n^m - X1_n^m\right) + u_2 \times \left(X_{r1}^m - X_{r2}^m\right)\right)/2 \tag{8}$$

$P_p^{m+1} = P_{LEO}$ *Else*

$$\vec{P}_{LEO}^{m} = X_{\text{best}} + f_1 \times \left(u_1 \times X_{\text{best}} - u_2 \times X_k^m\right) + f_2 \times \rho_1 \times \left(u_3 \times \left(X2_n^m - X1_n^m\right) + u_2 \times \left(X_{r1}^m - X_{r2}^m\right)\right)/2 \tag{9}$$

$P_p^{m+1} = P_{LEO}$

End

End

Here $\vec{P}_n^m$ is the current tunicate position, X_{best} is the best scored position, pr is the probability of performing LEO strategy where $pr = 0.3$, $rand$ represents a random value in range $\in [0, 1]$, f1 and f2 are uniformly distributed random values $\in [-1, 1]$, X_{r1}^m and X_{r2}^m represent two random solutions chosen from the population, $X1_n^m$ and $X2_n^m$ are two solutions which are randomly generated as shown in Eq10 from the current population.

$$\mathrm{X1_n^m}, \mathrm{X2_n^m} = LB + rand(Dim) \times (UB - LB) \tag{10}$$

where LB, UB are the lower and upper bounds, Dim is the dimension of any solution. Moreover, n and m represent the coordinates of the solution ($n = 1, 2, 3, \ldots, N$) and ($m = 1, 2, 3, \ldots, Dim$). In addition, $u_1, u_2,$ *and* u_3 are three variables that are randomly generated as following:

$$u_1 = L_1 \times 2 \times rand + (1 - L_1) \tag{11}$$

$$u_2 = L_1 \times rand + (1 - L_1) \tag{12}$$

$$u_3 = L_1 \times rand + (1 - L_1) \tag{13}$$

where L_1 is a binary parameter (L1 = 1 if $\mu_1 < 0.5$, and 0 otherwise), μ_1 is a number in the range of [0, 1].

Moreover ρ_1 is introduced to balance the exploration and exploitation searching processes, and it can be expressed as:

$$\rho_1 = 2 \times \text{rand} \times \alpha - \alpha \tag{14}$$

$$\alpha = \left|\beta \times \sin\left(\frac{3\pi}{2} + \sin\left(\beta \times \frac{3\pi}{2}\right)\right)\right| \tag{15}$$

$$\beta = \beta_{\min} + (\beta_{\max} - \beta_{\min}) \times \left(1 - \left(\frac{t}{Max_{iterations}}\right)^3\right)^2 \tag{16}$$

where $\beta_{\min}$ and $\beta_{\max}$ are set to 0.2 and 1.2 respectively, t is the current iteration, and $Max_{iterations}$ is the maximum number of iterations. To balance the exploration and exploitation processes, parameter ρ_1 changes based on the sine function α.

To determine the solution X_k^m in Eq. (28), the following scheme is suggested.

$$X_k^m = \begin{cases} x_{\text{rand}} & \text{if } \mu_2 < 0.5 \\ x_p^m & \text{otherwise} \end{cases} \tag{17}$$

where x_{rand} is a new solution that can be calculated as shown in Eq18, x_p^m is a random solution selected from the population ($p \in [1, 2, \ldots N]$), μ_2 is a random number in the range of [0,1].

$$x_{\text{rand}} = X_{\min} + \text{rand}(0, 1) \times (X_{\max} - X_{\min}) \tag{18}$$

Eq17 can be simplified as follows:

$$X_k^m = L_2 \times x_p^m + (1 - L_2) \times x_{\text{rand}} \tag{19}$$

where L_2 is a binary parameter with a value of 0 or 1. If parameter μ_1 is less than 0.5, the value of L_1 is 1, otherwise, it is 0.

III. THE PROPOSED TSA-LEO

This section illustrates the implementation of the proposed TSA–LEO method to improve the ability of the original TSA by allowing it to visit promising regions. LEO is specifically used to improve the performance of the best solutions of the original TSA. The TSA–LEO algorithm follows the main steps of the original TSA, and employs the LEO operator to encourage the visitation of new regions. LEO improves the search for global optima and convergence rate of the algorithm, dynamically evading stagnation in local optima. In the following section, the implementation of the proposed TSA–LEO is given in detail.

A. PRIMITIVE STEP OF TSA-LEO

The proposed TSA–LEO method, like numerous other optimization algorithms, begins by randomly initializing its parameters, $\vec{A}, \vec{G}, \vec{F}, \vec{M}$ as shown in Eqs. 1 to 4, respectively. Moreover, creating the initial population $\vec{P}_p$ as shown below.

$$\vec{P}_p = LB + rand(N, Dim) \times (UB - LB) \tag{20}$$

where $\vec{P}_p$ is the initial population, and N denotes the number of random solutions $i \in \{1, 2, \ldots, N\}$, each solution is limited between the upper and lower boundaries (UB *and* LB) with a dimension of Dim in the search space.

B. UPDATING SOLUTION SCENARIOS

The position updating process is conducted based on two scenarios. First, generating a two-agent solution as shown in Eq. 7, or based on the best position obtained so-far using Eq. 6 and saving results. In this step, the original TSA is executed conventionally. In the second scenario, to the solution is updated using the LEO strategy to improve the solution efficiency. The LEO distinction between two paths depends on a specific condition as shown in Eqs. 8, and 9. If $rand < 0.5$, the first path is selected to perform the process of solution updating as shown in Eq8; otherwise, the second path Eq.9 is selected to find the new solution.

C. OPTIMIZATION SCENARIOS

This step is performed to evaluate the vector of solutions generated from the previous phase in each iteration to enhance the quality of the further solutions. Accordingly, TSA–LEO computes the fitness value $f(\vec{P}_p)$ of each tunicate position in the current population. The best-scoring solution X_{best} is then determined, saved, and extracted at the updating stage.

D. TERMINATION CRITERIA

After completing the optimization scenarios and iterating until reaching the stopping criteria, the proposed TSA–LEO retrieves the optimal solution according to the best fitness. Algorithm 1 gives the pseudo code of the TSA–LEO algorithm, and a detailed flowchart is shown in Fig. 1.

Algorithm 1 The Proposed TSA–LEO Algorithm

```
procedure TSA–LEO
    Initialize the first population P_p randomly.
    while x < Max_iterations do
        for i = 1 to N do
            X_best ← Best(f(P_p))
            /*Jet propulsion behavior*/
            Calculate the parameters A, G, F, M, and PD
using Eqs.(1 to 5) respectively.
            /*Swarm behavior*/
            if r_rand ≥ 0.5 then
                P_p ← P_p + X_best + A × PD
            else
                P_p ← P_p + X_best − A × PD
            end if
        end for

        /*Local escaping operator (LEO)*/
        if rand < pr then
            if rand < 0.5 then
                Update P_p using Eq8
            else
                Update P_p using Eq9
            end if
        end if
        X_best ← Best(f(P_p))
        x ← x + 1
    end while
    return X_best
end procedure
```

E. COMPUTATIONAL COMPLEXITY OF THE PROPOSED TSA-LEO

This subsection reports and estimates the computational complexity of the proposed TSA-LEO algorithm in terms of time and space complexities.

1) TIME COMPLEXITY

TSA-LEO starts by creating an initial population of size N for each problem dimension Dim, such that the complexity of initialization is $\mathcal{O}(N \times Dim)$ time complexity. Furthermore, TSA-LEO computes the fitness of each population, so the complexity of this process is $\mathcal{O}(Max_{iterations} \times N \times Dim)$, where $Max_{iterations}$ denotes the maximum number of iterations. In addition, TSA-LEO needs $\mathcal{O}(T)$ time complexity to perform its main processes, where T represents the number of jet propulsion, swarm behaviors, and the LEO processes. The overall time complexity of the proposed TSA-LEO can be represented by $\mathcal{O}(Max_{iterations} \times T \times N \times Dim)$.

2) SPACE COMPLEXITY

Space complexity defines the total amount of space occupied by the algorithm. Now, TSA-LEO takes $\mathcal{O}(N \times Dim)$ space complexity.

IV. PERFORMANCE EVALUATION OF TSA-LEO

A. PARAMETER SETTINGS

To accurately evaluate the effectiveness of the proposed TSA-LEO, the algorithm was competed against seven other algorithms, namely, MFO [2], WOA [3], SCA [4], SOA [5], BMO [7], CTSA, and the original TSA. Each method was executed 30 times through (at most) 1000 iterations. The user population size was set to 30. The parameters of each algorithm were set to the values of the first-published standard versions. Table 1 lists the parameters and setting positions of TSA–LEO.

B. DEFINITION OF CEC'17 TEST SUITE FUNCTIONS

The CEC'17 test suite was selected as a test problem because it has high complexity and is customized for global optimization. The CEC'17 test suite contains 30 functions, but function F2 was excluded because to its instability. Therefore, the used benchmark contained 29 test functions. The test suite contains 29 functions and is composed of unimodal shifted and rotated functions; multimodal shifted and rotated functions; hybrid functions; and composition functions as shown in [51].

Fig. 2 shows the landscapes of 16 selected functions in two-dimensional space and provides an intuitive understanding of the functional differences and nature of the problems.

C. STATISTICAL RESULTS ANALYSIS

The CEC'17 benchmark functions are employed to assess the performance of advanced TSA–LEO. Mean and standard deviation (STD) values of each run's best solutions are used to measure the algorithm efficiency. Table 2 represents the mean and STD obtained from the proposed TSA–LEO and other comparative algorithms for each CEC'17 function with 50-dimension; the best results (minimum values) are highlighted in bold. Regarding the best optimal fitness results shown in Table2, the proposed TSA-LEO algorithm gains the best fitness results in 20 functions (0 unimodal functions, 5 multimodal functions, 8 in hybrid functions, and 7 in composition functions) gaining the first rank with overall ratio (69%) of test functions, whereas the CTSA algorithm gains

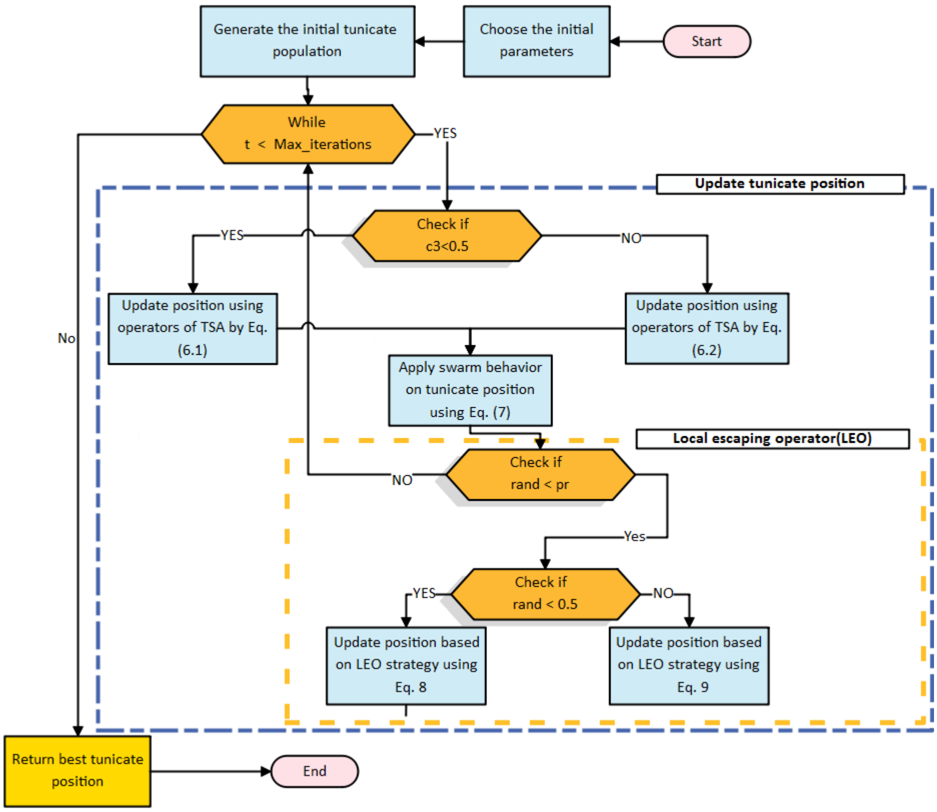

FIGURE 1. Flowchart of the proposed TSA–LEO algorithm.

TABLE 1. Parameter settings of TSA–LEO and competing algorithms.

Algorithms	Parameters setting
Common Settings	Population size: $N = 30$ Maximum iterations: $t_{max} = 1000$ Problem dimensions $Dim = 50$ Number of independent runs 30
MFO	$b = 1$ and a decreases linearly from -1 to -2 (Default)
WOA	α variable decreases linearly from 2 to 0 (Default) $a2$ linearly decreases from -1 to -2 (Default)
SCA	$A = 2$ (Default)
SOA	$A = [0, 2]$ and $f_c = 2$ (Default)
BMO	$pl = 7$ (Default)
TSA and CTSA	$P_{min} = 1$ and $P_{max} = 4$
TSA–LEO	$P_{min} = 1$, $P_{max} = 4$ and $pr = 0.3$

the best fitness of 9 functions gaining the second rank with overall ratio (31%) of test functions, while the other competing algorithms fail to gain the best fitness in any test function. This means that the proposed TSA-LEO algorithm can effectively solve multimodal functions (F4 to F10), hybrid functions (F11 to F20), and composition functions (F21 to F30). Table 3 shows the rank-sum results for fitness according to Wilcoxon rank-sum test. After applying the rank-sum test between the proposed TSA-LEO algorithm and each of the other algorithms (MFO, WOA, SCA, SOA, BMO, TSA, CTSA, and TSA-LEO) a difference between all competitors in contrast to the proposed TSA-LEO is noticed. TSA-LEO vs MFO has a significant difference with a ratio of (96.55%), TSA-LEO vs WOA has a significant difference with a ratio of (100%), TSA-LEO vs SCA has a significant difference with a ratio of (93.10%), TSA-LEO vs SOA has a significant difference with a ratio of (86.20%), TSA-LEO vs BMO has a significant difference with a ratio of (100%), TSA-LEO vs TSA has a significant difference with a ratio of (82.75%), TSA-LEO vs CTSA has a significant difference with a ratio of (82.75%); this means that the proposed TSA-LEO algorithm has a significant development. Moreover, based on

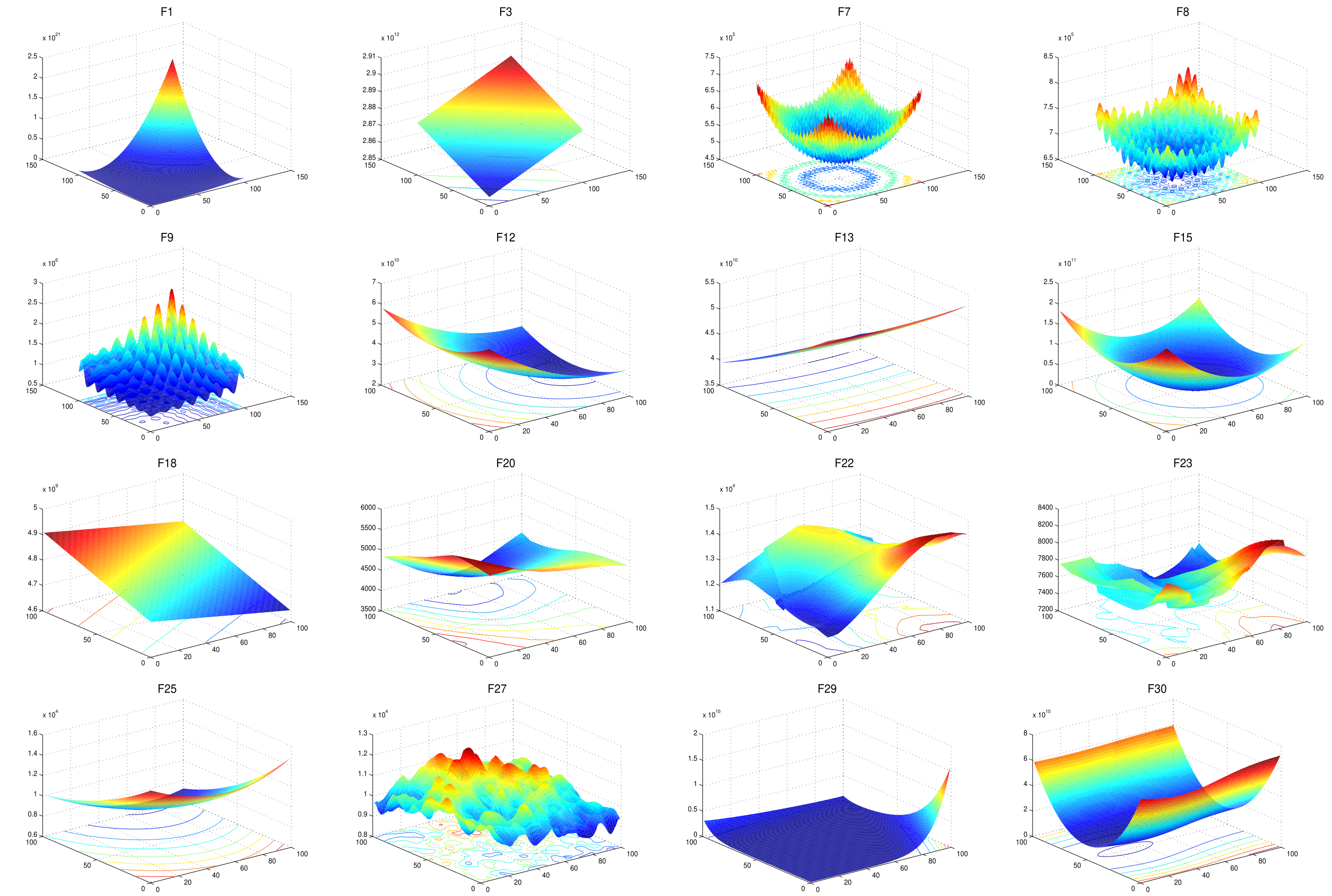

FIGURE 2. Two-dimensional view of some CEC'17 benchmark functions.

Friedman's mean rank test results, the proposed TSA–LEO ranks first compared to the other algorithms. Overall statistical results showed that in solving different advanced benchmarks, the proposed method was more effective than other well-known optimization methods.

D. BOXPLOT BEHAVIOR ANALYSIS

Data distribution characteristics can be displayed by boxplot analysis. Boxplots are efficient for depicting data distributions into quartiles. The minimum and maximum edges of the whiskers are the lowest and largest data points reached by the algorithm. The ends of the rectangles define the lower and upper quartile. A narrow boxplot signifies a high agreement between data. Due to space limitations, Fig. 6 illustrates 15 functions. Figure 3 shows the analyses of F1–F30 functions boxplot for Dim = 50. For most functions, boxplots of the proposed TSA–LEO algorithm are narrow compared with other algorithm distributions and thus have the lowest values. Indeed, the proposed TSA–LEO algorithm performs better than other algorithms for most of the test functions.

E. CONVERGENCE BEHAVIOR ANALYSIS

Fig. 4 shows the convergence plots of MFO, WOA, SCA, SOA, BMO, TSA, and TSA–LEO on the CEC'17 functions. The proposed TSA–LEO achieved (near)-optimal solutions and fast convergence on most functions; hence, it can solve problems requiring fast computation, such as online problems. Furthermore, the algorithm exhibited stable behavior, and its solutions smoothly converged in most of the tested problems. Due to space limitations, Fig. 4 illustrates 15 functions.

F. EXPLORATION AND EXPLOITATION ANALYSIS

Fig.5 records exploration-exploitation ratios during search maintained by the proposed TSA-LEO while solving a set of CEC'17 test functions with dimension of 30. From Fig.5 it is noticeable that the proposed TSA-LEO starts with a high exploration ratio and low exploitation ratio, but mostly later transformed into exploitation strategy during most of the iterations in most of the CEC'17 functions. This indicates that the proposed TSA-LEO balances effectively between exploration and exploitation phases.

G. QUALITATIVE METRICS ANALYSIS

Fig. 6 shows the collective behavior of foraging tunicates. The first pillar represents a set of the CEC'17 functions as shapes in two-dimensional space. The second pillar illustrates the search history of the tunicates, show-

TABLE 2. Mean and STD of the fitness values of different optimization algorithms, obtained from 30 runs of 50-dimensional CEC'17 functions.

	MFO		WOA		SCA		SOA		BMO		TSA		CTSA		TSA-LEO	
CEC-Function	**MEAN**	**STD**	**MEAN**	**STD**	**MEAN**	**STD**	**MEAN**	**STD**	**MEAN**	**STD**	**MEAN**	**STD**	**MEAN**	**STD**	**MEAN**	**STD**
F1	1.26E+11	2.83E+08	9.15E+09	2.85E+09	6.00E+10	6.93E+09	4.09E+10	8.15E+09	1.31E+11	5.55E+09	4.60E+10	9.73E+09	**6.77E+07**	1.98E+07	7.05E+08	8.86E+08
F3	2.20E+05	2.89E+04	2.51E+05	7.75E+04	1.74E+05	2.58E+04	1.39E+05	1.79E+04	3.00E+05	5.60E+04	1.17E+05	1.65E+04	**6.65E+03**	2.10E+03	6.44E+04	8.79E+03
F4	5.74E+04	8.30E+02	2.66E+03	5.61E+02	1.09E+04	2.34E+03	5.16E+03	1.78E+03	5.18E+04	4.57E+03	8.98E+03	3.35E+03	**5.39E+02**	4.08E+01	5.80E+02	7.25E+01
F5	1.39E+03	8.10E+01	1.06E+03	8.11E+01	1.11E+03	3.59E+01	9.47E+02	3.75E+01	1.31E+03	1.88E+01	1.19E+03	9.31E+01	7.38E+02	3.81E+01	**7.07E+02**	3.71E+01
F6	7.13E+02	5.04E+00	6.92E+02	1.26E+01	6.79E+02	5.90E+00	6.68E+02	9.73E+00	7.08E+02	4.50E-02	7.00E+02	1.09E+01	6.64E+02	1.08E+01	**6.47E+02**	9.87E+00
F7	2.04E+03	4.18E+01	1.84E+03	9.55E+01	1.82E+03	1.02E+02	1.64E+03	1.09E+02	2.20E+03	5.89E+00	1.81E+03	1.39E+02	**1.06E+03**	8.92E+01	1.14E+03	8.41E+01
F8	1.69E+03	1.13E+02	1.36E+03	9.40E+01	1.43E+03	3.15E+01	1.26E+03	5.55E+01	1.59E+03	1.21E+01	1.47E+03	7.65E+01	9.88E+02	2.72E+01	**9.62E+02**	2.48E+01
F9	5.58E+04	7.18E+03	3.25E+04	9.03E+03	3.17E+04	5.19E+03	2.32E+04	4.89E+03	5.36E+04	2.05E+03	4.91E+04	1.28E+04	6.65E+03	1.11E+03	**5.11E+03**	5.76E+02
F10	1.19E+04	6.96E+02	1.23E+04	1.12E+03	1.53E+04	3.88E+02	1.26E+04	1.18E+03	1.70E+04	6.36E+02	1.35E+04	1.04E+03	6.08E+03	6.23E+02	**5.22E+03**	4.27E+02
F11	1.91E+04	1.46E+03	5.43E+03	1.32E+03	1.03E+04	2.18E+03	8.18E+03	2.97E+03	4.48E+04	1.20E+04	1.28E+04	4.46E+03	**1.38E+03**	5.86E+01	1.56E+03	3.90E+02
F12	1.03E+11	2.47E+09	1.80E+09	7.66E+08	1.82E+10	5.06E+09	6.71E+09	2.90E+09	1.21E+11	1.54E+10	2.41E+10	1.14E+10	4.91E+07	3.75E+07	**5.16E+06**	4.60E+06
F13	1.10E+11	5.83E+09	1.72E+08	1.02E+08	5.39E+09	2.90E+09	1.46E+09	1.71E+09	7.34E+10	2.01E+10	1.59E+10	9.51E+09	2.19E+06	3.81E+06	**3.31E+04**	2.69E+04
F14	1.04E+09	2.56E+08	5.60E+06	4.84E+06	6.85E+06	3.52E+06	1.88E+06	2.01E+06	2.35E+08	9.66E+07	1.54E+07	2.80E+07	**6.27E+04**	5.58E+04	4.93E+05	4.43E+05
F15	2.29E+10	9.82E+07	2.02E+07	2.10E+07	7.82E+08	3.67E+08	1.18E+08	2.21E+08	1.72E+10	3.79E+09	1.45E+09	1.57E+09	9.78E+04	6.89E+04	**5.05E+03**	6.32E+03
F16	2.01E+04	8.30E+02	6.09E+03	8.97E+02	6.14E+03	4.06E+02	4.55E+03	6.49E+02	1.50E+04	2.77E+03	5.78E+03	1.13E+03	2.86E+03	3.70E+02	**2.71E+03**	3.51E+02
F17	1.34E+05	3.72E+04	4.53E+03	4.86E+02	4.89E+03	3.31E+02	3.84E+03	3.60E+02	7.62E+04	5.65E+04	5.67E+03	4.07E+03	2.41E+03	2.28E+02	**2.34E+03**	1.91E+02
F18	7.46E+08	1.24E+08	3.41E+07	3.47E+07	3.85E+07	2.01E+07	1.10E+07	6.40E+06	8.56E+08	3.07E+08	3.77E+07	4.00E+07	**1.06E+06**	8.29E+05	1.20E+06	1.22E+06
F19	1.19E+10	5.07E+08	1.06E+07	1.40E+07	4.84E+08	1.97E+08	1.46E+08	2.84E+08	9.43E+09	1.54E+09	1.72E+09	1.56E+09	2.11E+06	1.85E+06	**5.82E+03**	2.57E+03
F20	4.06E+03	2.64E+02	3.84E+03	3.72E+02	4.21E+03	2.35E+02	3.86E+03	3.85E+02	4.83E+03	5.60E+01	3.85E+03	3.29E+02	2.70E+03	2.29E+02	**2.67E+03**	2.41E+02
F21	3.72E+03	6.87E+01	3.04E+03	1.06E+02	2.95E+03	3.90E+01	2.75E+03	5.33E+01	3.58E+03	1.14E+02	3.04E+03	9.21E+01	2.53E+03	4.31E+01	**2.47E+03**	3.66E+01
F22	1.34E+04	5.24E+02	1.43E+04	1.05E+03	1.67E+04	5.73E+02	1.45E+04	1.15E+03	1.88E+04	4.27E+02	1.49E+04	8.23E+02	4.81E+03	2.67E+03	**2.76E+03**	1.30E+03
F23	5.51E+03	1.10E+02	3.83E+03	1.84E+02	3.68E+03	7.51E+01	3.23E+03	8.10E+01	4.83E+03	1.95E+02	4.04E+03	2.05E+02	3.07E+03	1.09E+02	**2.81E+03**	4.71E+01
F24	6.09E+03	4.55E+02	3.85E+03	1.53E+02	3.84E+03	7.24E+01	3.34E+03	5.50E+01	4.65E+03	1.43E+02	4.10E+03	1.67E+02	3.20E+03	1.14E+02	**2.96E+03**	3.50E+01
F25	1.60E+04	6.41E+01	4.12E+03	2.95E+02	8.20E+03	1.15E+03	5.83E+03	6.88E+02	1.89E+04	9.88E+02	7.13E+03	1.61E+03	2.94E+03	**2.47E+01**	2.97E+03	3.17E+01
F26	1.87E+04	7.26E+02	1.45E+04	1.58E+03	1.35E+04	7.67E+02	8.84E+03	6.18E+02	1.93E+04	5.21E+02	1.42E+04	1.13E+03	7.24E+03	1.33E+03	**5.36E+03**	1.71E+03
F27	7.93E+03	2.32E+02	4.65E+03	5.76E+02	4.82E+03	2.22E+02	3.90E+03	1.84E+02	6.94E+03	5.70E+02	4.95E+03	5.05E+02	3.39E+03	1.08E+02	**3.24E+03**	1.95E+01
F28	1.76E+04	5.41E+02	5.27E+03	3.97E+02	8.25E+03	8.76E+02	9.02E+03	1.67E+03	1.77E+04	1.61E+03	6.57E+03	9.68E+02	3.31E+03	**2.84E+01**	3.37E+03	4.31E+01
F29	4.19E+05	1.68E+05	8.65E+03	1.44E+03	8.24E+03	7.90E+02	7.27E+03	1.39E+03	1.21E+06	1.23E+06	9.23E+03	4.48E+03	4.80E+03	3.71E+02	**4.04E+03**	2.81E+02
F30	1.98E+10	4.29E+08	2.57E+08	1.09E+08	1.13E+09	3.83E+08	2.70E+08	1.68E+08	1.76E+10	3.45E+09	1.33E+09	1.47E+09	1.09E+07	8.18E+06	**4.16E+04**	5.86E+04
Fridman mean rank	**7.03**		**3.9**		**4.9**		**3.34**		**7.24**		**5.31**		**2.93**		**1.34**	
Rank	**7**		**4**		**5**		**3**		**8**		**6**		**2**		**1**	

TABLE 3. Comparison of the p-values obtained from the Wilcoxon signed-rank test between the pairs of TSA–LEO vs. MFO, TSA–LEO vs. WOA, TSA–LEO vs. SCA, TSA–LEO vs. SOA, TSA–LEO vs. BMO, TSA–LEO vs. TSA, and TSA–LEO vs. CTSA for CEC'17 test functions in terms of Fitness results.

	MFO		WOA		SCA		SOA		BMO		TSA		CTSA	
CEC17 Functions	**P**	**H**	**P**	**H**	**P**	**H**	**P**	**H**	**P**	**H**	**P**	**H**	**P**	**H**
F1	3.02E-11	1	3.02E-11	1	3.02E-11	1	3.02E-11	1	3.02E-11	1	2.28E-05	1	2.03E-09	1
F3	3.02E-11	1	3.02E-11	1	3.02E-11	1	3.02E-11	1	3.02E-11	1	3.02E-11	1	3.02E-11	1
F4	3.02E-11	1	3.02E-11	1	3.02E-11	1	3.02E-11	1	3.02E-11	1	9.94E-01	0	3.39E-02	1
F5	3.02E-11	1	3.02E-11	1	3.02E-11	1	3.02E-11	1	3.02E-11	1	1.41E-04	1	4.86E-03	1
F6	3.02E-11	1	3.02E-11	1	3.02E-11	1	3.02E-11	1	3.02E-11	1	1.07E-09	1	5.19E-07	1
F7	3.02E-11	1	3.02E-11	1	3.02E-11	1	3.02E-11	1	3.02E-11	1	7.98E-02	0	8.12E-04	1
F8	3.02E-11	1	3.02E-11	1	3.02E-11	1	3.02E-11	1	3.02E-11	1	6.97E-03	1	1.11E-03	1
F9	3.02E-11	1	3.02E-11	1	1.20E-08	1	1.67E-01	0	3.02E-11	1	1.61E-06	1	5.19E-07	1
F10	3.02E-11	1	3.02E-11	1	2.15E-10	1	8.88E-01	0	3.02E-11	1	1.16E-07	1	8.20E-07	1
F11	3.82E-10	1	3.02E-11	1	3.02E-11	1	3.02E-11	1	3.02E-11	1	6.10E-03	1	3.99E-04	1
F12	3.02E-11	1	3.02E-11	1	3.02E-11	1	3.02E-11	1	3.02E-11	1	2.87E-10	1	1.78E-10	1
F13	3.02E-11	1	5.57E-10	1	3.02E-11	1	3.02E-11	1	3.02E-11	1	3.02E-11	1	3.02E-11	1
F14	3.02E-11	1	3.02E-11	1	3.02E-11	1	3.02E-11	1	3.02E-11	1	2.38E-07	1	4.69E-08	1
F15	3.04E-01	0	8.48E-09	1	1.37E-03	1	5.56E-04	1	3.02E-11	1	4.08E-11	1	4.98E-11	1
F16	5.07E-10	1	3.02E-11	1	3.02E-11	1	3.34E-11	1	3.02E-11	1	3.52E-07	1	9.05E-02	0
F17	3.02E-11	1	3.02E-11	1	3.02E-11	1	3.02E-11	1	3.02E-11	1	6.97E-03	1	2.97E-01	0
F18	3.02E-11	1	3.02E-11	1	3.02E-11	1	3.02E-11	1	3.02E-11	1	2.46E-01	0	7.39E-01	0
F19	9.51E-06	1	1.07E-07	1	6.67E-03	1	4.83E-01	0	3.02E-11	1	3.02E-11	1	3.02E-11	1
F20	3.02E-11	1	3.02E-11	1	3.02E-11	1	3.02E-11	1	3.02E-11	1	1.81E-01	0	6.41E-01	0
F21	3.02E-11	1	3.02E-11	1	3.02E-11	1	3.02E-11	1	3.02E-11	1	5.97E-09	1	3.01E-07	1
F22	8.48E-09	1	3.02E-11	1	8.48E-09	1	8.48E-09	1	3.02E-11	1	4.23E-03	1	2.71E-01	0
F23	3.02E-11	1	3.02E-11	1	3.02E-11	1	3.02E-11	1	3.02E-11	1	5.49E-11	1	3.69E-11	1
F24	3.02E-11	1	3.02E-11	1	3.02E-11	1	3.02E-11	1	3.02E-11	1	6.07E-11	1	4.08E-11	1
F25	3.02E-11	1	3.02E-11	1	3.02E-11	1	3.02E-11	1	3.02E-11	1	8.68E-03	1	2.25E-04	1
F26	1.11E-06	1	3.02E-11	1	1.58E-01	0	3.55E-01	0	3.02E-11	1	6.35E-02	0	3.16E-05	1
F27	3.02E-11	1	3.02E-11	1	3.02E-11	1	3.02E-11	1	3.02E-11	1	1.78E-10	1	6.07E-11	1
F28	3.64E-02	1	3.02E-11	1	3.02E-11	1	3.02E-11	1	3.02E-11	1	1.44E-03	1	4.11E-07	1
F29	3.02E-11	1	3.02E-11	1	7.39E-01	0	9.47E-03	1	3.02E-11	1	3.08E-08	1	2.67E-09	1
F30	3.02E-11	1	3.02E-11	1	3.02E-11	1	3.02E-11	1	3.02E-11	1	3.02E-11	1	3.02E-11	1

ing their exploitation behavior to achieve the desired results. The third pillar displays the average fitness over 100 iterations, explaining how diversified new agents assist in the search of the best solution. The proposed TSA–LEO can find the areas with the best fitness for most functions according to the search history pillar. In terms of average fitness history, all curves are decreasing, which means that the population improves at each iteration.

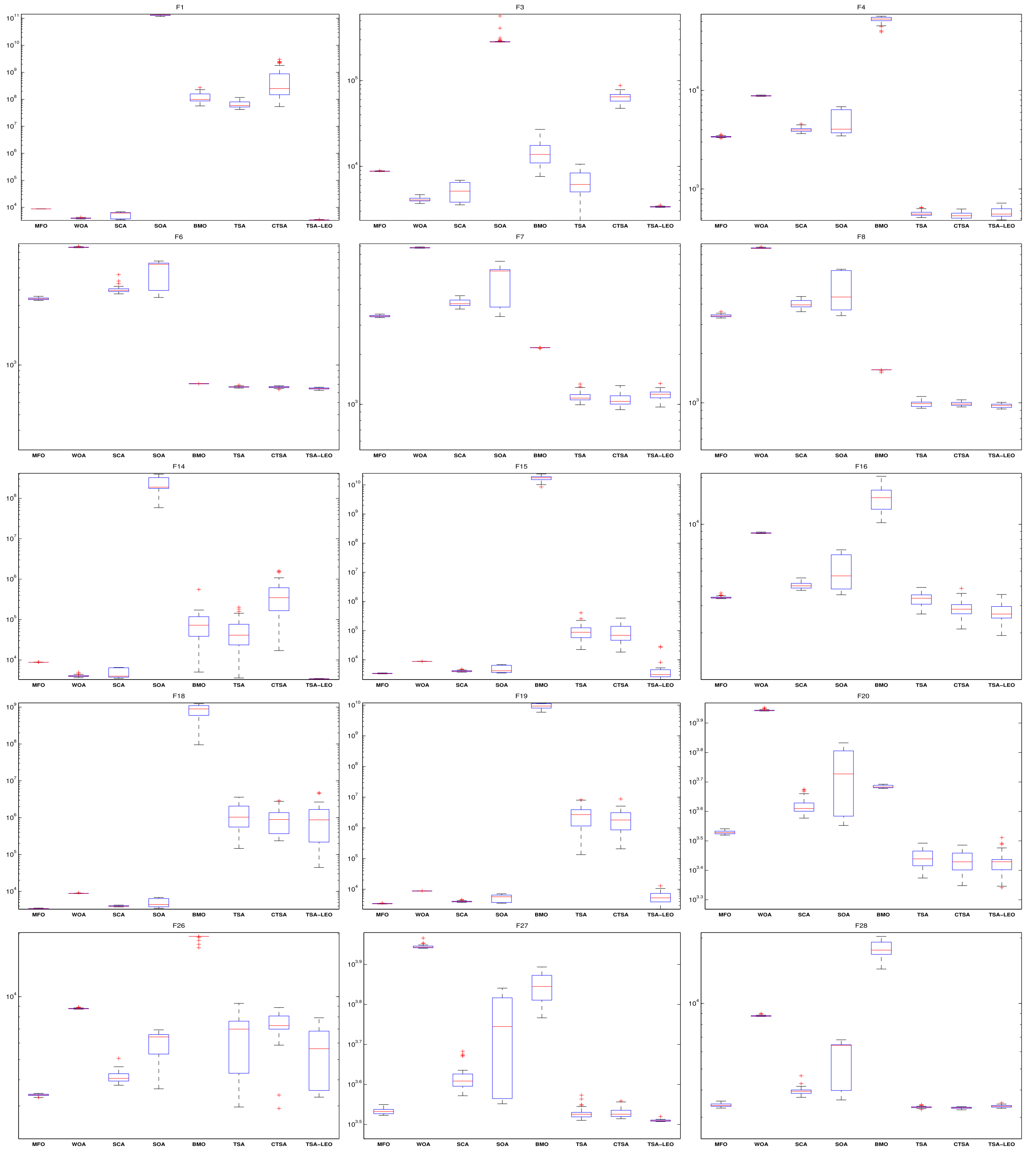

FIGURE 3. **Boxplots analysis for the proposed TSA-LEO and the competitor algorithms on the CEC'17 test functions with *Dim* = 50.**

This constant improvement substantiates a collaborative searching behavior and supports the efficiency of updating particle law. Finally, convergence curve and optimization history revealed the progress of fitness over several iterations. The decrease in optimization history indicates that the solutions are optimized during iterations until reaching the optimal solution.

V. EXPERIMENTAL RESULTS AND ANALYSIS

This section employs the proposed TSA–LEO to solve thresholding-based image segmentation problems. In this evaluation, TSA–LEO was expected to select the thresholds that best segmented a set of benchmark images by maximizing a well-known thresholding technique, namely, Otsu's objective function.

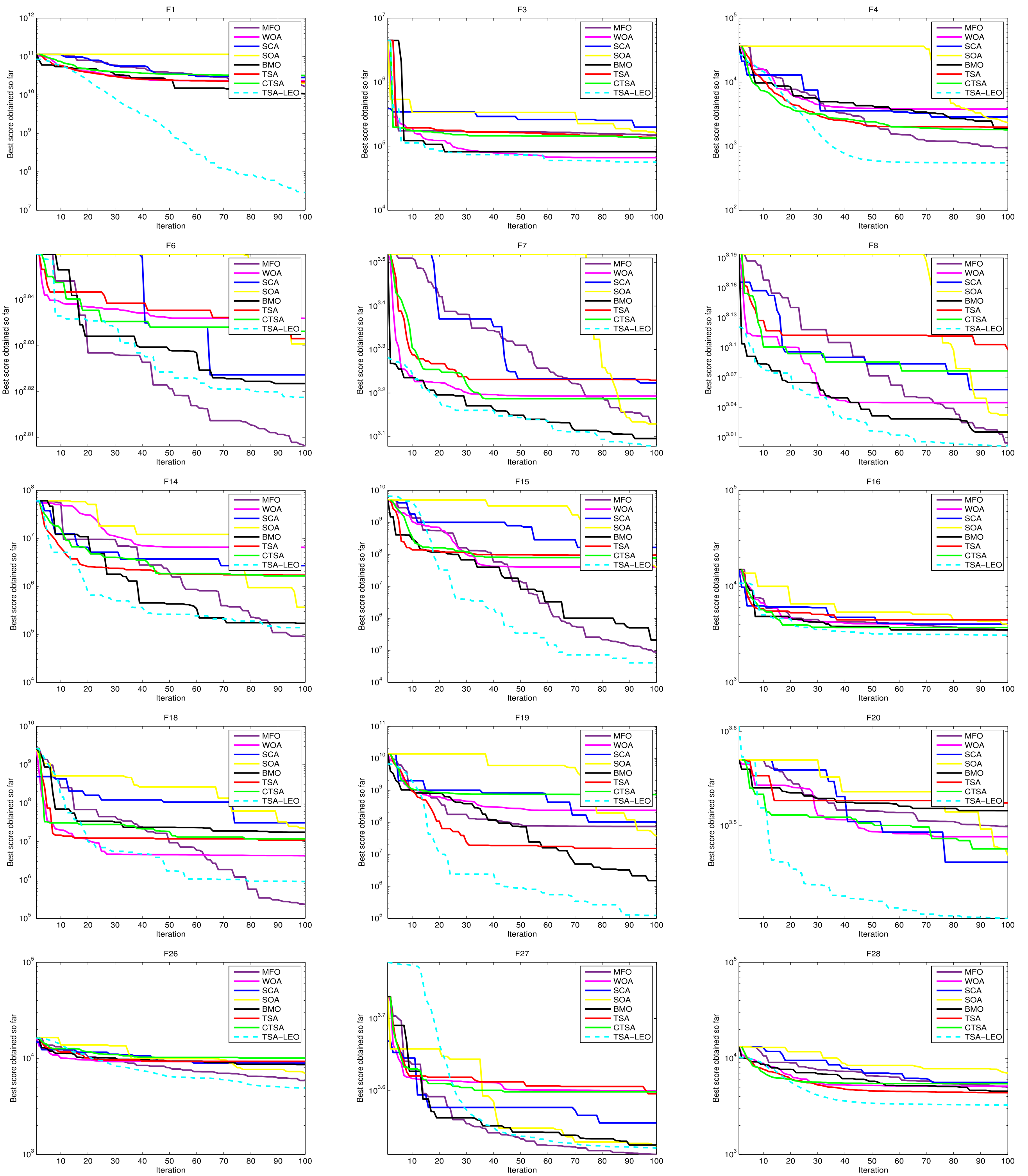

FIGURE 4. **Convergence curves for the proposed TSA-LEO and the competitor algorithms on the CEC'17 test functions with *Dim* = 50.**

A. MULTI-THRESHOLDING IMAGE SEGMENTATION STUDIES

In this research, image thresholding shows the efficiency of metaheuristic algorithms in the relevant method [35], [47], [52]. In this regard, there are numerous examples of meta-heuristic applications; however, a few prominent state-of-the-art research works are given. To tackle the problems of multi-thresholding, Upadhyay and Chhabra [53] used the crow search algorithm (CSA) to maximize Kapur's method. The proposed model was compared with a set of

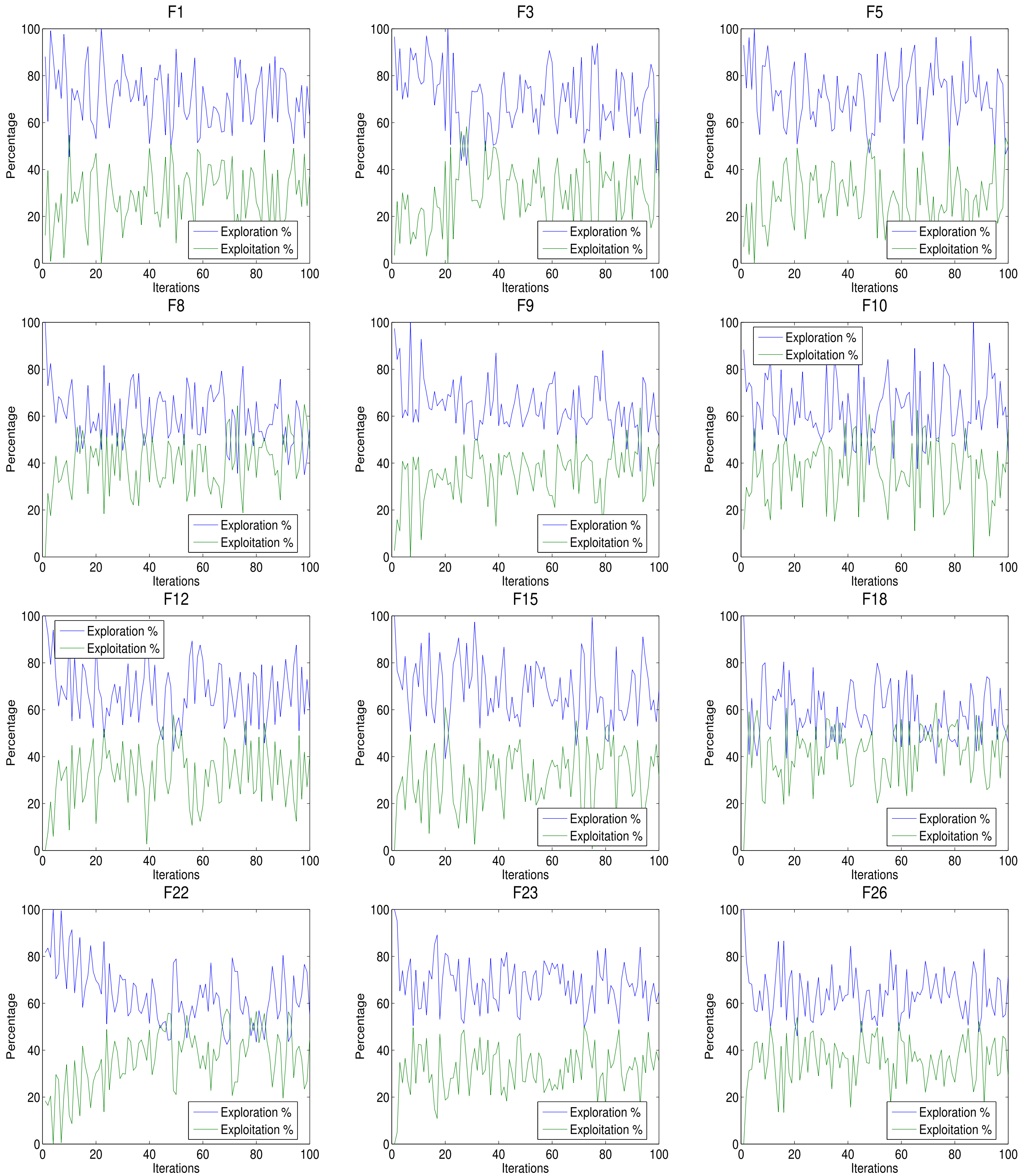

FIGURE 5. The Graphical representation of the exploration and exploitation phases for the proposed TSA-LEO over the CEC'17 functions with *Dim* = 50.

well-known metaheuristic algorithms, namely, PSO, DE, GWO, MFO, and CSA. The authors chose CSA because of its balance between exploration and exploitation, as well as less parameters to tune. Through most commonly used evaluation metrics, the authors contended to have achieved comparatively better results when tested on a set of benchmark images using multiple threshold values. Despite the success in this work, CSA has a slow convergence. Khairuzzaman and Chaudhury [54]used GWO to produce efficient image-segmentation results while finding the optimal set of

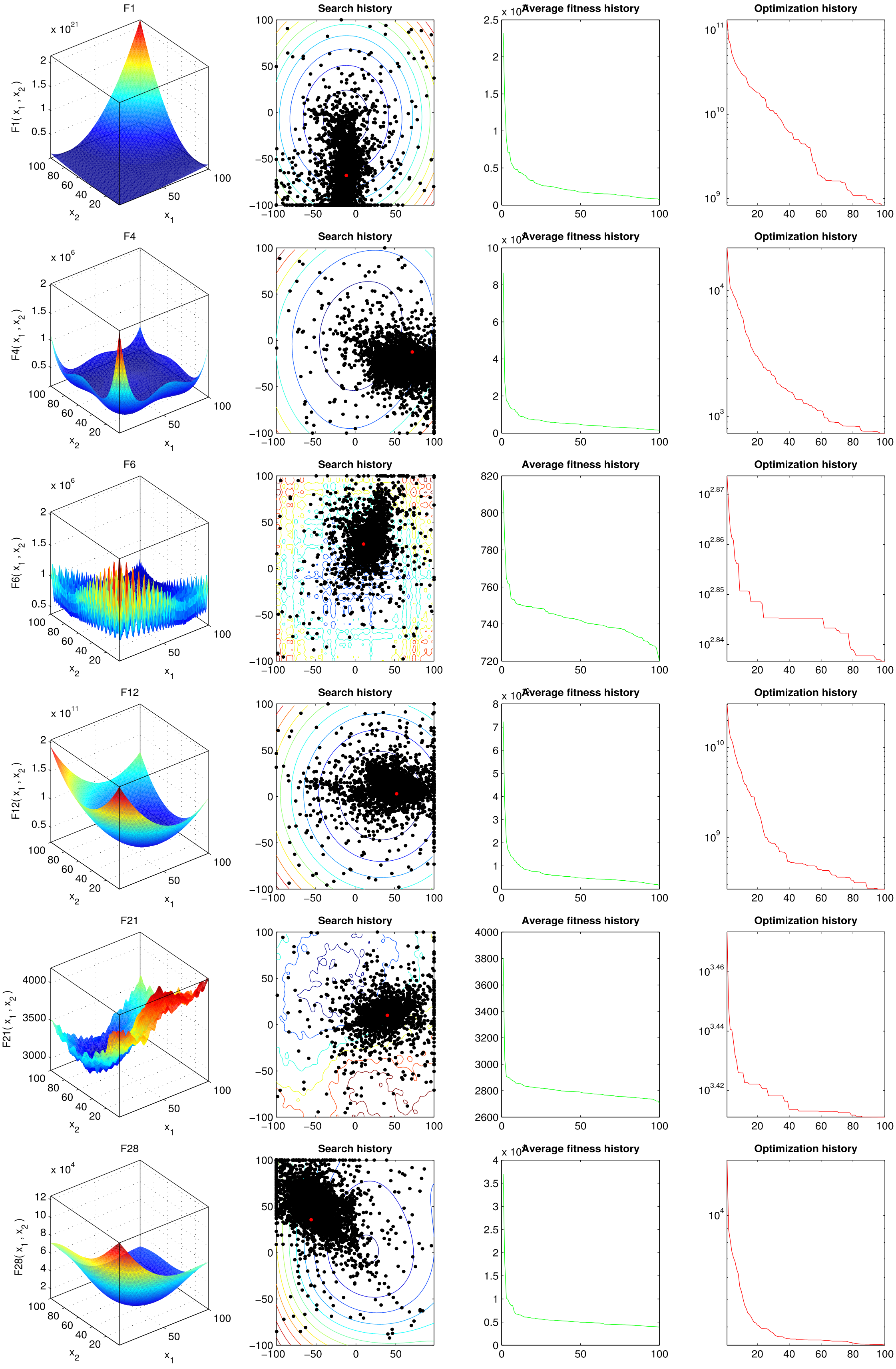

FIGURE 6. Qualitative metrics on F1, F4, F6, F12, F21, and F28: 2D views of the functions, search history, average fitness history, and optimization history.

TABLE 4. Results after applying TSA-LEO on Kapur to the set of benchmark images.

Image	Level = 2	Level = 3	Level = 4	Level = 5
Cameraman	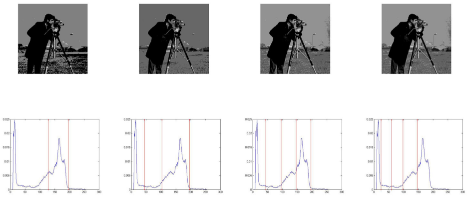			
Lena	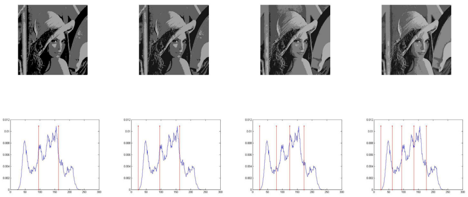			
Baboon	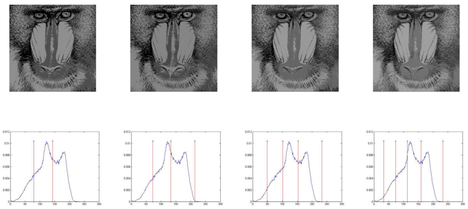			
Hunter	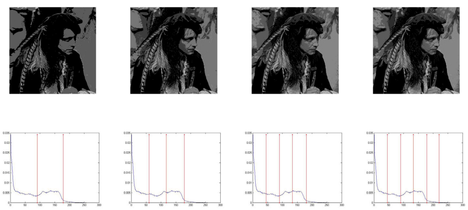			
Airplane	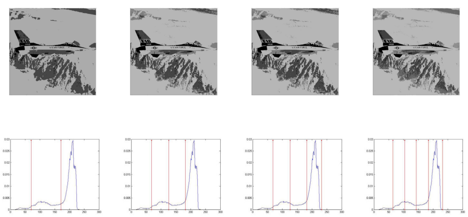			

TABLE 5. Results after applying TSA-LEO on Kapur to the set of benchmark images.

Image	Level = 2	Level = 3	Level = 4	Level = 5
Pepper	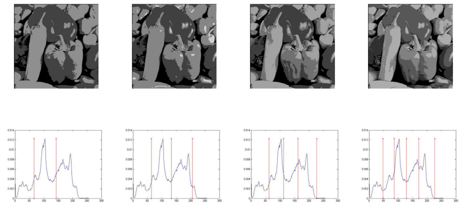			
Living-Room	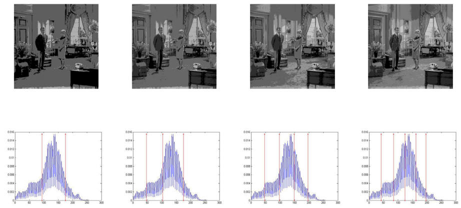			
Woman	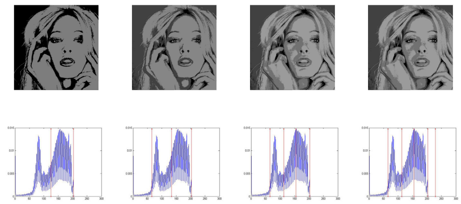			
Bridge	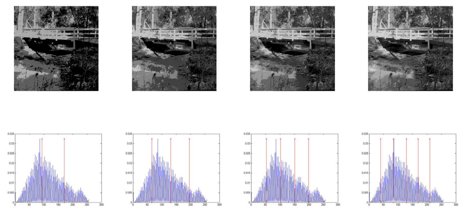			
Butter-Fly	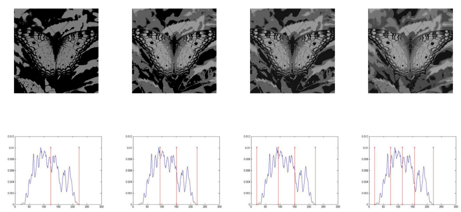			

thresholds using Otsu's and Kapur's functions. GWO converged to better optimum solutions than bacterial foraging optimization (BFO) and PSO; however, the proposed algorithms also posed certain disadvantages: a) its efficiency reduced when employed on noisy images and b) GWO was slower than PSO regarding the computational time. The research maintained a major weakness; it did not provide a comprehensive comparison with other well-known and established metaheuristic algorithms, but merely used PSO and BFO for comparison. To optimize threshold values for multilevel image thresholding, a modified grasshopper optimization algorithm (GOA) with Lévy flight was introduced based on Tsallis cross-entropy as the objective function [55]. The proposed model was tested on benchmark images and plant stomata. Compared with standard GOA, WOA, flower pollination algorithm (FPA), PSO, and bat algorithm (BA), the proposed GOA variant produced better segmentation accuracy with enhanced multilevel segmentation convergence on energy-based Tsallis entropy. One limitation of this study is that it did not experiment with relatively increased thresholds for high-dimensional optimization problems.

The study in [56] used the EO algorithm and Kapur's entropy as objective function to achieve the optimal threshold values for grayscale images. To achieve enhanced search ability, the researchers improved EO with adaptive parameters. The proposed method was evaluated using several solution quality metrics such as the signal-to-noise ratio, structured similarity index, some accuracy measures like mean absolute error, and the computation time for resource complexity. The proposed EO outperformed WOA, BA, SCA, SSA, harris hawk's optimizer (HHO), CSA, and PSO techniques. The significance of this study can be determined with the level of thresholds used in the experiment. The researchers used up to 50 threshold levels. However, the proposed EO variant comparatively underperformed considering standard deviation values and computational time. HHO is another recent metaheuristic technique that was implemented in a similar domain using Otsu's and Kapur's objective functions [57]. Comparisons of the proposed method with PSO, DE, harmony search (HS), ABC, and SCA, show that it produced efficient results in terms of quality, consistency, and accuracy. However, the results of HHO were also compared with two machine learning techniques, K-means and fuzzy IterAg, revealing that these techniques performed the least in the overall image-segmentation exercise. Another limitation of this study is that it was not evaluated on color images, and the number of thresholds was manually set. Meanwhile, Díaz-Cortés *et al.* [58] resolved the problem of unclear regional borders in low-resolution thermography images in health-care using the dragonfly algorithm (DA). In addition, the DA technique is used to find optimum threshold values for energy curves in thermal images for breast cancer diagnosis. Based on the objective functions of Otsu's and Kapur's, the authors evaluated solution quality and found that DA outperformed GA, PSO, runner-root algorithm and krill-herd algorithm on a set of eight images retrieved from the DA-Breast Thermography database.

To improve the optimal threshold selection in this study, the proposed TSA-LEO algorithm was integrated with Otsu' and Kapur's objective functions.

B. OTSU's OBJECTIVE FUNCTION

Otsu was selected because it is commonly used for thresholding images, segmented by maximizing the between-class variation. TSA–LEO optimizer maximizes the Otsu objective function and determines the best-fit thresholds. The objective function of Otsu considers L intensity levels of a gray image, and the probability distribution is computed in Eq. 21. This method can be used for RGB color images in which Otsu is separately applied to each channel.

$$h_i = \frac{h_i}{NP}, \sum_{i=1}^{NP} Ph_i = 1 \tag{21}$$

where i is an intensity level defined in the range of $(0 \leq i \leq L-1)$. NP is the total number of pixels in an image. h_i denotes the number of occurrence of intensity i in the image represented by the histogram. The histogram is normalized in a probability distribution Ph_i. Based on the probability distribution or threshold value (th), the classes are computed for bi-level segmentation as follows:

$$C_1 = \frac{Ph_1}{\omega_0(th)}, \ldots, \frac{Ph_{th}}{\omega_0(th)} \text{ and } C_2 = \frac{Ph^c_{th+1}}{\omega_1(th)}, \ldots, \frac{Ph_L}{\omega_1(th)} \tag{22}$$

where $\omega_0(th)$ and $\omega_1(th)$ are cumulative probability distributions for C_1 and C_2, as it is shown by Eq. (23).

$$\omega_0(th) = \sum_{i=1}^{th} Ph_i \text{ and } \omega_1(th) = \sum_{th+1}^{L} Ph_i \tag{23}$$

It is mandatory to find the average intensity levels μ_0 and μ_1 that define the classes using Eq. (24). Once those values are calculated, the Otsu based between-class σ_B^2 is calculated using Eq. (25).

$$\mu_0 = \sum_{i=1}^{th} \frac{iPh_i}{\omega_0(th)} \text{ and } \mu_1 = \sum_{i=th+1}^{L} \frac{iPh_i}{\omega_1(th)} \tag{24}$$

$$\sigma_B^2 = \sigma_1 + \sigma_2 \tag{25}$$

Notice that σ_1 and σ_2 in Eq. (25) are the variances of C_1 and C_2 which are defined as follow:

$$\sigma_1 = \omega_0(\mu_0 + \mu_T)^2 \text{ and } \sigma_2 = \omega_1(\mu_1 + \mu_T)^2 \tag{26}$$

where $\mu_T = \omega_0\mu_0 + \omega_1\mu_1$ and $\omega_0 + \omega_1 = 1$ based on the values σ_1 and σ_2, Eq. (27) presents the objective function. Therefore, the optimization problem is reduced to find the intensity level that maximizes Eq. (27)

$$F_{otsu}(th) = \max(\sigma_B^2(th)) \text{ where } 0 \leq th \leq L-1 \tag{27}$$

where $\sigma_B^2(th)$ is the Otsu's variance for a given th value. Otsu's method is applied for a single component of an image, that means for RGB images it is necessary to apply separation into single component images. The previous illustration of such bi-level method can be modified for multiple thresholds. The objective function $F_{otsu}(th)$ in Eq. (27) can also be modified for multiple thresholds as follows:

$$F_{otsu}(TH) = Max(\sigma_B^2(th)) \text{ where } 0 \leq th \leq L-1 \text{ and } i = [1, 2, 3, \ldots, k] \tag{28}$$

where $TH = [th_1, th_2, \ldots, th_k - 1]$ is a vector containing multiple thresholds, L denotes maximum grey level, whereas the variances are computed through Eq. (29).

$$N\sigma_B^2 = \sum_{i=1}^{k} \sigma_i = \sum_{i=1}^{k} \omega_1(\mu_1 - \mu_T)^2 \tag{29}$$

where i represents a specific class. ω_i and μ_j are the probability of occurrence and the mean of a class respectively. For multi-level thresholding, such values are obtained as:

$$\omega_{k-1}(th) = \sum_{i=th_k+1}^{L} Ph_i \tag{30}$$

for mean values:

$$\mu_{k-1} = \sum_{i=th_k+1}^{L} \frac{iPh_i}{\omega_1(th_k)} \tag{31}$$

C. KAPUR's OBJECTIVE FUNCTION

Another thresholding technique used to apply the concept of segmentation is the Kapur's method [43]. Kapur's method selects the optimal threshold values based on maximizing the entropy. The mathematical model is described as follows:

$$F_{kapur}(th) = H_1 + H_2 \tag{32}$$

where the entropies H_1 and H_2 are computed as:

$$H_1 = \sum_{i=1}^{th} \frac{Ph_i}{\omega_0} ln(\frac{Ph_i}{\omega_0}) \text{ and } H_2 = \sum_{i=th+1}^{L} \frac{Ph_i}{\omega_1} ln(\frac{Ph_i}{\omega_1}) \quad (33)$$

where Ph_i is the probability distribution of the intensity levels which is obtained using Eq. (13), $\omega_0(th)$ and $\omega_1(th)$ are probabilities distributions for the classes C_1 and C_2. $ln(.)$ is the natural logarithm. Similar to the Otsu's method, the entropy-based approach can be modified for multi-thresholding values; for such a case, it is necessary to divide the image into k classes using $k-1$ thresholds. The objective function then can be modified as follows:

$$F_{kapur}(TH) = \sum_{i=1}^{k} H_i \quad (34)$$

where $TH = [th_1, th_2, \ldots, th_{k-1}]$ is a vector that contains the multiple thresholds. Each entropy is computed separately with its respective (th) value, so Eq. (34) is expanded for k entropies as:

$$H_k^c = \sum_{i=th_{k+1}}^{L} \frac{Ph_i}{\omega_{k-1}} ln(\frac{Ph_i}{\omega_{k-1}}) \quad (35)$$

Here the values of the probability occurrence $(\omega_0^c, \omega_1, \ldots, \omega_{k-1})$ of the k classes are obtained using Eq. (20) and the probability distribution Ph_i with Eq. (13).

For the ease of understanding TSA-LEO implementation on image segmentation, the following steps are given in brief.

1) Read the image in grayscale.
2) Obtain the histogram of the selected image.
3) Calculate the probability distribution using Eq23.
4) Initialize TSA–LEO parameters.
5) Initialize the first population of tunicates $\vec{P_p}$ with the dimension of Dim.
6) Evaluate the initial population using Otsu (F_{otsu}) Eq28 or Kapur (F_{kapur}) Eq34.
7) Calculate the parameters $\vec{A}$, $\vec{G}$, $\vec{F}$, $\vec{M}$, and $\vec{PD}$ using Eqs.(1-5) respectively.
8) Update the positions of each agent using Eqs.(6 or 7).
9) Determine the optimal position X_{best}.
10) Apply LEO strategy if $rand < pr$ and update the value of $\vec{P_p}$ based on Eq.8 if $rand < 0.5$ or 9 if $rand \geq 0.5$.
11) Evaluate the new population and save best results.
12) Select tunicate with the best solution according to the objective function.
13) If maximum iteration or the stop conditions are not met, go to Step 7.
14) To segment the image, use tunicate with the best threshold values.

D. ENVIRONMENTAL SETUP

The results of advanced TSA–LEO with the objective functions of Otsu and Kapur were compared with those of MFO [2], WOA [3], SCA [4], SOA [5], BMO [7], CTSA, and original TSA. All algorithms were executed 35 times per algorithm under the same stopping criteria (350 iterations at most) with 50 search agents to evaluate their performances. The parameters of each algorithm were maintained at their standard versions' values. All tested algorithms were programmed and operated in the same experimental environment (Intel Core-I5 processor, 8 GB memory, Matlab-2013, and Windows 8.1-64).

E. EVALUATION CRITERIA

Evaluating segmented images is essential for validating the performance and accuracy of any algorithm. Three measures were used to evaluate the degree of segmentation: PSNR [59], SSIM [60], and FSIM [61]. Wilcoxon rank-sum was used to evaluate the significance of the proposed TSA–LEO, and the variations between the proposed method and competing algorithms were assessed in Friedman's non-parametric statistical tests [62], [63].

1) QUALITY METRICS

The **PSNR** distinguishes between the qualities of the initial and resulting images. The PSNR is defined as

$$PSNR = 20log_{10}\frac{255}{RMSE}$$
$$RMSE = \sqrt{\frac{\sum_{i=1}^{M}\sum_{j=1}^{N}((I(i,j) - Seg(i,j))^2)}{M \times N}} \quad (36)$$

where $RMSE$ is the root-mean-squared error, and I and Seg are the initial and final images, respectively. All images are sized M $\times$ N.

The **SSIM** determines the similarity between the original and segmented images. The SSIM is defined as

$$SSIM(I, Seg) = \frac{(2\mu_1\mu_{Seg} + c_1)(2\sigma_{1,Seg} + c_2)}{(\mu_I^2 + \mu_{Seg}^2 + c1)(\sigma_I^1 + \sigma_{Seg}^2 + c2)} \quad (37)$$

where μ_I and μ_{Seg} are the mean intensities of the original image I and segmented image Seg, respectively, and σ_I and σ_{Seg} are their respective standard deviations. $\sigma_{I,Seg}$ is the covariance of the original and segmented images, and c1 and c2 are two constants.

The **FSIM** measures the similarities in the mapped features. The FSIM mainly depends on the phase congruency (PC) and gradient magnitude (GM). The PC is a new measure applied to the features of an image. The GM computes the image gradient, as traditionally done in digital image processing. The similarity between the two images was first obtained as

$$S_{PC} = \frac{2PC_1PC_2 + T_1}{PC_1^2 + PC_2^2 + T_1} \quad (38)$$

where T_1 is a positive constant that increases the stability of S_{PC}. PC_1 and PC_2 are the PCs of the original and segmented images, respectively, and SG is the similarity between G_1 and G_2, which is computed as:

$$S_G = \frac{2G_1G_2 + T_2}{G_1^2 + G_2^2 + T_2} \quad (39)$$

Here, G_1 and G_2 are the gradients of the original and segmented images, respectively, and T_2 is a positive constant that depends on the dynamic range of GM values. From Eqs. (38) and (39), the similarity is computed as

$$S_L(x) = [S_{PC}(x)]^{\alpha}[S_G(x)]^{\beta} \tag{40}$$

The parameters α and β adjust the relative importances of the PC and GM features. Note that high values of fitness, PSNR, SSIM, and FSIM indicate a high-performing algorithm .

2) NON-PARAMETRIC STATISTICAL TESTS

The **Wilcoxon rank-sum test** rank-sum test is a non-parametric measure that analyzes the results of pairs of methods. The null hypothesis implies that the ranks of the results of the comparative methods are not significantly different. The alternative hypothesis examines whether the results of the comparative methods can be distinguished by rank. The Wilcoxon rank-sum was calculated at the 5% significance level. The significance levels (P) and hypothesis (H) values in terms of fitness obtained with Otsu's method are shown in Table 19. If $P > 0.05$ or $H = 0$, then the null hypothesis is accepted, whereas if $P < 0.05$ or $H = 1$, the alternative hypothesis is accepted.

The **Friedman mean rank test** is another non-parametric analysis that compares three or more matched groups. In the present study, the Friedman mean rank was applied for checking the performances of the competitive algorithms. The Friedman statistic determines the mean ranked value. Whether the critical values reach the assigned significance level is evaluated using Friedman's statistics, and whether the null hypothesis is accepted or declined is then judged.

F. ANALYSIS OF MULTI-THRESHOLDING IMAGE SEGMENTATION RESULTS

This section reports and discusses the experimental results of multilevel level thresholding Otsu and Kapur objective functions described above to tackle multilevel thresholding image-segmentation problems.

1) MULTI-THRESHOLDING SEGMENTATION EXPERIMENTS OF OTSU AND KAPUR METHODS IN TABLES AND FIGURES

Image-segmentation experiments were performed using Otsu and Kapur methods as the objective functions in two separate experiments on a set of ten benchmark images at four thresholding levels (Level = 2, 3, 4, and 5). In total, 40 cases were tested. Fig. 7 illustrates a set of benchmark images with their respective histograms namely Cameraman, Lena, Baboon, Hunter, Airplane, Pepper, Living room, Woman, Bridge, and Butter-Fly. Figures (12, 13, TSA-LEO Otsu) and (12, 13, TSA-LEO Kapur) show the segmented image results with their respective selected thresholds over histograms obtained from applying the proposed TSA–LEO with Otsu and Kapur methods. In addition, Tables (14, TSA-LEO OTSU) and (6, TSA-LEO Kapur) show the optimal thresholds obtained from TSA–LEO and other competitors under the condition of level = 2, 3, 4, and 5 for Otsu and Kapur objective functions. Tables(15, 16, 17, 18, TSA-LEO Otsu) and (7, 8, 9, and 10, TSA-LEO Kapur) represent the fitness, PSNR, SSIM, and SSIM results, for Otsu and Kapur methods respectively. Moreover, Tables (19 and 19) show the results of the Wilcoxon rank-sum test of TSA–LEO and other seven algorithms with Otsu and Kapur methods. Table.20 also provides convergence curves on Otsu and Kapur objective functions for samples of test images on various thresholds for the proposed TSA-LEO and other competitive algorithm.

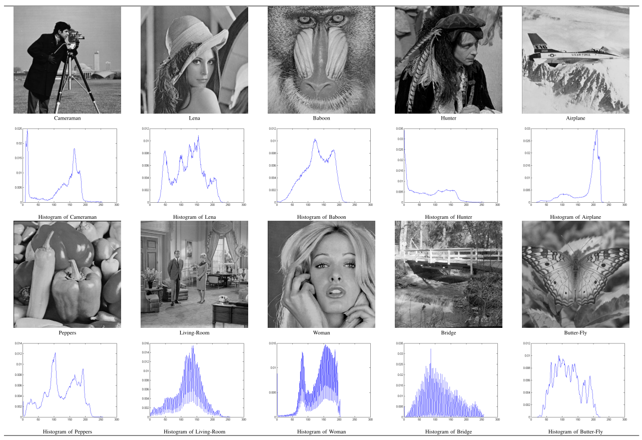

FIGURE 7. Set of benchmark images and relative histograms.

2) MULTI-THRESHOLDING SEGMENTATION ANALYSIS OF OTSU AND KAPUR METHODS

From the optimal thresholds selected on the basis of Otsu and Kapur objective functions, we can conclude that the Kapur segmentation process is more decentralized and has wider coverage, such as the optimal threshold value of the test image, namely, Cameraman at Level = 4 is 22, 59, 98, 145, 196, as shown in Table 6, and 36, 82, 122, 149, 173 shown in Table 14. Notably, the optimal thresholds for Otsu's objective function are closer than Kapur's objective function, revealing that segmentation based on Kapur's objective function is better than Otsu's objective function, which is also evident from the results of the segmented images based on Otsu and Kapur objective functions in Figures.(12, 13, 4, and 5). In terms of quality metrics (PSNR, SSIM, and FSIM), the quality of the segmented image based on Kapur's is better than Otsu's objective function. For example, the PSNR value of starfish in Test 9 image at Level = 4 is 1.90E + 01 in Table 8 and $1.89E + 01$ in Table 16, SSIM value is $8.70E - 01$ 8 and $8.46E - 01$ 16, FSIM value is $9.00E - 01$ in Table 8 and $8.86E - 01$ 16. The values of the Otsu-based method are smaller than those of Kapur's entropy-based method, and the segmentation effect in Tables. 4,5 is clearer than in Tables. 12,13, especially in the case with higher number of thresholds. Generally, in the given segmentation image and the same number of threshold levels, the method based on Kapur's is significantly better than Otsu-based method for the same optimization algorithm.

TABLE 6. Optimal thresholds obtained by Kapur's objective function.

Test Image	Level	MFO	WOA	SCA	SOA	BMO	TSA	CTSA	TSA-LEO
Test 1	2	128 196	128 196	128 196	127 195	128 196	123 190	128 196	128 196
	3	44 103 196	44 103 196	63 118 196	43 104 195	45 104 196	44 103 196	44 103 196	44 103 196
	4	42 96 145 196	44 96 146 196	42 96 145 196	38 93 143 194	43 96 145 196	43 96 146 196	44 96 146 196	44 96 146 196
	5	22 59 98 145 196	24 60 98 146 196	26 63 99 146 196	25 60 100 144 197	27 67 106 154 199	25 63 101 149 197	24 60 98 146 196	24 60 98 146 196
Test 2	2	96 163	96 163	96 163	95 163	96 163	96 163	96 163	96 163
	3	23 96 163	47 108 167	54 111 168	29 101 164	31 100 164	68 119 171	23 96 163	47 108 167
	4	23 80 125 173	23 79 124 173	24 81 125 173	22 75 121 170	23 80 125 173	37 85 128 174	23 80 125 173	23 79 124 173
	5	23 62 95 135 177	23 65 99 139 179	23 70 108 146 181	21 67 104 140 180	23 68 104 143 181	32 70 104 143 181	23 62 94 135 177	23 65 99 139 179
Test 3	2	79 143	79 143	79 143	79 143	79 143	79 143	79 143	79 143
	3	58 116 185	50 103 157	79 143 233	47 100 152	55 110 171	49 101 153	72 133 214	50 103 157
	4	46 99 152 233	40 87 133 197	48 100 152 233	37 87 139 214	42 90 138 205	34 77 119 171	49 101 153 233	40 87 133 197
	5	32 72 112 159 233	33 72 112 157 227	33 73 113 159 233	31 68 112 163 228	33 73 112 155 220	31 68 107 147 201	33 73 113 159 233	33 72 112 157 227
Test 4	2	91 179	91 179	91 179	90 178	91 179	91 179	91 179	91 179
	3	59 118 179	60 118 179	60 118 179	58 116 179	60 118 179	60 118 179	60 118 179	60 118 179
	4	44 90 133 180	44 89 133 180	44 90 134 181	43 87 132 180	45 90 134 181	44 90 134 181	45 90 134 181	44 89 133 180
	5	40 85 130 178 218	42 86 128 172 213	44 90 133 179 220	36 77 117 162 202	38 78 118 159 199	35 74 114 155 195	45 90 133 179 220	42 86 128 172 213
Test 5	2	70 171	70 171	70 171	70 171	70 171	70 171	70 171	70 171
	3	68 126 182	68 126 182	68 127 183	68 126 180	68 126 182	68 126 182	68 126 182	68 126 182
	4	67 125 181 232	66 116 165 211	63 121 177 227	64 116 165 215	67 122 175 223	66 115 164 210	68 126 182 232	66 116 165 211
	5	42 86 134 182 232	59 98 138 179 225	48 93 137 181 229	26 71 117 163 213	53 94 134 176 222	51 87 127 171 217	64 104 143 184 232	59 98 138 179 225
Test 6	2	66 143	66 143	66 143	66 142	66 143	66 143	66 143	66 143
	3	62 116 171	61 111 161	63 120 180	62 115 167	62 115 169	61 112 162	64 133 206 255	61 111 161
	4	61 111 161 227	61 111 161 225	61 111 161 227	60 108 161 225	61 111 160 225	57 104 156 222	62 112 162 227 255	61 111 161 225
	5	45 84 126 170 227	48 86 128 172 227	52 94 136 179 227	42 81 125 172 226	51 91 132 175 227	42 83 125 170 227	48 87 129 172 227 255	48 86 128 172 227
Test 7	2	94 175	92 173	93 174	90 173	93 174	93 174	94 175	92 173
	3	47 103 175	47 103 175	47 103 175	48 104 174	47 103 175	47 103 175	47 103 175	47 103 175
	4	46 98 149 197	46 97 148 195	47 100 152 197	46 96 144 191	47 99 150 196	46 97 148 196	47 98 149 197	46 97 148 195
	5	41 83 121 161 197	41 84 123 162 197	43 86 126 165 202	35 73 112 155 195	43 86 124 163 199	39 79 116 159 197	42 85 124 162 197	41 84 123 162 197
Test 8	2	125 203	125 203	125 203	125 203	125 203	108 189	125 203	125 203
	3	65 133 203	65 134 203	72 136 203	65 131 205	65 134 203	65 134 203	65 134 203	65 134 203
	4	65 112 154 203	65 113 155 203	65 115 157 203	63 111 155 204	65 113 155 203	65 112 154 203	65 113 155 203	65 113 155 203
	5	64 102 141 184 216	65 102 139 178 212	64 108 147 188 218	52 93 128 165 209	64 105 142 182 215	61 94 132 172 209	65 113 155 203 229	65 102 139 178 212
Test 9	2	94 171	95 172	94 171	96 173	93 172	94 171	94 171	95 172
	3	65 130 193	65 130 193	64 130 193	63 128 190	65 129 192	65 130 194	65 131 195	65 130 193
	4	53 100 148 198	53 102 149 199	52 101 149 199	51 100 148 199	53 100 149 199	52 100 148 198	53 102 151 199	53 102 149 199
	5	40 80 123 168 207	41 82 125 167 207	43 86 128 170 209	41 82 125 165 209	43 85 128 168 208	38 77 119 161 203	40 84 129 170 210	41 82 125 167 207
Test 10	2	124 222	122 217	124 222	124 222	124 222	97 159	124 222	122 217
	3	93 150 222	91 149 219	94 151 222	87 149 222	94 151 222	85 139 203	94 151 222	91 149 219
	4	58 108 155 222	72 114 156 222	58 108 154 220	47 101 155 223	74 115 157 222	59 106 150 212	20 94 151 222	72 114 156 222
	5	31 81 121 161 222	36 85 124 163 222	53 96 134 170 222	21 69 111 159 222	42 87 126 166 219	37 82 122 163 222	19 74 115 157 222	36 85 124 163 222

TABLE 7. Average and STD of Kapur's fitness obtained from all algorithms.

		MFO		WOA		SCA		SOA		BMO		TSA		CTSA		TSA-LEO	
Test Image	Level	Mean	STD	Mean	STD	Mean	STD	Mean	STD	Mean	STD	Mean	STD	Mean	STD	Mean	STD
Test 1	2	1.76E+01	3.17E-01	1.76E+01	2.23E-04	1.76E+01	5.60E-03	1.76E+01	4.59E-04	1.75E+01	3.17E-01	1.75E+01	4.43E-02	1.75E+01	3.13E-01	**1.76E+01**	7.21E-15
	3	2.20E+01	2.52E-02	2.20E+01	4.60E-02	2.20E+01	3.07E-02	2.20E+01	5.78E-03	2.20E+01	2.52E-02	2.19E+01	4.97E-02	2.20E+01	3.05E-02	**2.20E+01**	3.67E-13
	4	2.65E+01	6.21E-03	2.66E+01	1.01E-02	2.64E+01	1.08E-01	2.65E+01	4.43E-02	2.66E+01	6.21E-03	2.63E+01	4.00E-04	2.66E+01	5.06E-03	**2.66E+01**	1.20E-03
	5	3.05E+01	5.01E-02	3.05E+01	3.66E-02	3.01E+01	5.40E-01	3.05E+01	4.97E-02	3.05E+01	5.01E-02	3.02E+01	5.09E-02	3.05E+01	2.96E-02	**3.05E+01**	5.01E-02
Test 2	2	1.78E+01	1.38E-04	**1.78E+01**	0.00E+00	1.78E+01	2.85E-03	1.78E+01	3.72E-04	1.78E+01	1.38E-04	1.77E+01	3.10E-03	1.78E+01	8.76E-02	**1.78E+01**	0.00E+00
	3	**2.23E+01**	9.64E-02	2.21E+01	4.57E-02	2.21E+01	4.30E-02	2.21E+01	5.09E-02	2.22E+01	9.64E-02	2.22E+01	1.31E-02	2.21E+01	5.08E-02	2.21E+01	4.94E-02
	4	**2.66E+01**	1.65E-01	2.64E+01	1.65E-01	2.63E+01	1.22E-01	2.65E+01	3.12E-03	2.65E+01	2.30E-01	2.64E+01	2.90E-03	2.65E+01	8.69E-02	2.64E+01	1.65E-01
	5	3.04E+01	1.79E-01	3.03E+01	2.01E-01	2.97E+01	8.29E-01	3.04E+01	1.31E-02	**3.05E+01**	6.78E-02	3.02E+01	1.91E-02	3.03E+01	1.84E-01	3.03E+01	1.79E-01
Test 3	2	1.76E+01	0.00E+00	**1.76E+01**	0.00E+00	1.76E+01	1.34E-03	1.76E+01	4.98E-05	1.76E+01	8.34E-04	1.76E+01	4.80E-02	**1.76E+01**	0.00E+00	**1.76E+01**	0.00E+00
	3	**2.21E+01**	2.06E-01	2.21E+01	7.56E-03	2.21E+01	6.77E-03	2.21E+01	1.94E-03	2.21E+01	1.76E-03	2.20E+01	1.05E-01	2.21E+01	2.30E-04	2.21E+01	1.06E-04
	4	**2.65E+01**	9.15E-04	2.65E+01	7.22E-03	2.62E+01	9.57E-02	2.63E+01	1.04E-01	2.62E+01	3.45E-03	2.62E+01	1.70E-03	2.63E+01	1.22E-01	2.62E+01	9.35E-02
	5	3.05E+01	3.24E-03	**3.06E+01**	4.11E-02	3.00E+01	1.80E-01	3.03E+01	2.06E-01	3.01E+01	2.61E-01	3.02E+01	3.21E-02	3.06E+01	2.64E-02	3.03E+01	2.79E-01
Test 4	2	1.79E+01	1.32E-02	1.79E+01	5.28E-06	1.79E+01	2.88E-03	1.79E+01	9.15E-04	1.78E+01	1.08E-01	1.78E+01	1.75E-01	**1.79E+01**	3.60E-15	**1.79E+01**	3.60E-15
	3	2.26E+01	6.12E-02	2.26E+01	1.31E-03	2.26E+01	1.91E-02	2.26E+01	3.24E-03	2.26E+01	8.58E-03	2.25E+01	2.46E-01	2.26E+01	3.56E-04	**2.26E+01**	3.36E-05
	4	2.68E+01	1.83E-04	2.68E+01	4.72E-04	2.67E+01	4.80E-02	2.68E+01	1.32E-02	2.68E+01	6.80E-03	2.66E+01	1.50E-03	2.68E+01	1.17E-03	**2.68E+01**	4.98E-04
	5	3.07E+01	1.08E-03	**3.08E+01**	2.01E-02	3.05E+01	1.05E-01	3.07E+01	6.12E-02	3.07E+01	5.48E-02	3.05E+01	1.65E-01	3.08E+01	7.23E-02	3.08E+01	7.97E-02
Test 5	2	1.76E+01	1.61E-01	**1.76E+01**	1.08E-14	1.76E+01	1.67E-03	1.76E+01	1.83E-04	1.76E+01	3.29E-04	1.76E+01	1.79E-01	**1.76E+01**	1.08E-14	**1.76E+01**	1.08E-14
	3	2.24E+01	1.80E-14	2.24E+01	2.95E-04	2.23E+01	3.21E-02	2.24E+01	1.08E-03	2.24E+01	2.24E-03	2.23E+01	0.00E+00	2.24E+01	4.98E-04	**2.24E+01**	1.80E-14
	4	**2.68E+01**	1.87E-01	2.68E+01	1.43E-01	2.64E+01	1.75E-01	2.66E+01	1.61E-01	2.64E+01	8.29E-02	2.66E+01	2.06E-01	2.67E+01	2.34E-01	2.65E+01	1.87E-01
	5	3.07E+01	3.54E-01	**3.08E+01**	1.75E-01	3.00E+01	2.46E-01	3.05E+01	2.29E-01	3.05E+01	3.30E-01	3.04E+01	9.00E-04	3.08E+01	1.42E-01	3.06E+01	3.54E-01
Test 6	2	1.82E+01	0.00E+00	**1.82E+01**	0.00E+00	1.82E+01	1.55E-03	1.82E+01	6.98E-05	1.82E+01	7.19E-04	1.81E+01	3.20E-03	**1.82E+01**	0.00E+00	**1.82E+01**	0.00E+00
	3	2.26E+01	9.78E-04	**2.26E+01**	2.86E-03	2.26E+01	1.32E-02	2.26E+01	1.48E-03	2.26E+01	1.05E-03	2.25E+01	1.32E-02	2.26E+01	1.30E-03	2.26E+01	9.78E-04
	4	2.70E+01	1.50E-01	2.70E+01	4.56E-02	2.68E+01	9.20E-02	2.70E+01	6.36E-02	2.67E+01	1.35E-01	2.68E+01	6.12E-02	**2.70E+01**	5.96E-03	2.70E+01	1.50E-01
	5	3.09E+01	1.20E-02	3.10E+01	4.68E-02	3.07E+01	1.57E-01	3.10E+01	9.52E-02	3.10E+01	2.15E-01	3.07E+01	2.00E-04	3.11E+01	1.80E-02	**3.11E+01**	1.20E-02
Test 7	2	1.79E+01	2.38E-04	1.79E+01	2.29E-04	1.79E+01	4.81E-03	1.79E+01	3.55E-04	1.79E+01	2.33E-03	1.78E+01	1.10E-03	**1.79E+01**	8.11E-05	1.79E+01	2.38E-04
	3	2.24E+01	1.08E-14	2.24E+01	3.81E-03	2.24E+01	2.32E-02	2.24E+01	4.72E-03	2.24E+01	2.28E-03	2.23E+01	1.08E-01	2.24E+01	1.94E-03	**2.24E+01**	1.08E-14
	4	2.66E+01	8.24E-03	2.66E+01	7.21E-03	2.65E+01	4.46E-02	2.66E+01	1.09E-02	2.66E+01	2.48E-02	2.65E+01	8.60E-03	2.66E+01	7.81E-03	**2.66E+01**	8.24E-03
	5	3.04E+01	1.35E-02	3.05E+01	3.80E-02	3.03E+01	1.01E-01	3.04E+01	6.19E-02	3.05E+01	2.54E-02	3.03E+01	6.80E-03	3.05E+01	8.40E-03	**3.05E+01**	1.35E-02
Test 8	2	**1.78E+01**	7.21E-15	1.77E+01	7.03E-03	1.77E+01	1.96E-02	1.77E+01	6.28E-03	1.72E+01	5.14E-01	1.77E+01	5.48E-02	1.77E+01	5.71E-02	1.77E+01	7.21E-15
	3	**2.24E+01**	1.08E-14	2.22E+01	1.81E-01	2.22E+01	9.78E-02	2.23E+01	1.83E-02	2.23E+01	4.02E-01	2.21E+01	3.00E-04	2.24E+01	5.92E-03	2.24E+01	1.08E-14
	4	2.63E+01	2.74E-01	2.63E+01	1.61E-01	2.60E+01	4.80E-01	2.63E+01	4.16E-02	2.64E+01	3.39E-01	2.60E+01	2.20E-03	2.64E+01	1.41E-02	**2.64E+01**	8.08E-03
	5	2.99E+01	6.41E-04	2.99E+01	1.80E-01	2.89E+01	9.80E-01	2.98E+01	2.74E-01	**3.01E+01**	1.49E-01	2.97E+01	8.29E-02	2.99E+01	2.66E-01	3.01E+01	3.90E-02
Test 9	2	1.57E+01	1.00E-02	1.57E+01	7.23E-05	1.57E+01	2.70E-03	1.57E+01	6.41E-04	1.57E+01	3.70E-03	1.57E+01	3.30E-01	**1.57E+01**	2.64E-05	1.57E+01	5.54E-05
	3	1.95E+01	2.15E-02	1.95E+01	6.45E-03	1.95E+01	2.16E-02	1.95E+01	1.00E-02	1.95E+01	8.38E-03	1.94E+01	7.00E-04	1.95E+01	5.37E-03	**1.95E+01**	5.90E-03
	4	2.28E+01	5.04E-02	2.29E+01	1.14E-02	2.28E+01	4.00E-02	2.28E+01	2.15E-02	2.28E+01	1.95E-02	2.27E+01	1.00E-03	2.29E+01	9.48E-03	**2.29E+01**	9.37E-03
	5	2.58E+01	2.83E-04	2.59E+01	1.39E-02	2.55E+01	6.88E-01	2.59E+01	5.04E-02	2.59E+01	2.87E-02	2.57E+01	5.60E-03	2.59E+01	1.55E-02	**2.59E+01**	1.45E-02
Test 10	2	1.77E+01	8.28E-02	1.77E+01	3.63E-03	1.76E+01	2.27E-02	1.72E+01	2.83E-04	**2.63E+01**	1.61E-01	1.77E+01	3.07E-02	1.72E+01	3.60E-15	1.75E+01	1.49E-01
	3	2.24E+01	1.08E-01	2.23E+01	2.07E-02	2.22E+01	1.87E-01	2.16E+01	8.28E-02	**2.99E+01**	1.80E-01	2.22E+01	1.08E-01	2.15E+01	1.74E-01	2.23E+01	2.36E-01
	4	**2.65E+01**	3.10E-04	2.65E+01	1.47E-01	2.61E+01	2.40E-01	2.55E+01	1.08E-01	1.57E+01	7.23E-05	2.62E+01	5.40E-01	2.56E+01	1.09E-01	2.65E+01	3.10E-04
	5	3.05E+01	1.39E-01	3.03E+01	9.29E-02	2.95E+01	5.48E-01	2.95E+01	1.93E-01	1.95E+01	6.45E-03	3.00E+01	2.90E-03	2.96E+01	3.38E-01	**3.05E+01**	1.39E-01
Fridman mean rank		4.4		5.58		1.99		3.91		4.43		4.35		5.09		6.26	
rank		5		2		8		7		4		6		3		1	

3) MULTI-THRESHOLDING SEGMENTATION ANALYSIS OF TSA-LEO AND OTHER SEVEN OPTIMIZATION ALGORITHMS

Fitness results in the basis of Kapur's objective function shown in Table 7 confirmed the superiority of TSA–LEO over other algorithms. TSA–LEO ranked first with 21 higher cases (52.5%); MFO and WOA ranked second with 8 higher fitness cases (20%); and CTSA ranked third with 7 higher cases (17.5%). Moreover, BMO ranked fourth with only 4 higher fitness cases (10%). All the remaining algorithms have no higher fitness cases. Regarding PSNR results

TABLE 8. Average and STD of PSNR based Kapur's objective function obtained from all algorithms.

		MFO		WOA		SCA		SOA		BMO		TSA		CTSA		TSA-LEO	
Test Image	**Level**	**Mean**	**STD**	**Mean**	**STD**	**Mean**	**STD**	**Mean**	**STD**	**Mean**	**STD**	**Mean**	**STD**	**Mean**	**STD**	**Mean**	**STD**
Test 1	**2**	1.36E+01	9.01E-15	1.36E+01	3.10E-02	1.36E+01	2.18E-01	1.37E+01	6.71E-02	1.36E+01	9.01E-15	13.4148	8.52E-02	1.37E+01	1.44E-01	**1.38E+01**	8.15E-01
	3	1.45E+01	5.41E-15	**1.56E+01**	1.90E+00	1.45E+01	5.47E-01	1.44E+01	1.53E-01	1.45E+01	5.41E-15	11.96899	3.088276	1.48E+01	1.24E+00	1.47E+01	1.02E+00
	4	2.02E+01	2.65E-03	**2.02E+01**	3.63E-02	1.94E+01	7.45E-01	2.00E+01	1.58E-01	2.02E+01	2.25E-02	12.44735	3.78E+00	2.01E+01	6.63E-02	2.01E+01	4.65E-02
	5	2.08E+01	4.89E-01	**2.09E+01**	5.51E-01	2.01E+01	1.21E+00	2.08E+01	4.81E-01	2.07E+01	2.42E-02	13.25437	3.951965	2.07E+01	1.41E-01	2.08E+01	4.78E-01
Test 2	**2**	1.46E+01	5.41E-15	1.46E+01	5.41E-15	1.46E+01	8.65E-02	**1.46E+01**	1.80E-02	1.46E+01	5.41E-15	13.55247	1.10E+00	1.46E+01	1.67E-01	1.46E+01	7.50E-03
	3	1.70E+01	5.21E-01	**1.71E+01**	4.80E-01	1.63E+01	5.51E-01	1.70E+01	5.33E-01	1.62E+01	7.21E-15	11.69355	3.41E+00	1.70E+01	5.35E-01	1.70E+01	5.60E-01
	4	1.93E+01	5.59E-02	1.93E+01	6.22E-02	1.87E+01	4.25E-01	1.93E+01	2.09E-02	**1.93E+01**	3.60E-15	15.10784	3.832912	1.93E+01	3.79E-02	1.92E+01	2.02E-01
	5	2.07E+01	3.36E-01	2.07E+01	3.80E-01	1.99E+01	6.69E-01	**2.09E+01**	7.37E-02	2.09E+01	4.07E-02	16.83521	3.929955	2.08E+01	3.05E-01	2.09E+01	1.68E-01
Test 3	**2**	1.60E+01	3.60E-15	1.60E+01	3.60E-15	1.60E+01	2.78E-02	1.60E+01	5.89E-03	1.60E+01	3.60E-15	13.63084	2.28E+00	1.60E+01	3.60E-15	**1.60E+01**	5.70E-04
	3	1.88E+01	2.07E-03	1.86E+01	6.47E-01	1.86E+01	1.90E-01	1.87E+01	7.05E-02	1.76E+01	1.46E+00	15.33114	3.36E+00	**1.88E+01**	8.96E-03	1.87E+01	5.59E-02
	4	2.02E+01	6.01E-01	1.86E+01	2.44E-01	1.89E+01	1.24E+00	1.96E+01	1.25E+00	1.86E+01	1.37E-01	14.71321	4.069417	1.97E+01	9.59E-01	**2.04E+01**	2.81E-02
	5	2.13E+01	9.33E-01	2.04E+01	1.40E-01	1.99E+01	1.63E+00	2.04E+01	1.17E+00	2.04E+01	6.81E-02	14.86649	4.215337	2.03E+01	2.14E-01	**2.19E+01**	7.01E-01
Test 4	**2**	1.52E+01	9.01E-15	1.52E+01	3.00E-03	1.52E+01	4.94E-02	1.52E+01	3.22E-02	1.52E+01	9.01E-15	15.02778	0.186838	1.52E+01	9.01E-15	**1.57E+01**	1.04E+00
	3	1.85E+01	1.59E-04	1.85E+01	1.38E-02	1.84E+01	9.61E-02	1.85E+01	1.93E-02	**1.85E+01**	1.59E-04	15.2745	2.45E+00	1.85E+01	6.73E-03	1.85E+01	5.72E-02
	4	2.10E+01	8.99E-03	2.10E+01	7.11E-03	2.06E+01	2.81E-01	2.10E+01	7.85E-02	2.10E+01	9.05E-03	16.7778	2.963764	**2.10E+01**	2.61E-02	2.10E+01	3.53E-02
	5	2.18E+01	8.68E-01	2.10E+01	1.38E-01	2.17E+01	9.03E-01	2.22E+01	9.09E-01	2.11E+01	3.24E-01	17.94948	3.928128	2.17E+01	8.90E-01	**2.25E+01**	7.27E-01
Test 5	**2**	1.58E+01	9.01E-15	1.58E+01	9.01E-15	**1.58E+01**	1.42E-01	1.58E+01	2.15E-02	1.58E+01	9.01E-15	12.13135	4.50E+00	1.58E+01	9.01E-15	1.58E+01	7.46E-03
	3	1.88E+01	3.60E-15	1.88E+01	6.55E-03	1.87E+01	3.56E-01	**1.88E+01**	5.74E-02	1.88E+01	3.60E-15	12.66649	5.23E+00	1.88E+01	7.40E-03	1.88E+01	8.61E-03
	4	1.99E+01	7.11E-01	1.88E+01	4.62E-02	1.88E+01	1.19E+00	1.92E+01	1.20E+00	1.88E+01	4.70E-02	12.317	5.22E+00	1.88E+01	5.94E-01	**2.01E+01**	4.82E-01
	5	2.08E+01	6.14E-01	2.04E+01	3.55E-01	1.97E+01	1.33E+00	1.97E+01	1.08E+00	1.97E+01	7.32E-01	12.17215	5.379873	2.01E+01	5.53E-01	2.05E+01	5.40E-01
Test 6	**2**	**1.63E+01**	3.60E-15	**1.63E+01**	3.60E-15	1.63E+01	2.75E-02	1.63E+01	2.13E-03	1.63E+01	3.60E-15	14.0264	2.87E+00	**1.63E+01**	3.60E-15	1.63E+01	8.43E-03
	3	**1.83E+01**	3.53E-01	1.77E+01	9.80E-01	1.80E+01	7.81E-01	1.82E+01	4.90E-01	1.81E+01	7.44E-01	14.60448	3.09E+00	1.82E+01	5.98E-01	**1.84E+01**	1.72E-02
	4	1.87E+01	8.19E-01	1.83E+01	1.25E-01	1.80E+01	4.48E-01	1.82E+01	2.19E-01	1.84E+01	2.06E-02	13.18489	3.29489	1.83E+01	8.91E-02	**2.01E+01**	8.57E-01
	5	2.05E+01	5.25E-01	2.00E+01	7.50E-01	1.94E+01	7.44E-01	1.99E+01	5.38E-01	2.05E+01	8.30E-02	15.13551	3.691575	2.05E+01	2.35E-01	**2.06E+01**	5.67E-01
Test 7	**2**	1.46E+01	1.73E-02	1.46E+01	6.03E-02	1.46E+01	1.42E-01	1.46E+01	9.69E-02	1.46E+01	5.41E-15	13.7211	7.28E-01	1.46E+01	5.89E-03	1.46E+01	6.88E-02
	3	**1.71E+01**	3.60E-15	1.72E+01	1.16E-01	1.72E+01	3.18E-01	**1.72E+01**	1.33E-01	1.71E+01	3.60E-15	13.96877	3.18E+00	1.71E+01	8.05E-02	1.71E+01	7.40E-02
	4	1.92E+01	1.77E-01	1.90E+01	2.45E-01	1.92E+01	6.37E-01	1.92E+01	3.10E-01	1.91E+01	5.32E-02	14.05711	3.61E+00	1.91E+01	2.59E-01	**1.95E+01**	3.05E-01
	5	2.10E+01	3.66E-01	2.06E+01	1.01E+00	2.05E+01	7.39E-01	2.07E+01	4.04E-01	**2.11E+01**	1.21E-01	15.32838	4.16489	2.10E+01	1.83E-01	2.10E+01	2.56E-01
Test 8	**2**	1.22E+01	1.80E-15	1.22E+01	1.49E-01	1.21E+01	2.34E-01	1.22E+01	1.14E-01	1.22E+01	1.80E-15	12.13652	0.033664	1.20E+01	5.96E-01	**1.44E+01**	2.52E+00
	3	1.69E+01	0.00E+00	1.64E+01	7.73E-01	1.63E+01	4.74E-01	1.67E+01	1.79E-01	1.69E+01	1.36E-02	14.39967	3.28E+00	1.68E+01	6.35E-02	**1.71E+01**	7.62E-01
	4	2.01E+01	4.19E-03	1.98E+01	8.71E-01	1.89E+01	1.05E+00	1.97E+01	3.71E-01	2.01E+01	4.77E-02	15.21108	3.563423	1.99E+01	1.60E-01	**2.01E+01**	3.28E-01
	5	2.18E+01	6.05E-01	2.10E+01	1.27E+00	1.99E+01	1.52E+00	2.11E+01	9.50E-01	2.09E+01	1.10E+00	15.41984	3.59453	2.14E+01	8.76E-01	2.13E+01	9.61E-01
Test 9	**2**	**1.34E+01**	2.06E-01	1.34E+01	3.19E-01	1.34E+01	3.61E-01	1.35E+01	4.44E-01	1.35E+01	1.26E-14	12.28385	1.058047	1.35E+01	9.80E-02	**1.36E+01**	3.29E-01
	3	1.68E+01	9.29E-02	1.68E+01	1.46E-01	1.68E+01	2.63E-01	1.69E+01	2.04E-01	1.68E+01	5.71E-02	13.39903	2.44E+00	1.68E+01	1.20E-01	**1.69E+01**	1.23E-01
	4	1.89E+01	6.42E-02	1.89E+01	9.65E-02	1.88E+01	3.06E-01	1.89E+01	2.12E-01	1.90E+01	6.43E-02	13.43293	2.79E+00	**1.90E+01**	1.15E-01	1.90E+01	1.02E-01
	5	2.05E+01	1.98E-01	2.03E+01	2.43E-01	2.01E+01	5.95E-01	**2.05E+01**	2.58E-01	2.05E+01	1.55E-01	13.5548	2.62713	2.05E+01	1.99E-01	2.05E+01	2.43E-01
Test 10	**2**	1.24E+01	1.75E+00	1.08E+01	1.29E-01	1.09E+01	4.83E-01	1.55E+01	6.41E-03	1.08E+01	5.41E-15	10.76443	0.01149	**1.55E+01**	1.80E-15	**1.55E+01**	1.80E-15
	3	1.46E+01	1.01E+00	1.42E+01	4.34E-01	1.41E+01	9.98E-01	1.58E+01	4.09E-01	1.43E+01	7.00E-02	13.45779	0.930439	**1.63E+01**	1.16E+00	**1.63E+01**	1.16E+00
	4	1.78E+01	1.67E-02	1.75E+01	7.64E-01	1.63E+01	1.41E+00	1.82E+01	1.24E+00	1.74E+01	8.23E-01	14.49837	2.62E+00	**1.83E+01**	7.89E-01	**1.83E+01**	7.89E-01
	5	1.95E+01	4.18E-01	1.94E+01	6.97E-01	1.79E+01	1.36E+00	**2.00E+01**	6.43E-01	1.95E+01	4.07E-01	13.67651	3.829981	2.00E+01	5.22E-01	2.00E+01	5.22E-01

TABLE 9. Average and STD of SSIM based Kapur's objective function obtained from all algorithms.

		MFO		WOA		SCA		SOA		BMO		TSA		CTSA		TSA-LEO	
Test Image	**Level**	**Mean**	**STD**	**Mean**	**STD**	**Mean**	**STD**	**Mean**	**STD**	**Mean**	**STD**	**Mean**	**STD**	**Mean**	**STD**	**Mean**	**STD**
Test 1	2	6.63E-01	3.38E-16	6.63E-01	1.10E-03	6.63E-01	8.61E-03	6.64E-01	2.78E-03	6.63E-01	3.38E-16	6.55E-01	3.54E-03	6.71E-01	2.61E-02	**6.71E-01**	2.80E-02
	3	7.72E-01	5.63E-16	**7.76E-01**	6.22E-03	7.71E-01	8.73E-03	7.71E-01	3.43E-03	7.72E-01	5.63E-16	6.34E-01	1.54E-01	7.73E-01	5.37E-03	7.73E-01	3.77E-03
	4	8.33E-01	2.28E-04	8.33E-01	1.11E-03	8.27E-01	1.33E-02	**8.36E-01**	3.92E-03	8.34E-01	7.89E-04	6.34E-01	1.52E-01	8.35E-01	3.36E-03	8.34E-01	2.25E-03
	5	8.51E-01	4.60E-03	8.52E-01	3.88E-03	8.45E-01	2.37E-02	**8.53E-01**	5.48E-03	8.51E-01	1.17E-03	6.53E-01	1.59E-01	8.51E-01	5.28E-03	8.51E-01	4.44E-03
Test 2	2	6.16E-01	1.13E-16	6.16E-01	1.13E-16	**6.18E-01**	7.18E-03	6.16E-01	1.74E-03	6.16E-01	1.13E-16	5.92E-01	2.19E-02	6.16E-01	4.63E-03	6.16E-01	7.71E-04
	3	7.23E-01	9.58E-03	7.21E-01	8.92E-03	7.27E-01	1.65E-02	7.23E-01	1.09E-02	**7.38E-01**	3.38E-16	5.40E-01	1.96E-01	7.23E-01	1.03E-02	7.25E-01	1.23E-02
	4	8.15E-01	1.08E-02	8.14E-01	1.13E-02	8.11E-01	1.64E-02	**8.19E-01**	2.12E-03	8.18E-01	3.38E-16	6.91E-01	1.60E-01	8.17E-01	5.97E-03	8.12E-01	1.76E-02
	5	8.49E-01	1.85E-02	8.45E-01	1.97E-02	8.34E-01	1.67E-02	8.60E-01	2.58E-03	**8.61E-01**	1.37E-03	7.56E-01	1.23E-01	8.53E-01	1.80E-02	8.58E-01	6.58E-03
Test 3	2	8.23E-01	4.51E-16	8.23E-01	4.51E-16	8.23E-01	9.05E-04	8.23E-01	1.53E-04	8.23E-01	4.51E-16	6.96E-01	1.24E-01	8.23E-01	4.51E-16	**8.23E-01**	3.31E-05
	3	9.00E-01	1.85E-04	8.96E-01	1.82E-02	8.98E-01	2.99E-03	9.00E-01	8.37E-04	8.67E-01	4.16E-02	7.55E-01	1.64E-01	**9.00E-01**	3.48E-04	9.00E-01	5.24E-04
	4	9.22E-01	9.03E-03	8.98E-01	2.91E-03	8.95E-01	2.73E-02	9.12E-01	2.03E-02	8.98E-01	1.64E-03	7.08E-01	2.07E-01	9.15E-01	1.47E-02	**9.26E-01**	2.85E-04
	5	9.38E-01	1.37E-02	9.25E-01	2.12E-03	9.12E-01	3.20E-02	9.24E-01	1.78E-02	9.25E-01	1.07E-03	7.11E-01	2.08E-01	9.22E-01	4.18E-03	**9.48E-01**	1.03E-02
Test 4	2	6.10E-01	1.13E-16	6.10E-01	6.73E-04	6.07E-01	7.83E-03	6.11E-01	2.23E-03	6.10E-01	1.13E-16	6.01E-01	8.11E-03	6.10E-01	1.13E-16	**6.30E-01**	4.24E-02
	3	7.53E-01	3.73E-04	7.52E-01	4.07E-03	7.52E-01	1.66E-02	**7.59E-01**	7.06E-03	7.53E-01	3.73E-04	6.57E-01	7.27E-02	7.53E-01	3.03E-03	7.55E-01	4.79E-03
	4	8.38E-01	1.26E-03	8.37E-01	1.69E-03	**8.45E-01**	1.44E-02	8.44E-01	7.34E-03	8.39E-01	1.38E-03	7.30E-01	9.65E-02	8.37E-01	2.94E-03	8.41E-01	4.23E-03
	5	8.61E-01	2.51E-02	8.34E-01	1.18E-02	8.68E-01	3.35E-02	8.81E-01	2.80E-02	8.50E-01	9.08E-03	7.63E-01	1.26E-01	8.60E-01	2.34E-02	**8.82E-01**	1.87E-02
Test 5	2	8.77E-01	4.51E-16	**8.77E-01**	4.51E-16	8.76E-01	3.08E-03	8.77E-01	5.37E-04	**8.77E-01**	4.51E-16	7.18E-01	1.96E-01	8.77E-01	4.51E-16	8.77E-01	1.34E-04
	3	9.23E-01	7.89E-16	9.23E-01	4.45E-05	9.20E-01	4.71E-03	9.23E-01	7.51E-04	9.23E-01	7.89E-16	7.28E-01	1.96E-01	9.23E-01	1.45E-04	9.23E-01	1.26E-04
	4	9.39E-01	1.03E-02	9.24E-01	1.69E-03	9.20E-01	1.95E-02	9.30E-01	1.39E-02	9.23E-01	6.05E-04	7.13E-01	1.99E-01	9.26E-01	6.75E-03	**9.43E-01**	6.17E-03
	5	**9.50E-01**	5.14E-03	9.45E-01	4.11E-03	9.33E-01	2.14E-02	9.41E-01	9.92E-03	9.39E-01	7.90E-03	7.10E-01	2.20E-01	9.43E-01	5.43E-03	9.50E-01	5.34E-03
Test 6	2	7.58E-01	4.51E-16	7.58E-01	4.51E-16	7.58E-01	4.23E-03	7.58E-01	5.38E-04	7.58E-01	4.51E-16	6.89E-01	8.45E-02	7.58E-01	4.51E-16	**7.58E-01**	1.10E-03
	3	8.05E-01	8.14E-03	7.91E-01	2.28E-02	8.00E-01	1.98E-02	8.04E-01	1.05E-02	8.00E-01	1.55E-02	7.06E-01	8.85E-02	8.02E-01	1.47E-02	**8.07E-01**	6.99E-04
	4	8.15E-01	1.98E-02	8.06E-01	3.77E-03	8.04E-01	1.44E-02	8.04E-01	6.87E-03	8.07E-01	7.75E-04	6.67E-01	9.95E-02	8.06E-01	3.10E-03	**8.51E-01**	2.09E-02
	5	8.57E-01	1.42E-02	8.41E-01	2.04E-02	8.45E-01	1.55E-02	8.58E-01	7.31E-03	8.62E-01	5.94E-04	7.35E-01	1.15E-01	8.60E-01	5.26E-03	**8.62E-01**	1.23E-02
Test 7	2	6.90E-01	5.00E-03	6.85E-01	2.36E-03	6.88E-01	4.08E-03	6.88E-01	4.86E-03	6.84E-01	4.51E-16	6.46E-01	3.36E-02	6.84E-01	1.70E-03	**6.92E-01**	3.66E-03
	3	8.24E-01	6.76E-16	8.24E-01	1.41E-03	8.22E-01	6.46E-03	**8.25E-01**	2.51E-03	8.24E-01	6.76E-16	6.84E-01	1.54E-01	8.24E-01	7.25E-04	8.24E-01	5.87E-04
	4	8.65E-01	4.54E-03	8.60E-01	5.06E-03	8.65E-01	1.63E-02	8.67E-01	7.25E-03	8.63E-01	1.15E-03	6.76E-01	1.60E-01	8.62E-01	5.67E-03	**8.73E-01**	7.78E-03
	5	9.05E-01	7.44E-03	8.96E-01	2.09E-02	8.96E-01	1.53E-02	9.01E-01	5.99E-03	**9.08E-01**	1.58E-03	7.23E-01	1.63E-01	9.05E-01	2.52E-03	9.06E-01	3.69E-03
Test 8	2	5.90E-01	1.13E-16	5.84E-01	1.41E-02	5.77E-01	2.48E-02	5.86E-01	1.30E-02	5.90E-01	1.13E-16	5.82E-01	2.82E-03	5.87E-01	7.69E-03	**7.09E-01**	1.23E-01
	3	8.34E-01	5.63E-16	8.03E-01	4.43E-02	8.14E-01	2.34E-02	8.34E-01	5.47E-03	8.34E-01	4.39E-04	7.46E-01	1.19E-01	8.32E-01	4.30E-03	**8.37E-01**	1.55E-02
	4	9.00E-01	1.37E-04	8.89E-01	2.68E-02	8.76E-01	2.36E-02	8.95E-01	5.62E-03	8.99E-01	8.57E-04	7.76E-01	1.16E-01	8.97E-01	4.62E-03	**9.01E-01**	4.95E-03
	5	**9.26E-01**	9.55E-03	9.13E-01	2.46E-02	8.95E-01	2.56E-02	9.18E-01	1.44E-02	9.12E-01	1.70E-02	7.74E-01	1.10E-01	9.21E-01	1.35E-02	9.19E-01	1.47E-02
Test 9	2	5.81E-01	1.64E-02	5.80E-01	2.52E-02	5.78E-01	2.83E-02	5.86E-01	3.48E-02	5.87E-01	0.00E+00	5.17E-01	5.99E-02	5.86E-01	7.83E-03	**5.94E-01**	2.56E-02
	3	7.88E-01	5.35E-03	7.87E-01	6.18E-03	7.86E-01	1.31E-02	7.91E-01	9.45E-03	7.88E-01	1.92E-03	6.36E-01	1.22E-01	7.87E-01	5.38E-03	**7.92E-01**	6.68E-03
	4	8.68E-01	2.04E-03	8.67E-01	3.02E-03	8.62E-01	1.04E-02	8.68E-01	5.41E-03	8.68E-01	2.11E-03	6.44E-01	1.45E-01	8.67E-01	3.37E-03	**8.70E-01**	3.41E-03
	5	9.06E-01	7.32E-03	9.01E-01	5.86E-03	8.95E-01	1.68E-02	**9.09E-01**	7.08E-03	9.08E-01	2.88E-03	6.55E-01	1.48E-01	9.05E-01	5.57E-03	9.08E-01	8.09E-03
Test 10	2	5.11E-01	1.18E-01	4.03E-01	1.08E-02	4.08E-01	4.12E-02	7.12E-01	1.87E-04	4.05E-01	2.25E-16	3.99E-01	2.15E-04	**7.12E-01**	0.00E+00	7.12E-01	1.87E-04
	3	6.52E-01	4.85E-02	6.31E-01	2.86E-02	6.33E-01	5.88E-02	7.37E-01	2.49E-02	6.39E-01	4.78E-03	5.96E-01	4.57E-02	**7.51E-01**	6.22E-02	7.37E-01	2.49E-02
	4	8.08E-01	6.97E-04	7.97E-01	2.50E-02	7.59E-01	6.45E-02	**8.44E-01**	3.94E-02	7.96E-01	2.25E-02	6.74E-01	1.30E-01	**8.54E-01**	2.88E-02	8.44E-01	8.54E-01
	5	8.69E-01	1.34E-02	**8.55E-01**	2.32E-02	8.20E-01	5.15E-02	8.97E-01	1.46E-02	**8.71E-01**	1.20E-02	6.20E-01	2.18E-01	8.93E-01	1.17E-02	**8.97E-01**	8.97E-01

shown in Table 8, the proposed TSA-LEO ranked first with 19 higher cases (47.5%) and CTSA ranked second with 7 higher cases (17.5%). Besides, SOA ranked third with 6 higher cases (15%). WOA ranked fourth with 5 higher best fitness cases (12.5%). MFO and BMO ranked fifth with 3 higher cases representing (7.5%) of overall higher cases. Finally, TSA took the last rank without any higher case. The proposed TSA-LEO ranked first in the SSIM results represented in Table 9, with 21 higher cases representing (52.5%) of overall test cases. However, SOA ranked second with 7 higher cases (17.5%). BMO gained third place with only 5 higher cases representing (12.5%) from overall cases.

TABLE 10. Average and STD of FSIM based Kapur's objective function obtained from all algorithms.

		MFO		WOA		SCA		SOA		BMO		TSA		CTSA		TSA-LEO	
Test Image	**Level**	**Mean**	**STD**	**Mean**	**STD**	**Mean**	**STD**	**Mean**	**STD**	**Mean**	**STD**	**Mean**	**STD**	**Mean**	**STD**	**Mean**	**STD**
Test 1	**2**	6.78E-01	3.38E-16	6.77E-01	7.06E-04	6.77E-01	5.76E-03	6.78E-01	1.63E-03	6.78E-01	3.38E-16	3.38E-16	6.85E-01	**6.86E-01**	2.68E-02	6.85E-01	2.60E-02
	3	**7.99E-01**	2.25E-16	7.94E-01	8.65E-03	7.97E-01	3.37E-03	7.98E-01	1.25E-03	7.99E-01	2.25E-16	1.90E-05	7.99E-01	7.98E-01	3.60E-03	7.99E-01	3.66E-03
	4	8.41E-01	2.55E-04	8.42E-01	1.48E-03	8.38E-01	1.64E-02	**8.46E-01**	6.49E-03	8.43E-01	1.29E-03	9.31E-04	8.43E-01	8.45E-01	5.22E-03	8.43E-01	3.90E-03
	5	8.62E-01	5.29E-03	8.64E-01	5.75E-03	8.57E-01	2.82E-02	**8.65E-01**	7.72E-03	8.62E-01	1.90E-03	6.14E-04	8.63E-01	8.64E-01	6.69E-03	8.63E-01	5.06E-03
Test 2	**2**	6.74E-01	4.51E-16	6.74E-01	4.51E-16	6.74E-01	3.54E-03	**6.74E-01**	6.54E-04	6.74E-01	4.51E-16	3.38E-16	6.74E-01	6.73E-01	6.88E-03	6.74E-01	2.45E-04
	3	7.29E-01	2.47E-02	**7.32E-01**	2.30E-02	7.00E-01	2.37E-02	7.28E-01	2.51E-02	6.91E-01	2.25E-16	2.25E-16	7.27E-01	7.28E-01	2.53E-02	7.27E-01	2.53E-02
	4	7.65E-01	1.02E-02	7.65E-01	1.02E-02	7.63E-01	1.25E-02	7.62E-01	1.02E-03	7.62E-01	3.38E-16	4.24E-04	7.67E-01	7.62E-01	5.47E-03	**7.67E-01**	1.18E-02
	5	8.13E-01	6.64E-03	**8.15E-01**	7.67E-03	7.96E-01	1.53E-02	8.14E-01	3.82E-03	8.13E-01	2.18E-03	7.24E-04	8.14E-01	8.14E-01	4.39E-03	8.14E-01	5.06E-03
Test 3	**2**	8.65E-01	4.51E-16	8.65E-01	4.51E-16	8.64E-01	1.46E-03	**8.65E-01**	1.62E-04	8.65E-01	4.51E-16	1.13E-16	8.65E-01	8.65E-01	5.63E-16	8.65E-01	2.33E-05
	3	**9.06E-01**	1.45E-04	9.04E-01	9.62E-03	9.03E-01	2.42E-03	9.06E-01	8.97E-04	8.85E-01	2.88E-02	3.12E-04	9.06E-01	9.06E-01	2.93E-04	9.06E-01	6.88E-04
	4	9.23E-01	7.01E-03	9.04E-01	2.78E-03	9.02E-01	2.37E-02	9.14E-01	1.67E-02	9.04E-01	1.58E-03	7.64E-04	9.25E-01	9.17E-01	1.19E-02	**9.25E-01**	5.29E-04
	5	9.39E-01	1.52E-02	9.26E-01	2.58E-03	9.19E-01	3.18E-02	9.25E-01	1.94E-02	9.25E-01	1.09E-03	8.76E-04	9.50E-01	9.23E-01	3.82E-03	**9.50E-01**	1.15E-02
Test 4	**2**	7.15E-01	0.00E+00	7.15E-01	3.61E-04	7.13E-01	5.27E-03	7.15E-01	1.47E-03	7.15E-01	0.00E+00	4.51E-16	7.29E-01	7.15E-01	0.00E+00	**7.29E-01**	2.89E-02
	3	8.24E-01	3.49E-05	8.23E-01	1.49E-03	8.21E-01	4.60E-03	**8.25E-01**	2.02E-03	8.24E-01	3.49E-05	5.63E-16	8.24E-01	8.24E-01	1.11E-03	8.24E-01	7.58E-04
	4	8.89E-01	8.00E-04	8.89E-01	7.57E-04	8.87E-01	7.26E-03	**8.92E-01**	3.04E-03	8.89E-01	7.98E-04	3.43E-04	8.91E-01	8.89E-01	1.38E-03	8.91E-01	2.19E-03
	5	9.06E-01	1.82E-02	8.88E-01	5.70E-03	9.06E-01	2.10E-02	9.18E-01	1.93E-02	8.96E-01	5.89E-03	2.40E-04	9.22E-01	9.05E-01	1.72E-02	**9.22E-01**	1.40E-02
Test 5	**2**	7.91E-01	4.51E-16	**7.91E-01**	4.51E-16	7.90E-01	2.87E-03	7.91E-01	3.62E-04	7.91E-01	4.51E-16	2.25E-16	7.91E-01	**7.91E-01**	4.51E-16	7.91E-01	2.58E-04
	3	8.61E-01	5.63E-16	**8.61E-01**	2.73E-04	8.58E-01	4.24E-03	8.61E-01	6.36E-04	8.61E-01	5.63E-16	1.29E-03	8.61E-01	8.61E-01	3.92E-04	8.61E-01	2.14E-04
	4	8.88E-01	1.73E-02	8.61E-01	1.11E-03	8.63E-01	2.49E-02	8.74E-01	2.16E-02	8.61E-01	6.02E-04	1.45E-03	8.93E-01	8.64E-01	1.07E-02	**8.93E-01**	1.31E-02
	5	**9.06E-01**	9.51E-03	8.96E-01	8.63E-03	8.79E-01	2.25E-02	8.88E-01	1.64E-02	8.83E-01	1.84E-02	8.57E-04	9.02E-01	8.94E-01	9.71E-03	9.02E-01	1.04E-02
Test 6	**2**	7.21E-01	3.38E-16	7.21E-01	3.38E-16	7.21E-01	1.57E-03	7.21E-01	1.83E-04	7.21E-01	3.38E-16	3.38E-16	7.22E-01	7.21E-01	2.25E-16	**7.22E-01**	4.30E-04
	3	7.78E-01	9.82E-03	7.62E-01	2.74E-02	7.72E-01	2.16E-02	7.76E-01	1.31E-02	7.72E-01	1.98E-02	3.38E-16	7.80E-01	7.75E-01	1.68E-02	**7.80E-01**	7.69E-04
	4	7.85E-01	1.69E-02	7.81E-01	2.50E-03	7.69E-01	1.16E-02	7.75E-01	9.80E-03	7.80E-01	6.47E-04	2.54E-04	8.15E-01	7.80E-01	2.57E-03	**8.15E-01**	1.69E-02
	5	8.22E-01	6.93E-03	8.14E-01	1.15E-02	8.05E-01	9.98E-03	8.12E-01	9.51E-03	8.24E-01	1.11E-03	3.92E-04	8.26E-01	8.21E-01	2.37E-03	**8.26E-01**	1.25E-02
Test 7	**2**	7.23E-01	5.77E-03	7.17E-01	2.76E-03	7.22E-01	5.53E-03	7.21E-01	5.97E-03	7.16E-01	5.63E-16	4.51E-16	7.26E-01	7.16E-01	1.96E-03	**7.26E-01**	4.61E-03
	3	7.99E-01	4.51E-16	8.00E-01	2.83E-03	**8.01E-01**	8.67E-03	8.01E-01	3.89E-03	7.99E-01	4.51E-16	1.41E-05	7.99E-01	7.99E-01	1.90E-03	7.99E-01	1.63E-03
	4	8.56E-01	4.28E-03	8.53E-01	2.91E-03	8.57E-01	1.23E-02	8.58E-01	5.90E-03	8.54E-01	3.56E-04	2.29E-04	8.64E-01	8.54E-01	4.10E-03	**8.64E-01**	7.83E-03
	5	9.00E-01	8.77E-03	8.92E-01	2.18E-02	8.87E-01	1.35E-02	8.96E-01	8.11E-03	**9.03E-01**	2.43E-03	1.07E-03	9.00E-01	9.01E-01	3.31E-03	9.00E-01	5.50E-03
Test 8	**2**	6.48E-01	1.13E-16	6.46E-01	5.33E-03	6.43E-01	8.61E-03	6.46E-01	4.43E-03	6.48E-01	1.13E-16	2.25E-16	6.92E-01	6.42E-01	1.63E-02	**6.92E-01**	5.47E-02
	3	7.46E-01	4.51E-16	7.46E-01	9.86E-03	7.36E-01	9.99E-03	7.45E-01	2.10E-03	7.46E-01	2.61E-04	1.52E-04	7.51E-01	7.46E-01	1.66E-03	**7.51E-01**	2.15E-02
	4	8.37E-01	4.81E-04	8.35E-01	7.86E-03	8.14E-01	2.58E-02	8.30E-01	1.16E-02	8.37E-01	1.63E-03	1.04E-03	8.38E-01	8.36E-01	4.51E-03	**8.38E-01**	8.42E-03
	5	**8.79E-01**	1.53E-02	8.67E-01	2.82E-02	8.35E-01	3.40E-02	8.67E-01	2.51E-02	8.56E-01	2.76E-02	9.60E-04	8.67E-01	8.72E-01	2.11E-02	8.67E-01	2.50E-02
Test 9	**2**	7.60E-01	5.19E-03	7.59E-01	6.38E-03	7.57E-01	6.96E-03	7.59E-01	6.83E-03	7.63E-01	2.25E-16	4.53E-05	7.64E-01	7.62E-01	2.47E-03	**7.64E-01**	3.65E-03
	3	8.47E-01	1.63E-03	8.47E-01	3.06E-03	8.44E-01	5.35E-03	8.46E-01	4.28E-03	8.48E-01	6.89E-04	2.03E-06	8.48E-01	8.47E-01	2.36E-03	**8.48E-01**	2.00E-03
	4	9.00E-01	5.75E-04	8.99E-01	1.38E-03	8.91E-01	5.17E-03	8.97E-01	2.51E-03	9.00E-01	3.50E-04	1.05E-03	9.00E-01	8.99E-01	1.12E-03	**9.00E-01**	1.12E-03
	5	**9.26E-01**	1.06E-03	9.24E-01	2.65E-03	9.11E-01	1.07E-02	9.23E-01	2.65E-03	9.25E-01	1.33E-03	1.05E-03	9.25E-01	9.23E-01	1.93E-03	9.25E-01	1.74E-03
Test 10	**2**	6.86E-01	4.35E-02	6.46E-01	4.78E-03	6.46E-01	1.55E-02	7.45E-01	4.33E-04	6.47E-01	1.13E-16	5.63E-16	7.45E-01	**7.45E-01**	1.13E-16	7.45E-01	4.33E-04
	3	7.40E-01	2.21E-02	7.32E-01	4.80E-03	7.24E-01	2.25E-02	7.48E-01	1.41E-02	7.34E-01	1.05E-03	3.20E-04	7.48E-01	**7.56E-01**	2.12E-02	7.48E-01	1.41E-02
	4	**8.11E-01**	2.37E-04	8.02E-01	2.15E-02	7.61E-01	3.30E-02	8.03E-01	2.74E-02	7.95E-01	2.45E-02	5.35E-04	8.03E-01	7.98E-01	1.78E-02	8.03E-01	2.74E-02
	5	8.41E-01	8.94E-03	**8.46E-01**	9.31E-03	7.99E-01	3.05E-02	8.42E-01	1.30E-02	8.39E-01	9.03E-03	5.26E-04	8.42E-01	8.39E-01	1.41E-02	8.42E-01	1.30E-02

TABLE 11. Comparison of the p-values obtained from the Wilcoxon signed-rank test between the pairs of TSA–LEO vs. MFO, TSA–LEO vs. WOA, TSA–LEO vs. SCA, TSA–LEO vs. SOA, TSA–LEO vs. BMO, TSA–LEO vs. TSA, and TSA–LEO vs. CTSA for Kapur's method in terms of Fitness results.

		MFO		WOA		SCA		SOA		BMO		TSA		CTSA	
Test Image	**Level**	**P**	**H**	**P**	**H**	**P**	**H**	**P**	**H**	**P**	**H**	**P**	**H**	**P**	**H**
Test 1	**2**	1.04E-16	1	3.31E-01	0	8.37E-12	1	1.45E-06	1	8.24E-15	1	8.37E-12	1	4.24E-02	1
	3	3.89E-16	1	1.95E-07	1	4.07E-14	1	1.25E-11	1	1.96E-03	1	4.07E-14	1	6.48E-08	1
	4	1.99E-02	1	8.31E-10	1	3.02E-14	1	5.36E-14	1	1.87E-12	1	3.02E-14	1	3.10E-13	1
	5	8.55E-06	1	7.89E-07	1	7.09E-13	1	4.49E-08	1	1.07E-01	0	7.09E-13	1	1.59E-07	1
Test 2	**2**	1.04E-16	1	NaN	0	1.52E-14	1	1.79E-05	1	1.43E-15	1	1.52E-14	1	3.31E-01	0
	3	1.29E-14	1	6.10E-02	0	6.66E-01	0	7.80E-05	1	2.01E-01	0	6.66E-01	0	6.53E-03	1
	4	6.80E-14	1	2.20E-01	0	7.49E-09	1	2.50E-08	1	4.98E-06	1	7.49E-09	1	7.64E-08	1
	5	5.63E-13	1	2.09E-01	0	4.05E-10	1	6.29E-01	0	4.59E-11	1	4.05E-10	1	8.14E-01	0
Test 3	**2**	1.04E-16	1	NaN	0	2.09E-13	1	2.61E-07	1	3.61E-15	1	1.04E-16	1	NaN	0
	3	1.38E-06	1	7.13E-01	0	4.07E-14	1	1.87E-11	1	4.03E-01	0	1.38E-06	1	7.13E-01	1
	4	2.04E-13	1	3.46E-08	1	2.51E-03	1	4.65E-03	1	8.94E-01	0	2.04E-13	1	3.46E-08	1
	5	3.99E-13	1	4.93E-01	0	8.89E-08	1	3.04E-02	1	5.42E-03	1	3.99E-13	1	4.93E-01	0
Test 4	**2**	1.04E-16	1	8.17E-02	0	2.53E-12	1	1.76E-04	1	4.30E-15	1	2.53E-12	1	NaN	0
	3	1.58E-11	1	2.75E-05	1	2.18E-14	1	2.17E-14	1	3.71E-02	1	2.18E-14	1	4.30E-08	1
	4	2.32E-01	0	6.50E-02	0	3.47E-13	1	2.13E-12	1	7.94E-13	1	3.47E-13	1	1.08E-08	1
	5	9.34E-01	0	6.89E-01	0	6.23E-12	1	3.16E-08	1	2.84E-04	1	6.23E-12	1	8.29E-04	1
Test 5	**2**	1.04E-16	1	NaN	0	2.10E-13	1	1.05E-07	1	3.62E-03	1	1.05E-07	1	NaN	0
	3	1.12E-01	0	2.21E-02	1	1.53E-14	1	7.48E-13	1	5.21E-10	1	7.48E-13	1	8.27E-12	1
	4	3.58E-13	1	7.31E-03	1	5.20E-03	1	2.83E-01	0	9.55E-04	1	2.83E-01	0	6.46E-01	0
	5	2.99E-12	1	7.24E-01	0	1.75E-07	1	1.65E-01	0	7.51E-01	0	1.65E-01	0	5.10E-01	0
Test 6	**2**	1.04E-16	1	NaN	0	2.51E-12	1	1.60E-01	0	2.95E-15	1	1.04E-16	1	NaN	0
	3	3.49E-11	1	5.39E-02	0	1.86E-12	1	8.25E-09	1	4.62E-01	0	3.49E-11	1	3.60E-05	1
	4	7.49E-05	1	1.94E-01	0	4.44E-07	1	1.66E-05	1	6.92E-09	1	7.49E-05	1	4.84E-04	1
	5	9.45E-04	1	1.59E-06	1	6.04E-13	1	8.90E-12	1	1.26E-01	0	9.45E-04	1	2.15E-08	1
Test 7	**2**	2.61E-14	1	5.77E-04	1	7.42E-09	1	5.71E-02	0	2.25E-11	1	7.42E-09	1	3.31E-07	1
	3	7.76E-15	1	6.29E-07	1	1.53E-14	1	7.42E-13	1	3.52E-03	1	1.53E-14	1	9.78E-08	1
	4	4.01E-01	0	1.37E-03	1	4.09E-13	1	1.04E-09	1	5.12E-09	1	4.09E-13	1	3.18E-06	1
	5	1.96E-01	0	9.36E-02	0	7.26E-13	1	7.23E-11	1	8.51E-01	0	7.26E-13	1	2.16E-08	1
Test 8	**2**	1.04E-16	1	1.49E-03	1	5.71E-14	1	6.28E-07	1	1.23E-01	0	5.71E-14	1	7.48E-04	1
	3	2.61E-16	1	5.77E-09	1	1.53E-14	1	5.78E-14	1	7.47E-13	1	1.53E-14	1	5.51E-09	1
	4	3.34E-14	1	4.58E-08	1	5.37E-14	1	3.74E-13	1	1.31E-11	1	5.37E-14	1	1.17E-10	1
	5	1.85E-13	1	1.86E-10	1	1.86E-13	1	2.30E-11	1	1.26E-08	1	1.86E-13	1	1.01E-09	1
Test 9	**2**	7.83E-16	1	1.30E-01	0	3.06E-11	1	6.72E-07	1	1.28E-14	1	3.06E-11	1	9.23E-02	0
	3	2.59E-07	1	1.19E-02	1	8.90E-13	1	1.66E-10	1	2.96E-01	0	8.90E-13	1	2.16E-02	1
	4	1.33E-02	1	1.22E-02	1	4.50E-13	1	9.51E-12	1	4.41E-13	1	4.50E-13	1	3.18E-07	1
	5	4.81E-01	0	5.92E-02	0	6.45E-13	1	2.93E-11	1	6.38E-01	0	6.45E-13	1	3.95E-09	1
Test 10	**2**	4.94E-15	1	2.04E-05	1	7.78E-01	0	2.44E-13	1	1.95E-13	1	7.78E-01	0	4.94E-15	1
	3	8.65E-15	1	4.13E-05	1	3.81E-10	1	8.93E-11	1	7.15E-14	1	3.81E-10	1	4.18E-11	1
	4	7.31E-14	1	2.13E-11	1	8.67E-14	1	8.67E-14	1	7.31E-14	1	8.67E-14	1	8.66E-14	1
	5	3.07E-06	1	1.93E-06	1	3.79E-13	1	3.79E-13	1	3.07E-06	1	3.79E-13	1	3.79E-13	1

MFO, WOA, SCA, and CTSA ranked fourth with 3 higher FSIM cases representing a (7.5%) of the total cases. Finally, TSA ranked last without any higher cases. Regarding the FSIM results shown in Table. 10, proposed TSA-LEO ranked first with 18 higher cases (45%). MFO was ranked second with 7 higher cases (17.5%) and WOA ranked third with 5 higher cases (12.5%). CTSA ranked fourth with 4 higher cases (10.5%). SCA and BMO ranked fifth with only one higher case with a percentage of (2.5%). In addition, TSA gained no higher FSIM cases.

TABLE 12. Segmented images after applying TSA–LEO on Otsu's method.

Image	level = 2	level = 3	level = 4	level = 5
Cameraman	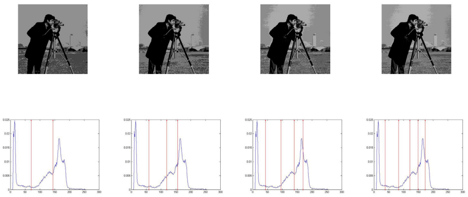			
Lena	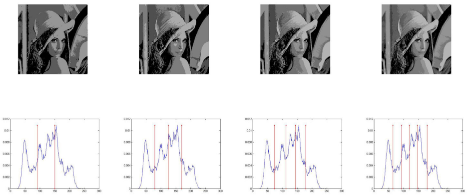			
Baboon	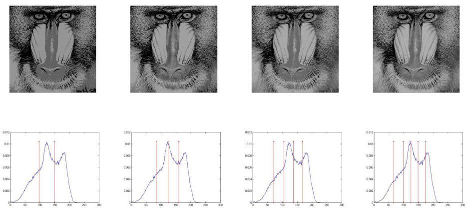			
Hunter	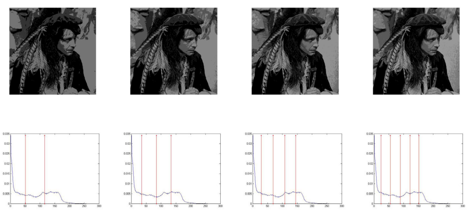			
Airplane	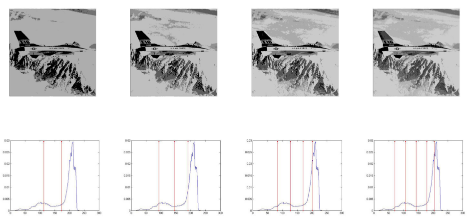			

TABLE 13. Segmented images after applying TSA–LEO on Otsu's method.

Image	level = 2	level = 3	level = 4	level = 5
Pepper	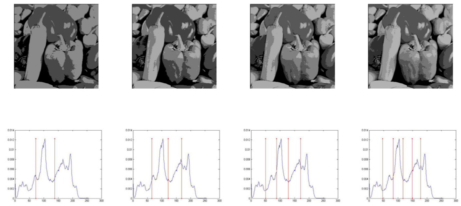			
Living-Room	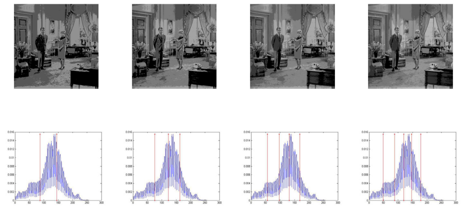			
Woman	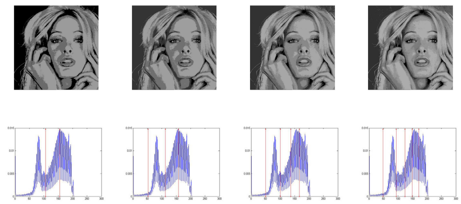			
Bridge	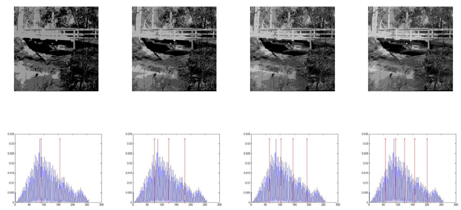			
Butter-Fly	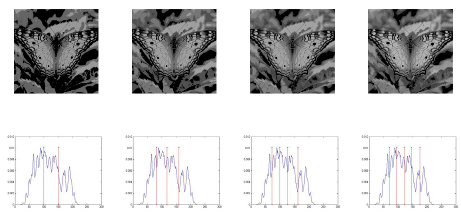			

Regarding the objective function of Otsu, the results of Otsu in terms of the mean of fitness provided in Table 15 confirmed the superiority of TSA–LEO over the other algorithms. Where the proposed TSA–LEO ranked first with 40 higher cases (100%), Table 16 shows the mean PSNR results and confirms that BMO ranked first with 10 higher cases (25%). Moreover, the proposed TSA-LEO and SCA ranked second with 9 higher cases (22.5%). MFO ranked third with 8 higher cases (20%) and CTSA ranked fourth with 4 higher best fitness cases (10%). The original TSA and SOA with 3 higher cases represent (7.5%) of overall higher cases. Finally, WOA ranked in the last place with only one higher case (2.5%). Table 17 represents the SSIM results of the proposed TSA-LEO as compared with other algorithms in terms of SSIM mean results. Remarkably, BMO ranked first with 15 higher cases representing (37.5%) of overall test cases. TSA-LEO ranked second with 13 higher cases (32.5%). MFO, SCA, SOA, and CTSA ranked third with 3 higher cases representing (7.5%) of overall cases. WOA and TSA ranked last with only one higher case representing (2.5%) of total cases. Table 18 provides the mean result of FSIM, which indicates that BMO ranked first with 14 higher cases representing (35%) of overall cases. TSA-LEO ranked second with 9 higher cases (22.5%). SCA ranked third with overall 5 higher cases (12.5%). Moreover, WOA, SOA, CTSA ranked fourth with 4 higher cases representing a percentage of (10%). Besides, TSA gained two higher FSIM cases with (5%) of overall cases. Finally, MFO ranked last with only one higher FSIM case representing (2.5%) of overall cases. According to the Wilcoxon rank sum test, Tables (11 and 19) represent P and H results of the Wilcoxon test in terms of fitness for Kapur and Otsu objective functions, respectively. When the number of thresholds is small (e.g., Level = 2,3), the segmentation results of each algorithm are almost the same, according to comparisons based on Kapur and For example, when Level = 2, the optimal threshold, PSNR, SSIM, and FSIM of the eight algorithms of Baboon are the same.

TABLE 14. Optimal thresholds obtained by Otsu's objective function.

Test Image	Th	MFO	WOA	SCA	SOA	BMO	TSA	CTSA	TSA-LEO
Test 1	2	70 144	70 144	70 144	70 144	70 144	70 144	70 144	70 144
	3	59 119 156	59 119 156	57 118 155	59 119 156	59 119 156	59 199 156	59 119 156	59 119 156
	4	42 95 140 170	42 95 140 170	34 89 136 167	42 95 140 170	42 95 140 170	40 94 140 170	42 95 140 170	42 95 140 170
	5	36 82 122 149 173	36 82 122 149 173	18 62 109 144 172	36 82 122 149 173	36 82 122 149 173	33 80 121 148 173	35 82 122 149 173	36 82 122 149 173
Test 2	2	91 150	91 150	90 149	91 150	91 150	91 150	91 150	91 150
	3	79 125 170	79 125 170	79 125 169	79 125 170	79 125 170	79 125 170	79 125 170	79 125 170
	4	73 112 143 178	73 112 144 179	45 98 135 174	73 112 143 178	73 112 144 179	63 107 141 177	73 112 144 179	73 112 143 178
	5	64 92 119 147 180	72 108 135 159 187	11 70 110 142 178	72 108 135 159 187	72 108 135 159 187	56 92 122 149 181	72 108 135 159 187	72 108 135 159 187
Test 3	2	97 149	97 149	96 149	97 149	97 149	97 149	97 149	97 149
	3	85 125 161	85 125 161	75 120 159	85 125 161	85 125 161	85 124 160	85 125 161	85 125 161
	4	72 106 137 168	72 106 137 168	49 98 133 166	72 106 137 168	72 106 137 168	65 104 136 167	72 106 137 168	72 106 137 168
	5	66 97 123 148 174	67 99 125 149 174	14 66 104 136 168	67 99 125 149 174	67 99 125 149 174	52 90 118 144 172	66 98 124 148 174	67 99 125 149 174
Test 4	2	51 116	51 116	51 116	51 116	51 116	51 116	51 116	51 116
	3	36 86 135	36 86 135	35 85 134	36 86 135	36 86 135	36 86 135	36 86 135	36 86 135
	4	30 71 110 146	30 71 110 146	27 65 104 143	30 71 110 146	30 71 110 146	27 66 105 143	30 71 110 146	30 71 110 146
	5	22 53 88 122 152	22 53 88 122 152	12 41 80 116 149	22 53 88 122 152	22 53 88 122 152	18 49 85 119 151	22 53 88 122 152	22 53 88 122 152
Test 5	2	113 173	113 173	112 173	113 173	113 173	113 173	113 173	113 173
	3	93 145 191	93 145 191	92 144 190	93 145 191	93 145 191	92 144 190	93 145 191	93 145 191
	4	84 129 172 203	84 129 172 203	62 117 163 199	84 129 172 203	84 129 172 203	83 128 172 202	84 129 172 203	84 129 172 203
	5	68 106 142 179 204	69 106 142 179 204	24 87 127 170 201	68 106 142 179 204	68 106 142 179 204	53 101 139 177 204	66 106 142 179 204	68 106 142 179 204
Test 6	2	72 138	72 138	71 138	72 138	72 138	72 138	72 138	72 138
	3	65 122 169	65 122 169	62 120 167	65 122 169	65 122 169	65 122 169	65 122 169	65 122 169
	4	50 88 128 171	50 88 128 171	33 82 126 170	50 88 128 171	50 88 128 171	44 85 128 171	50 88 128 171	50 88 128 171
	5	48 85 118 150 179	49 85 118 150 179	17 58 96 134 173	48 85 118 150 179	48 85 118 150 179	37 77 112 145 177	48 85 118 151 180	48 85 118 150 179
Test 7	2	87 145	87 145	87 145	87 145	87 145	87 145	87 145	87 145
	3	76 123 163	76 123 163	73 122 162	76 123 163	76 123 163	76 123 163	76 123 163	76 123 163
	4	56 97 132 168	56 97 132 168	43 92 130 166	56 97 132 168	56 97 132 168	52 95 132 168	56 97 132 168	56 97 132 168
	5	49 88 120 146 178	49 89 120 146 178	25 71 108 139 173	49 88 120 146 178	49 88 120 146 178	42 84 118 145 178	45 86 119 146 178	49 88 120 146 178
Test 8	2	106 155	106 155	106 155	106 155	106 155	106 155	106 155	106 155
	3	53 112 158	53 112 158	49 112 157	53 112 158	53 112 158	52 112 158	53 112 158	53 112 158
	4	50 101 137 167	50 101 137 167	24 99 135 166	50 101 137 167	50 101 137 167	39 101 137 167	49 101 137 167	50 101 137 167
	5	48 94 124 149 172	48 95 125 150 173	5 58 104 139 167	48 94 124 149 172	48 95 125 150 173	30 83 117 146 171	47 95 124 150 173	48 94 124 149 172
Test 9	2	91 156	91 156	91 156	91 156	91 156	91 157	91 156	91 156
	3	75 124 180	75 124 180	71 122 179	75 124 180	75 124 180	74 122 179	75 124 180	75 124 180
	4	63 103 145 193	63 103 145 193	50 96 140 190	63 103 145 193	63 103 145 193	60 101 143 192	63 103 145 193	63 103 145 193
	5	55 88 120 157 200	55 91 124 159 201	19 70 107 147 197	55 88 120 157 200	55 88 120 156 200	48 83 116 154 198	55 91 124 159 201	55 88 120 157 200
Test 10	2	100 152	100 152	99 151	100 152	100 152	102 153	100 152	100 152
	3	81 118 159	81 118 159	76 116 159	81 118 159	81 118 159	77 114 157	81 118 159	81 118 159
	4	71 99 127 162	72 99 127 162	33 88 122 160	71 99 127 162	72 99 127 162	64 103 136 169	72 99 127 162	71 99 127 162
	5	71 98 124 152 179	71 98 124 152 179	24 73 106 134 166	71 98 124 152 179	71 98 124 152 179	53 101 139 177 204	71 97 124 152 179	71 98 124 152 179

TABLE 15. Average and STD of Otsu's fitness obtained from all algorithms.

		MFO		WOA		SCA		SOA		BMO		TSA		CTSA		TSA-LEO	
Test Image	**Level**	**Mean**	**STD**	**Mean**	**STD**	**Mean**	**STD**	**Mean**	**STD**	**Mean**	**STD**	**Mean**	**STD**	**Mean**	**STD**	**Mean**	**STD**
Test 1	2	3.64E+03	1.92E+02	3.65E+03	2.67E+00	3.65E+03	5.49E+00	3.65E+03	6.47E+00	3.65E+03	1.50E+00	3.64E+03	6.47E+00	3.65E+03	1.57E+00	**3.65E+03**	1.81E+00
	3	3.72E+03	1.84E+02	3.73E+03	2.12E+00	3.72E+03	8.41E+00	3.71E+03	8.55E+00	3.73E+03	1.63E+00	3.72E+03	8.55E+00	3.72E+03	2.69E+00	**3.73E+03**	2.24E+00
	4	3.77E+03	1.50E+02	3.78E+03	3.07E+00	3.76E+03	9.25E+00	3.75E+03	1.33E+01	3.78E+03	3.32E+00	3.77E+03	1.33E+01	3.78E+03	2.65E+00	**3.78E+03**	3.04E+00
	5	3.81E+03	1.28E+02	3.81E+03	3.44E+00	3.78E+03	7.70E+00	3.78E+03	1.06E+01	3.81E+03	3.53E+00	3.80E+03	1.06E+01	3.81E+03	3.05E+00	**3.81E+03**	3.07E+00
Test 2	2	1.96E+03	1.04E+02	1.96E+03	1.69E+00	1.96E+03	5.78E+00	1.96E+03	6.26E+00	1.96E+03	1.64E+00	1.96E+03	6.26E+00	1.96E+03	2.05E+00	**1.96E+03**	1.61E+00
	3	2.12E+03	1.11E+02	2.13E+03	4.30E+00	2.11E+03	1.56E+01	2.10E+03	2.31E+01	2.13E+03	4.47E+00	2.12E+03	2.31E+01	2.13E+03	5.07E+00	**2.13E+03**	3.82E+00
	4	2.19E+03	1.01E+02	2.19E+03	4.76E+00	2.15E+03	1.38E+01	2.15E+03	1.85E+01	2.19E+03	6.81E+00	2.18E+03	1.85E+01	2.19E+03	4.37E+00	**2.19E+03**	4.59E+00
	5	2.21E+03	8.99E+01	2.22E+03	4.02E+00	2.18E+03	1.27E+01	2.18E+03	1.52E+01	2.22E+03	4.35E+00	2.21E+03	1.52E+01	2.22E+03	3.65E+00	**2.22E+03**	3.77E+00
Test 3	2	1.55E+03	8.27E+01	1.55E+03	3.04E+00	1.55E+03	8.77E+00	1.54E+03	9.62E+00	1.55E+03	1.71E+00	1.55E+03	9.62E+00	1.55E+03	2.81E+00	**1.55E+03**	2.33E+00
	3	1.64E+03	8.52E+01	1.64E+03	3.69E+00	1.63E+03	1.09E+01	1.61E+03	1.73E+01	1.64E+03	2.95E+00	1.64E+03	1.73E+01	1.64E+03	3.40E+00	**1.64E+03**	3.32E+00
	4	1.69E+03	8.30E+01	1.70E+03	4.42E+00	1.66E+03	1.35E+01	1.65E+03	1.50E+01	1.70E+03	4.90E+00	1.69E+03	1.50E+01	1.69E+03	4.11E+00	**1.70E+03**	4.17E+00
	5	1.72E+03	7.76E+01	1.72E+03	3.93E+00	1.68E+03	1.10E+01	1.69E+03	1.35E+01	1.72E+03	3.83E+00	1.71E+03	1.35E+01	1.72E+03	3.44E+00	**1.72E+03**	4.11E+00
Test 4	2	3.05E+03	1.62E+02	3.06E+03	2.30E+00	3.06E+03	3.79E+00	3.06E+03	7.00E+00	3.06E+03	1.58E+00	3.05E+03	9.95E+00	3.06E+03	2.34E+00	**3.06E+03**	2.54E+00
	3	3.20E+03	1.58E+02	3.21E+03	4.32E+00	3.21E+03	1.12E+01	3.19E+03	1.75E+01	3.21E+03	3.26E+00	3.20E+03	1.18E+01	3.21E+03	3.73E+00	**3.21E+03**	4.95E+00
	4	3.26E+03	1.42E+02	3.27E+03	3.74E+00	3.24E+03	9.95E+00	3.24E+03	1.50E+01	3.27E+03	3.50E+00	3.25E+03	3.93E+00	3.27E+03	2.75E+00	**3.27E+03**	3.48E+00
	5	3.30E+03	1.21E+02	3.31E+03	4.12E+00	3.28E+03	1.18E+01	3.27E+03	1.38E+01	3.31E+03	3.97E+00	3.29E+03	6.75E+00	3.31E+03	3.37E+00	**3.31E+03**	3.34E+00
Test 5	2	1.94E+03	1.04E+02	1.95E+03	1.09E+00	1.95E+03	3.93E+00	1.95E+03	4.27E+00	1.95E+03	1.07E+00	1.94E+03	7.99E+00	1.95E+03	1.24E+00	**1.95E+03**	1.17E+00
	3	2.02E+03	1.02E+02	2.03E+03	1.64E+00	2.01E+03	6.75E+00	2.01E+03	7.18E+00	2.02E+03	2.67E+00	2.02E+03	8.04E+00	2.03E+03	1.54E+00	**2.03E+03**	1.69E+00
	4	2.07E+03	9.37E+01	2.07E+03	2.85E+00	2.04E+03	7.99E+00	2.04E+03	8.79E+00	2.07E+03	3.11E+00	2.06E+03	7.59E+00	2.07E+03	2.76E+00	**2.07E+03**	2.62E+00
	5	2.09E+03	8.03E+01	2.10E+03	2.77E+00	2.06E+03	8.04E+00	2.07E+03	9.40E+00	2.10E+03	4.19E+00	2.09E+03	1.61E+01	2.09E+03	2.93E+00	**2.10E+03**	3.03E+00
Test 6	2	2.43E+03	1.26E+02	2.44E+03	2.06E+00	2.44E+03	7.59E+00	2.43E+03	6.53E+00	2.44E+03	1.80E+00	2.43E+03	1.14E+01	2.44E+03	2.89E+00	**2.44E+03**	2.49E+00
	3	2.58E+03	1.24E+02	2.59E+03	4.71E+00	2.57E+03	1.61E+01	2.56E+03	1.75E+01	2.59E+03	3.46E+00	2.58E+03	1.03E+01	2.59E+03	3.37E+00	**2.59E+03**	3.97E+00
	4	2.65E+03	1.08E+02	2.66E+03	4.45E+00	2.62E+03	1.14E+01	2.62E+03	1.46E+01	2.66E+03	4.43E+00	2.64E+03	5.02E+00	2.66E+03	4.26E+00	**2.66E+03**	3.82E+00
	5	2.69E+03	8.92E+01	2.69E+03	4.42E+00	2.64E+03	1.03E+01	2.65E+03	1.63E+01	2.69E+03	5.14E+00	2.68E+03	1.02E+02	2.69E+03	4.50E+00	**2.70E+03**	4.75E+00
Test 7	2	1.62E+03	8.38E+01	1.63E+03	2.58E+00	1.63E+03	5.02E+00	1.62E+03	8.96E+00	1.63E+03	1.91E+00	1.62E+03	9.37E+01	1.63E+03	3.03E+00	**1.63E+03**	2.03E+00
	3	1.76E+03	8.35E+01	1.76E+03	3.44E+00	1.75E+03	1.12E+01	1.74E+03	1.64E+01	1.76E+03	4.13E+00	1.75E+03	8.03E+01	1.76E+03	3.28E+00	**1.76E+03**	3.46E+00
	4	1.82E+03	7.35E+01	1.83E+03	4.50E+00	1.80E+03	1.28E+01	1.79E+03	1.52E+01	1.83E+03	4.45E+00	1.82E+03	1.26E+02	1.83E+03	3.73E+00	**1.83E+03**	3.57E+00
	5	1.87E+03	6.67E+01	1.87E+03	4.23E+00	1.82E+03	9.90E+00	1.83E+03	1.52E+01	1.87E+03	4.79E+00	1.86E+03	1.24E+02	1.87E+03	4.69E+00	**1.87E+03**	4.06E+00
Test 8	2	1.54E+03	8.24E+01	1.54E+03	2.92E+00	1.54E+03	8.56E+00	1.54E+03	7.85E+00	1.54E+03	1.94E+00	1.54E+03	1.08E+02	1.54E+03	2.93E+00	**1.54E+03**	2.07E+00
	3	1.64E+03	8.21E+01	1.64E+03	3.27E+00	1.63E+03	8.62E+00	1.62E+03	1.18E+01	1.64E+03	2.61E+00	1.63E+03	8.92E+01	1.64E+03	3.73E+00	**1.64E+03**	3.04E+00
	4	1.70E+03	7.92E+01	1.70E+03	4.94E+00	1.67E+03	9.72E+00	1.66E+03	1.36E+01	1.70E+03	4.46E+00	1.69E+03	8.38E+01	1.70E+03	3.91E+00	**1.70E+03**	3.84E+00
	5	1.73E+03	7.30E+01	1.73E+03	4.17E+00	1.69E+03	8.53E+00	1.69E+03	1.16E+01	1.73E+03	4.14E+00	1.72E+03	8.35E+01	1.73E+03	3.66E+00	**1.73E+03**	3.37E+00
Test 9	2	2.53E+03	1.24E+02	2.53E+03	2.56E+00	2.53E+03	7.64E+00	2.53E+03	8.70E+00	2.53E+03	1.88E+00	2.53E+03	7.35E+01	2.53E+03	2.86E+00	**2.53E+03**	2.15E+00
	3	2.72E+03	1.15E+02	2.72E+03	3.47E+00	2.71E+03	1.36E+01	2.70E+03	1.88E+01	2.72E+03	3.24E+00	2.71E+03	6.67E+01	2.72E+03	3.13E+00	**2.72E+03**	2.83E+00
	4	2.82E+03	9.88E+01	2.82E+03	4.54E+00	2.77E+03	1.48E+01	2.78E+03	1.65E+01	2.82E+03	5.79E+00	2.81E+03	8.24E+01	2.82E+03	4.38E+00	**2.82E+03**	3.99E+00
	5	2.87E+03	8.35E+01	2.88E+03	4.18E+00	2.82E+03	1.52E+01	2.83E+03	1.46E+01	2.87E+03	6.75E+00	2.86E+03	8.21E+01	2.87E+03	4.55E+00	**2.88E+03**	4.26E+00
Test 10	2	1.55E+03	8.31E+01	1.56E+03	2.44E+00	1.55E+03	5.63E+00	1.55E+03	7.55E+00	1.56E+03	2.19E+00	1.55E+03	7.92E+01	1.56E+03	2.71E+00	**1.56E+03**	2.12E+00
	3	1.67E+03	8.77E+01	1.67E+03	4.51E+00	1.63E+03	1.11E+01	1.64E+03	1.89E+01	1.67E+03	3.91E+00	1.66E+03	7.30E+01	1.67E+03	5.35E+00	**1.67E+03**	4.33E+00
	4	1.71E+03	8.78E+01	1.71E+03	3.87E+00	1.67E+03	1.24E+01	1.68E+03	1.58E+01	1.71E+03	4.69E+00	1.70E+03	1.24E+02	1.71E+03	4.22E+00	**1.71E+03**	3.63E+00
	5	1.73E+03	7.75E+01	1.74E+03	3.88E+00	1.69E+03	1.10E+01	1.70E+03	1.39E+01	1.74E+03	4.36E+00	1.73E+03	2.56E+00	1.73E+03	3.87E+00	**1.74E+03**	4.02E+00
Friedman mean rank		**2.6**		**5.4**		**2**		**1.43**		**4.7**		**4.88**		**5.4**		**7**	
Rank		**5**		**2**		**6**		**7**		**4**		**3**		**2**		**1**	

When the number of thresholds is large (e.g., Level = 4, 5), the numerical difference of segmentation results is obvious. For example, the PSNR values of image Test 4 at Level = 5 are different: 21.78 Table (8, MFO), 20.99 Table (8, WOA),

TABLE 16. Average and STD of PSNR based Otsu's objective function obtained from all algorithms.

		MFO		WOA		SCA		SOA		BMO		TSA		CTSA		TSA-LEO	
Test Image	**Level**	**Mean**	**STD**	**Mean**	**STD**	**Mean**	**STD**	**Mean**	**STD**	**Mean**	**STD**	**Mean**	**STD**	**Mean**	**STD**	**Mean**	**STD**
Test 1	**2**	1.72E+01	1.08E-14	1.72E+01	1.08E-14	**1.73E+01**	7.51E-02	1.72E+01	1.25E-02	1.72E+01	1.08E-14	1.72E+01	1.08E-14	1.72E+01	1.08E-14	1.72E+01	1.22E-02
	3	2.02E+01	6.06E-03	2.02E+01	1.88E-02	2.00E+01	6.93E-01	2.01E+01	4.94E-01	**2.02E+01**	2.22E-02	2.02E+01	1.02E-02	2.02E+01	8.45E-03	2.02E+01	1.17E-02
	4	2.15E+01	2.15E-02	2.15E+01	4.78E-02	2.12E+01	5.91E-01	2.13E+01	3.02E-01	2.15E+01	1.16E-01	2.15E+01	4.45E-02	2.15E+01	3.89E-02	**2.15E+01**	5.59E-02
	5	2.33E+01	1.84E-02	2.33E+01	4.68E-02	2.21E+01	7.97E-01	2.28E+01	5.43E-01	2.33E+01	2.66E-02	2.33E+01	4.34E-02	2.33E+01	3.84E-02	**2.33E+01**	3.54E-02
Test 2	**2**	1.54E+01	7.21E-15	1.54E+01	7.21E-15	**1.54E+01**	3.75E-02	1.54E+01	5.97E-03	1.54E+01	4.29E-03	1.54E+01	7.21E-15	1.54E+01	7.21E-15	1.54E+01	7.21E-15
	3	1.74E+01	1.31E-02	1.74E+01	1.12E-03	1.73E+01	4.55E-01	1.74E+01	4.09E-02	**1.74E+01**	1.94E-02	1.74E+01	1.08E-14	1.74E+01	1.08E-14	1.74E+01	1.08E-14
	4	1.88E+01	4.28E-03	1.88E+01	1.81E-02	1.81E+01	6.76E-01	1.86E+01	3.89E-01	**1.88E+01**	1.71E-02	1.88E+01	2.05E-02	1.88E+01	3.96E-03	1.87E+01	2.13E-01
	5	1.96E+01	3.32E-01	1.95E+01	2.58E-01	1.89E+01	7.18E-01	1.98E+01	6.86E-01	**1.99E+01**	3.07E-01	1.95E+01	2.45E-01	1.95E+01	2.83E-01	1.94E+01	4.69E-02
Test 3	**2**	1.54E+01	1.26E-14	1.54E+01	1.26E-14	**1.54E+01**	5.33E-02	1.54E+01	9.82E-04	1.54E+01	1.26E-14	1.54E+01	1.26E-14	1.54E+01	1.26E-14	1.54E+01	1.26E-14
	3	1.77E+01	3.41E-02	1.77E+01	3.92E-02	1.76E+01	7.43E-01	1.76E+01	5.28E-01	**1.78E+01**	1.19E-01	1.77E+01	2.65E-03	1.77E+01	3.69E-03	1.77E+01	7.21E-15
	4	2.02E+01	3.64E-02	2.03E+01	6.09E-02	1.91E+01	1.14E+00	1.98E+01	1.02E+00	2.03E+01	5.85E-02	2.03E+01	4.55E-02	**2.03E+01**	3.62E-02	2.02E+01	4.41E-02
	5	2.17E+01	1.10E-01	2.17E+01	1.13E-01	2.03E+01	1.24E+00	**2.19E+01**	6.35E-01	2.19E+01	2.16E-01	2.16E+01	8.55E-02	2.17E+01	7.55E-02	2.16E+01	1.26E-01
Test 4	**2**	1.79E+01	0.00E+00	1.79E+01	0.00E+00	**1.79E+01**	1.88E-02	1.79E+01	3.93E-03	1.79E+01	5.19E-03	1.79E+01	0.00E+00	1.79E+01	0.00E+00	1.79E+01	0.00E+00
	3	2.03E+01	6.08E-03	2.03E+01	9.49E-03	2.03E+01	1.02E-01	2.03E+01	1.74E-02	2.03E+01	1.81E-02	2.03E+01	1.08E-14	**2.03E+01**	3.62E-03	**2.03E+01**	1.08E-14
	4	**2.22E+01**	1.77E-02	2.22E+01	1.68E-02	2.14E+01	8.01E-01	2.21E+01	1.26E-01	2.22E+01	2.95E-02	**2.22E+01**	9.70E-03	2.22E+01	1.29E-02	2.22E+01	7.74E-03
	5	2.37E+01	7.81E-03	2.37E+01	2.16E-02	2.27E+01	6.78E-01	2.33E+01	4.74E-01	2.37E+01	4.38E-02	2.37E+01	1.79E-02	2.37E+01	2.65E-02	**2.37E+01**	1.28E-02
Test 5	**2**	1.50E+01	1.26E-14	1.50E+01	1.26E-14	**1.50E+01**	5.39E-02	1.50E+01	2.97E-02	1.50E+01	1.90E-02	1.50E+01	1.26E-14	1.50E+01	1.26E-14	1.50E+01	1.26E-14
	3	1.88E+01	4.51E-02	1.88E+01	4.80E-02	1.84E+01	1.08E+00	**1.89E+01**	9.24E-02	1.89E+01	8.56E-02	1.88E+01	4.40E-02	1.88E+01	2.58E-02	1.88E+01	1.44E-14
	4	2.08E+01	3.78E-02	2.08E+01	5.60E-02	1.99E+01	1.29E+00	2.06E+01	6.26E-01	**2.08E+01**	1.19E-01	**2.08E+01**	4.74E-02	2.08E+01	3.45E-02	2.07E+01	1.89E-02
	5	**2.31E+01**	3.86E-02	2.31E+01	5.27E-02	2.14E+01	1.04E+00	2.26E+01	8.92E-01	2.31E+01	8.97E-02	2.31E+01	3.94E-02	2.31E+01	3.61E-01	2.31E+01	3.91E-01
Test 6	**2**	1.63E+01	1.08E-14	1.63E+01	1.08E-14	**1.63E+01**	2.04E-02	1.63E+01	1.06E-03	1.63E+01	1.08E-14	1.63E+01	1.08E-14	1.63E+01	1.08E-14	1.63E+01	1.08E-14
	3	1.84E+01	4.67E-03	1.84E+01	7.86E-03	1.82E+01	4.76E-01	**1.84E+01**	2.11E-02	1.84E+01	1.35E-02	1.84E+01	1.44E-14	1.84E+01	1.44E-14	1.84E+01	5.42E-03
	4	2.07E+01	8.37E-03	2.07E+01	2.35E-02	1.97E+01	1.06E+00	2.04E+01	8.07E-01	2.07E+01	1.62E-02	2.07E+01	2.15E-02	2.07E+01	9.98E-03	**2.07E+01**	2.68E-02
	5	**2.23E+01**	8.83E-03	2.23E+01	2.46E-02	2.04E+01	1.16E+00	2.19E+01	5.89E-01	2.23E+01	2.94E-02	2.23E+01	1.79E-02	2.23E+01	2.10E-02	2.23E+01	2.58E-01
Test 7	**2**	1.60E+01	5.41E-15	1.60E+01	5.41E-15	**1.60E+01**	2.24E-02	1.60E+01	4.85E-03	1.60E+01	1.17E-02	1.60E+01	5.41E-15	1.60E+01	5.41E-15	1.60E+01	5.41E-15
	3	**1.82E+01**	7.21E-15	1.82E+01	2.57E-02	1.81E+01	3.84E-01	1.82E+01	3.14E-02	1.82E+01	2.43E-02	1.82E+01	9.46E-03	**1.82E+01**	7.21E-15	1.82E+01	1.54E-02
	4	2.07E+01	2.47E-04	2.07E+01	2.52E-02	2.01E+01	8.95E-01	2.06E+01	4.31E-01	2.07E+01	2.36E-02	2.07E+01	2.72E-02	2.07E+01	1.91E-02	**2.07E+01**	3.39E-02
	5	2.22E+01	2.93E-02	2.22E+01	3.68E-02	2.05E+01	1.00E+00	2.20E+01	3.98E-01	2.22E+01	6.55E-02	2.22E+01	2.82E-02	2.22E+01	3.38E-02	**2.22E+01**	3.19E-02
Test 8	**2**	**1.46E+01**	0.00E+00	**1.46E+01**	0.00E+00	1.46E+01	5.29E-02	1.46E+01	1.05E-02	1.46E+01	3.96E-03	1.46E+01	0.00E+00	**1.46E+01**	0.00E+00	**1.46E+01**	0.00E+00
	3	1.92E+01	3.60E-15	1.91E+01	4.54E-02	1.83E+01	1.70E+00	1.91E+01	1.48E-01	1.91E+01	1.99E-02	1.91E+01	2.55E-02	1.92E+01	3.60E-15	**1.92E+01**	1.77E-01
	4	**2.12E+01**	2.14E-02	2.11E+01	8.61E-02	1.72E+01	1.88E+00	1.90E+01	2.14E+00	2.11E+01	6.45E-02	2.11E+01	7.96E-02	2.10E+01	7.60E-01	2.10E+01	4.31E-01
	5	**2.24E+01**	2.54E-02	2.23E+01	1.43E-01	2.04E+01	1.90E+00	2.16E+01	1.14E+00	2.23E+01	7.07E-02	2.22E+01	1.72E-01	2.22E+01	1.80E-01	2.21E+01	3.96E-01
Test 9	**2**	1.40E+01	1.33E-02	1.40E+01	1.33E-02	**1.40E+01**	2.60E-02	1.40E+01	1.43E-02	1.40E+01	1.29E-02	**1.40E+01**	1.42E-02	1.40E+01	1.36E-02	1.40E+01	1.40E-02
	3	1.66E+01	1.58E-01	1.66E+01	1.33E-02	1.65E+01	7.21E-01	1.67E+01	1.87E-01	**1.68E+01**	2.24E-01	1.66E+01	4.28E-03	1.66E+01	1.08E-14	1.66E+01	1.08E-14
	4	1.89E+01	1.05E-01	1.88E+01	3.04E-02	1.79E+01	1.10E+00	1.87E+01	7.65E-01	**1.90E+01**	1.48E-01	1.89E+01	5.54E-02	1.89E+01	2.17E-02	1.89E+01	2.29E-02
	5	2.06E+01	1.21E-01	2.05E+01	8.81E-02	1.93E+01	1.15E+00	2.03E+01	8.36E-01	**2.08E+01**	1.75E-01	2.05E+01	7.38E-02	2.06E+01	5.74E-02	2.06E+01	5.51E-02
Test 10	**2**	1.37E+01	0.00E+00	1.37E+01	0.00E+00	**1.38E+01**	8.15E-02	1.37E+01	3.24E-02	1.37E+01	3.68E-02	1.37E+01	0.00E+00	1.37E+01	0.00E+00	1.37E+01	0.00E+00
	3	**1.70E+01**	0.00E+00	1.70E+01	1.83E-02	1.60E+01	1.41E+00	1.69E+01	5.38E-01	1.70E+01	5.09E-04	1.70E+01	1.80E-02	1.70E+01	0.00E+00	1.69E+01	3.78E-02
	4	1.91E+01	3.41E-02	1.92E+01	6.39E-02	1.76E+01	1.02E+00	1.89E+01	7.89E-01	1.92E+01	6.38E-02	1.92E+01	6.30E-02	**1.92E+01**	6.39E-02	1.91E+01	3.54E-01
	5	1.98E+01	1.06E-01	1.98E+01	7.41E-02	1.85E+01	1.36E+00	1.98E+01	3.46E-01	**2.00E+01**	1.96E-01	1.98E+01	5.92E-02	1.98E+01	9.28E-02	1.97E+01	1.14E-01

TABLE 17. Average and STD of SSIM based Otsu's objective function obtained from all algorithms.

		MFO		WOA		SCA		SOA		BMO		TSA		CTSA		TSA-LEO	
Test Image	**Level**	**Mean**	**STD**	**Mean**	**STD**	**Mean**	**STD**	**Mean**	**STD**	**Mean**	**STD**	**Mean**	**STD**	**Mean**	**STD**	**Mean**	**STD**
Test 1	**2**	7.68E-01	4.51E-16	7.68E-01	2.48E-04	7.67E-01	1.86E-03	7.68E-01	2.42E-04	7.68E-01	4.51E-16	7.68E-01	4.51E-16	7.68E-01	4.51E-16	**7.78E-01**	4.51E-16
	3	8.07E-01	4.11E-05	8.07E-01	2.91E-04	8.05E-01	1.01E-02	8.07E-01	5.53E-03	8.09E-01	3.25E-03	8.06E-01	4.80E-03	8.06E-01	2.66E-04	**8.11E-01**	7.89E-16
	4	8.31E-01	6.13E-04	8.31E-01	5.47E-04	8.25E-01	7.97E-03	8.29E-01	3.44E-03	8.30E-01	1.94E-03	8.30E-01	2.75E-03	8.31E-01	5.56E-04	**8.31E-01**	4.51E-16
	5	8.58E-01	6.55E-04	8.58E-01	5.99E-04	8.45E-01	1.16E-02	8.54E-01	6.09E-03	**8.59E-01**	1.37E-03	8.57E-01	4.34E-03	8.58E-01	1.03E-03	8.58E-01	2.04E-03
Test 2	**2**	6.46E-01	1.13E-16	6.46E-01	1.13E-16	**6.47E-01**	3.21E-03	6.46E-01	4.21E-04	6.46E-01	3.02E-04	6.46E-01	1.13E-16	6.46E-01	1.13E-16	6.46E-01	1.13E-16
	3	7.22E-01	1.05E-03	7.22E-01	4.51E-16	7.16E-01	1.72E-02	7.22E-01	2.78E-03	**7.23E-01**	1.53E-03	7.22E-01	2.06E-03	7.22E-01	2.45E-04	7.22E-01	4.51E-16
	4	7.65E-01	1.32E-04	7.63E-01	6.36E-03	7.44E-01	2.12E-02	7.62E-01	1.06E-02	**7.65E-01**	7.18E-04	7.63E-01	1.03E-02	7.65E-01	6.52E-04	7.65E-01	4.51E-16
	5	7.94E-01	1.11E-02	7.86E-01	8.63E-04	7.72E-01	2.27E-02	8.02E-01	2.23E-02	**8.04E-01**	1.05E-02	7.91E-01	1.09E-02	7.91E-01	8.75E-03	7.90E-01	8.87E-03
Test 3	**2**	7.89E-01	1.13E-16	7.89E-01	1.13E-16	**7.89E-01**	2.71E-03	7.89E-01	1.59E-05	7.89E-01	1.13E-16	7.89E-01	1.13E-16	7.89E-01	1.13E-16	7.89E-01	1.13E-16
	3	8.54E-01	8.07E-04	8.54E-01	7.89E-16	8.51E-01	2.05E-02	8.52E-01	1.45E-02	8.56E-01	3.04E-03	8.55E-01	1.61E-03	8.55E-01	9.38E-04	**8.56E-01**	7.89E-16
	4	9.13E-01	8.49E-04	9.13E-01	9.92E-04	8.88E-01	2.68E-02	9.04E-01	2.32E-02	9.14E-01	1.34E-03	9.12E-01	9.34E-03	**9.14E-01**	1.38E-03	9.12E-01	3.29E-04
	5	9.34E-01	1.50E-03	9.33E-01	1.13E-03	9.12E-01	2.51E-02	**9.39E-01**	9.66E-03	9.37E-01	2.87E-03	9.32E-01	4.52E-03	9.35E-01	1.79E-03	9.33E-01	6.84E-05
Test 4	**2**	7.58E-01	2.25E-16	7.58E-01	2.25E-16	7.57E-01	1.18E-03	7.58E-01	3.61E-04	**7.58E-01**	1.37E-04	7.58E-01	2.25E-16	7.58E-01	2.25E-16	7.58E-01	2.25E-16
	3	8.47E-01	6.52E-04	8.47E-01	5.63E-16	8.48E-01	2.75E-03	**8.48E-01**	9.86E-04	8.48E-01	1.22E-03	8.47E-01	9.32E-04	8.47E-01	1.02E-03	8.47E-01	5.63E-16
	4	8.88E-01	2.88E-03	8.86E-01	3.26E-04	8.78E-01	1.87E-02	8.92E-01	4.08E-03	**8.93E-01**	4.62E-03	8.87E-01	2.42E-03	8.87E-01	2.16E-03	8.86E-01	3.71E-04
	5	9.22E-01	2.25E-04	9.22E-01	2.56E-04	9.05E-01	1.59E-02	9.18E-01	1.03E-02	9.23E-01	6.38E-04	9.22E-01	6.12E-04	9.22E-01	4.50E-04	**9.32E-01**	6.73E-05
Test 5	**2**	8.39E-01	2.25E-16	8.39E-01	2.25E-16	8.39E-01	2.17E-03	**8.40E-01**	1.20E-03	8.40E-01	1.39E-03	8.39E-01	2.25E-16	8.39E-01	2.25E-16	8.39E-01	2.25E-16
	3	8.91E-01	2.37E-03	8.89E-01	2.25E-16	8.84E-01	1.85E-02	8.92E-01	4.13E-03	**8.95E-01**	6.28E-03	8.93E-01	2.11E-03	8.92E-01	2.23E-03	8.89E-01	2.25E-16
	4	9.11E-01	8.69E-04	9.10E-01	4.89E-04	9.01E-01	1.77E-02	9.10E-01	6.32E-03	**9.12E-01**	2.32E-03	9.11E-01	4.21E-03	9.11E-01	1.12E-03	9.10E-01	4.51E-16
	5	9.45E-01	7.57E-04	9.45E-01	5.56E-03	9.22E-01	1.45E-02	9.40E-01	1.18E-02	9.45E-01	1.60E-03	9.43E-01	5.13E-03	9.45E-01	8.80E-04	**9.46E-01**	4.92E-04
Test 6	**2**	7.59E-01	3.38E-16	7.59E-01	3.38E-16	7.59E-01	1.89E-03	7.59E-01	4.80E-04	7.59E-01	3.38E-16	7.59E-01	3.38E-16	7.59E-01	3.38E-16	**7.60E-01**	3.38E-16
	3	7.99E-01	2.56E-05	7.99E-01	5.75E-04	7.95E-01	9.39E-03	7.98E-01	1.06E-03	7.99E-01	1.51E-04	7.99E-01	8.44E-04	7.99E-01	4.30E-05	**7.99E-01**	0.00E+00
	4	8.61E-01	6.99E-05	8.61E-01	3.50E-04	8.36E-01	2.77E-02	8.53E-01	2.10E-02	8.61E-01	1.79E-04	**8.62E-01**	5.86E-04	8.61E-01	2.94E-04	8.61E-01	1.81E-05
	5	8.84E-01	3.84E-04	8.84E-01	3.29E-03	8.50E-01	2.87E-02	8.81E-01	8.42E-03	**8.85E-01**	7.51E-04	8.84E-01	3.36E-03	8.84E-01	3.93E-04	8.84E-01	8.43E-05
Test 7	**2**	7.31E-01	0.00E+00	7.31E-01	0.00E+00	7.31E-01	9.90E-04	7.31E-01	4.14E-04	**7.31E-01**	6.24E-04	7.31E-01	0.00E+00	7.31E-01	0.00E+00	7.31E-01	0.00E+00
	3	**8.08E-01**	2.25E-16	8.08E-01	3.06E-04	8.05E-01	1.35E-02	8.07E-01	7.13E-04	8.08E-01	6.40E-04	8.07E-01	5.18E-04	8.07E-01	5.37E-04	**8.08E-01**	2.25E-16
	4	8.86E-01	4.78E-06	8.86E-01	1.19E-03	8.69E-01	2.95E-02	8.86E-01	1.38E-02	8.87E-01	1.20E-03	8.87E-01	1.78E-03	**8.87E-01**	1.10E-03	8.86E-01	5.63E-16
	5	9.18E-01	6.97E-04	9.19E-01	1.57E-03	8.83E-01	3.05E-02	9.18E-01	7.62E-03	9.20E-01	1.98E-03	9.20E-01	2.13E-03	9.20E-01	1.53E-03	**9.21E-01**	5.51E-05
Test 8	**2**	7.01E-01	4.51E-16	7.01E-01	4.51E-16	7.00E-01	2.84E-03	7.00E-01	2.81E-04	**7.01E-01**	4.10E-04	7.01E-01	4.51E-16	7.01E-01	4.51E-16	7.01E-01	4.51E-16
	3	8.83E-01	2.25E-16	**8.83E-01**	3.49E-03	8.50E-01	6.75E-02	8.82E-01	3.24E-03	8.83E-01	5.63E-04	8.83E-01	9.73E-04	8.82E-01	9.06E-04	8.83E-01	2.25E-16
	4	**9.23E-01**	2.87E-04	9.20E-01	8.02E-03	8.10E-01	5.99E-02	8.64E-01	6.48E-02	9.22E-01	8.46E-04	9.17E-01	2.54E-02	9.21E-01	1.26E-03	9.23E-01	4.25E-04
	5	9.42E-01	2.46E-04	9.38E-01	5.16E-03	8.98E-01	5.16E-02	9.26E-01	2.89E-02	9.42E-01	9.87E-04	9.40E-01	4.35E-03	9.41E-01	1.75E-03	**9.42E-01**	2.45E-04
Test 9	**2**	6.14E-01	1.12E-04	6.14E-01	1.18E-04	6.15E-01	8.71E-04	6.14E-01	1.20E-04	6.14E-01	1.09E-04	6.14E-01	1.16E-04	6.14E-01	1.12E-04	**6.18E-01**	1.20E-04
	3	7.60E-01	7.48E-03	7.57E-01	2.25E-16	7.56E-01	4.13E-02	7.63E-01	9.26E-03	**7.67E-01**	1.06E-02	7.58E-01	3.33E-03	7.57E-01	6.42E-05	7.57E-01	2.25E-16
	4	8.47E-01	4.18E-03	8.46E-01	3.99E-04	8.11E-01	4.29E-02	8.43E-01	2.92E-02	**8.50E-01**	6.07E-03	8.46E-01	5.79E-04	8.46E-01	3.49E-04	8.46E-01	4.51E-16
	5	8.93E-01	4.03E-03	8.92E-01	5.82E-04	8.59E-01	3.91E-02	8.89E-01	2.44E-02	**9.00E-01**	6.44E-03	8.91E-01	7.71E-03	8.92E-01	1.99E-03	8.92E-01	5.96E-05
Test 10	**2**	5.99E-01	1.13E-16	5.99E-01	1.13E-16	**6.03E-01**	5.08E-03	6.00E-01	1.99E-03	6.00E-01	2.26E-03	5.99E-01	1.13E-16	5.99E-01	1.13E-16	5.99E-01	1.13E-16
	3	**7.64E-01**	4.51E-16	7.63E-01	1.92E-03	7.15E-01	6.98E-02	7.59E-01	2.67E-02	7.64E-01	9.99E-05	7.57E-01	2.64E-02	7.64E-01	9.16E-04	**7.64E-01**	4.51E-16
	4	8.41E-01	1.21E-03	8.40E-01	1.24E-02	7.87E-01	3.85E-02	8.34E-01	2.80E-02	8.43E-01	2.27E-03	8.38E-01	1.61E-02	**8.43E-01**	2.09E-03	8.41E-01	5.63E-16
	5	8.58E-01	3.14E-03	8.56E-01	2.64E-03	8.18E-01	5.11E-02	8.61E-01	9.42E-03	**8.64E-01**	5.75E-03	8.59E-01	7.97E-03	8.58E-01	2.32E-03	8.57E-01	7.08E-04

21.71 Table (8, SCA), 22.22 Table (8, SOA), 21.05 Table (8, BMO), 17.94 Table (8, TSA), 22.48 Table (8, CTSA), and 3.08E+01 Table (8, TSA-LEO); SSIM and FSIM also have similar differences. In Kapur's method, it is noticeable that the value based on TSA-LEO occupies the most advantages. However, results based on the Otsu method are close to that of

TABLE 18. Average and STD of FSIM based Otsu's objective function obtained from all algorithms.

		MFO		WOA		SCA		SOA		BMO		TSA		CTSA		TSA-LEO	
Test Image	**Level**	**Mean**	**STD**	**Mean**	**STD**	**Mean**	**STD**	**Mean**	**STD**	**Mean**	**STD**	**Mean**	**STD**	**Mean**	**STD**	**Mean**	**STD**
Test 1	**2**	7.71E-01	3.38E-16	**7.71E-01**	1.14E-04	7.70E-01	2.44E-03	7.71E-01	1.98E-04	7.71E-01	3.38E-16	7.71E-01	3.38E-16	7.71E-01	3.38E-16	7.71E-01	3.38E-16
	3	8.15E-01	1.13E-05	8.15E-01	2.42E-04	8.12E-01	1.11E-02	8.14E-01	7.48E-03	**8.16E-01**	1.55E-03	8.13E-01	7.39E-03	8.15E-01	1.84E-04	8.15E-01	2.25E-16
	4	8.47E-01	6.83E-04	8.47E-01	9.71E-04	8.40E-01	1.27E-02	8.43E-01	7.35E-03	8.46E-01	2.09E-03	8.46E-01	5.84E-03	8.47E-01	9.56E-04	**8.48E-01**	5.63E-16
	5	8.86E-01	2.73E-04	**8.87E-01**	5.31E-04	8.60E-01	1.94E-02	8.79E-01	1.25E-02	8.86E-01	4.43E-04	8.84E-01	8.87E-03	8.86E-01	5.82E-04	8.86E-01	2.50E-03
Test 2	**2**	6.98E-01	3.38E-16	6.98E-01	3.38E-16	**7.00E-01**	2.01E-03	6.99E-01	3.86E-04	6.98E-01	2.77E-04	6.98E-01	3.38E-16	6.98E-01	3.38E-16	6.98E-01	3.38E-16
	3	7.54E-01	7.98E-04	7.54E-01	3.38E-16	7.50E-01	1.38E-02	7.54E-01	1.53E-03	**7.55E-01**	1.17E-03	7.54E-01	1.34E-03	7.54E-01	4.80E-04	7.54E-01	2.25E-16
	4	8.03E-01	3.35E-04	8.02E-01	8.29E-03	7.76E-01	2.45E-02	7.97E-01	1.63E-02	8.03E-01	6.68E-04	7.99E-01	1.30E-02	8.03E-01	4.34E-04	**8.04E-01**	3.38E-16
	5	8.33E-01	6.14E-04	8.31E-01	7.34E-03	8.01E-01	2.11E-02	8.24E-01	1.55E-02	8.32E-01	9.18E-04	8.31E-01	6.69E-03	**8.33E-01**	7.54E-04	8.33E-01	4.46E-04
Test 3	**2**	8.45E-01	1.13E-16	8.45E-01	0.00E+00	**8.45E-01**	1.62E-03	8.45E-01	3.47E-04	8.45E-01	1.13E-16	8.45E-01	0.00E+00	8.45E-01	0.00E+00	8.45E-01	1.13E-16
	3	8.88E-01	6.66E-04	**8.88E-01**	5.63E-16	8.85E-01	1.29E-02	8.86E-01	9.63E-03	8.87E-01	1.08E-03	8.88E-01	9.85E-04	8.88E-01	7.19E-04	**8.88E-01**	7.89E-16
	4	9.24E-01	4.42E-04	9.24E-01	6.51E-04	9.08E-01	1.85E-02	9.18E-01	1.47E-02	9.24E-01	8.16E-04	9.23E-01	6.14E-03	**9.24E-01**	1.03E-03	9.24E-01	2.11E-04
	5	9.40E-01	8.00E-04	9.40E-01	1.44E-03	9.23E-01	1.76E-02	**9.42E-01**	6.61E-03	9.40E-01	1.03E-03	9.39E-01	4.14E-03	9.41E-01	1.42E-03	9.40E-01	3.57E-04
Test 4	**2**	7.95E-01	4.51E-16	7.95E-01	5.63E-16	**7.95E-01**	4.36E-04	7.95E-01	1.00E-04	7.95E-01	8.99E-05	7.95E-01	5.63E-16	7.95E-01	5.63E-16	7.95E-01	4.51E-16
	3	8.74E-01	1.90E-04	**8.74E-01**	3.38E-16	8.72E-01	9.43E-04	8.73E-01	2.94E-04	8.73E-01	3.44E-04	8.73E-01	2.72E-04	8.73E-01	2.97E-04	**8.74E-01**	5.63E-16
	4	9.12E-01	4.00E-04	9.11E-01	1.71E-04	8.96E-01	1.68E-02	9.12E-01	2.08E-03	**9.12E-01**	3.45E-04	9.12E-01	6.42E-04	9.12E-01	4.42E-04	9.11E-01	9.00E-05
	5	9.37E-01	1.55E-04	9.37E-01	3.92E-05	9.21E-01	1.28E-02	9.33E-01	8.77E-03	9.37E-01	4.17E-04	**9.38E-01**	4.37E-04	9.38E-01	2.08E-04	9.37E-01	6.54E-05
Test 5	**2**	8.11E-01	2.25E-16	8.11E-01	2.25E-16	8.11E-01	9.07E-04	**8.11E-01**	8.77E-04	8.11E-01	3.03E-04	8.11E-01	2.25E-16	8.11E-01	2.25E-16	8.11E-01	2.25E-16
	3	8.51E-01	1.39E-03	8.50E-01	2.25E-16	8.47E-01	1.27E-02	8.52E-01	2.36E-03	**8.53E-01**	4.51E-03	8.52E-01	1.22E-03	8.51E-01	1.28E-03	8.50E-01	1.13E-16
	4	8.85E-01	1.17E-03	8.85E-01	5.16E-04	8.67E-01	1.96E-02	8.81E-01	1.08E-02	**8.86E-01**	1.73E-03	8.85E-01	6.35E-03	8.85E-01	1.24E-03	8.84E-01	3.38E-16
	5	9.17E-01	1.00E-03	9.17E-01	5.30E-03	8.90E-01	1.69E-02	9.10E-01	1.34E-02	9.17E-01	1.88E-03	9.15E-01	5.66E-03	9.16E-01	1.08E-03	**9.18E-01**	6.70E-04
Test 6	**2**	7.24E-01	3.38E-16	7.24E-01	3.38E-16	7.24E-01	5.28E-04	**7.24E-01**	5.67E-07	7.24E-01	3.38E-16	7.24E-01	3.38E-16	7.24E-01	3.38E-16	7.24E-01	3.38E-16
	3	7.81E-01	8.10E-05	7.81E-01	2.09E-04	7.78E-01	1.35E-02	7.81E-01	5.51E-04	7.81E-01	2.00E-04	7.81E-01	4.37E-04	7.81E-01	1.36E-04	**7.81E-01**	3.38E-16
	4	8.23E-01	8.65E-05	8.24E-01	2.34E-04	8.05E-01	1.89E-02	8.18E-01	1.52E-02	8.23E-01	2.07E-04	**8.24E-01**	3.78E-04	8.24E-01	2.74E-04	8.23E-01	6.22E-05
	5	8.58E-01	4.10E-04	8.57E-01	5.75E-03	8.18E-01	2.31E-02	8.51E-01	1.41E-02	**8.58E-01**	7.34E-04	8.57E-01	5.79E-03	8.58E-01	3.80E-04	8.58E-01	2.69E-05
Test 7	**2**	7.57E-01	4.51E-16	7.57E-01	5.63E-16	7.57E-01	2.90E-04	7.57E-01	1.81E-04	**7.57E-01**	3.22E-04	7.57E-01	5.63E-16	7.57E-01	5.63E-16	7.57E-01	4.51E-16
	3	8.29E-01	2.25E-16	8.29E-01	1.36E-04	8.26E-01	1.21E-02	8.29E-01	3.86E-04	**8.29E-01**	3.07E-04	8.29E-01	1.96E-04	8.29E-01	3.82E-05	8.29E-01	2.25E-16
	4	8.83E-01	9.91E-05	8.83E-01	4.51E-04	8.69E-01	1.99E-02	8.82E-01	9.18E-03	**8.83E-01**	2.11E-04	8.83E-01	5.14E-04	8.83E-01	3.16E-04	8.83E-01	3.38E-16
	5	9.11E-01	5.87E-04	9.12E-01	1.27E-03	8.78E-01	2.17E-02	9.10E-01	8.18E-03	9.12E-01	1.23E-03	9.13E-01	1.14E-03	**9.13E-01**	1.11E-03	9.11E-01	1.94E-04
Test 8	**2**	7.57E-01	2.25E-16	7.57E-01	2.25E-16	7.57E-01	7.05E-04	**7.58E-01**	3.94E-04	7.57E-01	2.02E-04	7.57E-01	2.25E-16	7.57E-01	2.25E-16	7.57E-01	2.25E-16
	3	8.35E-01	4.51E-16	8.35E-01	1.49E-03	8.21E-01	2.84E-02	8.35E-01	1.53E-03	**8.35E-01**	2.82E-04	8.35E-01	3.15E-04	8.35E-01	2.72E-04	8.35E-01	4.51E-16
	4	8.93E-01	1.29E-04	8.93E-01	3.95E-03	8.41E-01	2.72E-02	8.67E-01	2.96E-02	8.93E-01	3.78E-04	8.92E-01	1.17E-02	8.93E-01	8.48E-04	**8.94E-01**	5.92E-04
	5	9.28E-01	1.50E-04	9.25E-01	7.11E-03	8.84E-01	2.50E-02	9.11E-01	1.96E-02	9.28E-01	8.82E-04	9.25E-01	7.38E-03	9.28E-01	9.80E-04	**9.28E-01**	1.20E-04
Test 9	**2**	7.66E-01	4.22E-05	7.66E-01	4.46E-05	**7.66E-01**	1.09E-03	7.66E-01	4.55E-05	7.66E-01	4.11E-05	7.66E-01	4.40E-05	7.66E-01	4.22E-05	7.66E-01	4.55E-05
	3	8.34E-01	1.38E-03	8.34E-01	0.00E+00	8.32E-01	1.84E-02	8.35E-01	2.11E-03	**8.35E-01**	2.18E-03	8.34E-01	8.92E-04	8.34E-01	1.12E-05	8.34E-01	2.25E-16
	4	8.86E-01	1.54E-03	8.86E-01	3.75E-04	8.64E-01	2.61E-02	8.83E-01	1.76E-02	**8.88E-01**	2.43E-03	8.86E-01	7.71E-04	8.86E-01	6.33E-04	8.86E-01	0.00E+00
	5	9.16E-01	1.24E-03	9.15E-01	1.05E-03	8.91E-01	2.05E-02	9.09E-01	1.48E-02	**9.16E-01**	1.39E-03	9.15E-01	5.10E-03	9.16E-01	1.17E-03	9.15E-01	8.45E-04
Test 10	**2**	7.29E-01	5.63E-16	7.29E-01	5.63E-16	**7.30E-01**	1.33E-03	7.29E-01	5.10E-04	7.29E-01	5.80E-04	7.29E-01	5.63E-16	7.29E-01	5.63E-16	7.29E-01	5.63E-16
	3	**8.03E-01**	5.63E-16	8.03E-01	6.73E-04	7.81E-01	3.24E-02	8.00E-01	1.22E-02	8.03E-01	5.27E-04	8.00E-01	1.22E-02	8.03E-01	3.20E-04	**8.03E-01**	5.63E-16
	4	8.50E-01	1.83E-04	8.49E-01	7.75E-03	8.17E-01	2.14E-02	8.44E-01	1.68E-02	8.50E-01	3.75E-04	8.47E-01	1.15E-02	**8.50E-01**	5.91E-04	8.50E-01	7.89E-16
	5	8.78E-01	4.91E-04	8.75E-01	7.77E-03	8.39E-01	2.99E-02	8.72E-01	1.25E-02	**8.79E-01**	1.62E-03	8.76E-01	6.63E-03	8.78E-01	6.35E-04	8.78E-01	8.33E-05

TABLE 19. Comparison of the p-values obtained from the Wilcoxon signed-rank test between the pairs of TSA–LEO vs. MFO, TSA–LEO vs. WOA, TSA–LEO vs. SCA, TSA–LEO vs. SOA, TSA–LEO vs. BMO, TSA–LEO vs. TSA, and TSA–LEO vs. CTSA for Otsu's method in terms of Fitness results.

		MFO		WOA		SCA		SOA		BMO		TSA		CTSA	
Test Image	**Level**	**P**	**H**	**P**	**H**	**P**	**H**	**P**	**H**	**P**	**H**	**P**	**H**	**P**	**H**
Test 1	**2**	NaN	0	3.31E-01	0	7.70E-11	1	3.31E-01	0	NaN	0	NaN	0	NaN	0
	3	4.00E-04	1	9.00E-03	1	4.39E-13	1	2.85E-08	1	8.00E-04	1	9.01E-02	0	4.00E-04	1
	4	9.58E-05	1	9.38E-02	0	5.90E-13	1	1.11E-10	1	3.83E-01	0	4.73E-05	1	9.58E-05	1
	5	2.75E-08	1	7.33E-08	1	6.48E-13	1	2.94E-11	1	4.81E-01	0	6.66E-10	1	2.75E-08	1
Test 2	**2**	NaN	0	NaN	0	7.94E-12	1	1.60E-01	0	3.31E-01	0	NaN	0	1.60E-01	0
	3	3.77E-01	0	1.60E-01	0	3.02E-14	1	1.21E-08	1	1.20E-03	1	5.33E-08	1	1.21E-08	1
	4	2.90E-02	1	3.00E-04	1	4.68E-13	1	1.10E-12	1	4.17E-01	0	9.40E-10	1	1.10E-12	1
	5	6.98E-01	0	4.37E-08	1	6.52E-13	1	2.15E-11	1	3.05E-06	1	2.25E-08	1	2.15E-11	1
Test 3	**2**	NaN	0	NaN	0	8.02E-11	1	8.17E-02	0	NaN	0	NaN	0	8.02E-11	1
	3	5.81E-01	0	7.00E-04	1	1.83E-13	1	8.09E-06	1	2.00E-04	1	4.80E-03	1	1.83E-13	1
	4	2.00E-03	1	7.25E-06	1	5.83E-13	1	6.59E-10	1	7.06E-01	0	1.77E-11	1	5.83E-13	1
	5	4.00E-02	1	7.33E-09	1	6.47E-13	1	7.42E-12	1	2.27E-05	1	8.02E-10	1	6.47E-13	1
Test 4	**2**	NaN	0	NaN	0	6.41E-10	1	3.31E-01	0	3.31E-01	0	NaN	0	NaN	0
	3	6.01E-02	0	1.50E-03	1	1.49E-13	1	3.76E-06	1	7.38E-02	0	5.77E-01	0	5.77E-01	0
	4	4.24E-01	0	3.76E-08	1	5.60E-13	1	4.72E-09	1	1.00E-04	1	7.00E-04	1	7.00E-04	1
	5	2.00E-04	1	7.20E-07	1	6.38E-13	1	1.89E-10	1	5.90E-03	1	1.42E-08	1	1.42E-08	1
Test 5	**2**	NaN	0	NaN	0	2.58E-07	1	1.50E-03	1	1.60E-01	0	NaN	0	1.60E-01	1
	3	1.63E-01	0	1.33E-06	1	3.75E-13	1	5.17E-07	1	4.73E-02	1	4.00E-04	1	4.73E-02	1
	4	1.00E-04	1	1.20E-09	1	6.20E-13	1	1.46E-10	1	3.57E-02	1	1.33E-09	1	3.57E-02	1
	5	1.02E-08	1	8.54E-10	1	6.51E-13	1	1.66E-12	1	8.83E-01	0	1.60E-08	1	0.8827	1
Test 6	**2**	NaN	0	NaN	0	2.41E-10	1	8.17E-02	0	NaN	0	NaN	0	NaN	0
	3	3.14E-01	0	9.23E-01	0	4.07E-14	1	3.90E-09	1	5.37E-02	0	4.24E-06	1	4.24E-06	1
	4	4.33E-08	1	4.68E-01	0	5.09E-13	1	8.44E-11	1	9.98E-05	1	9.18E-07	1	9.18E-07	1
	5	2.80E-03	1	1.20E-03	1	6.16E-13	1	1.60E-11	1	1.98E-01	0	5.13E-10	1	5.13E-10	1
Test 7	**2**	NaN	0	NaN	0	3.98E-08	1	5.80E-03	1	1.60E-01	0	NaN	0	NaN	0
	3	7.00E-04	1	1.10E-01	0	1.72E-13	1	1.86E-08	1	5.03E-02	0	4.08E-02	1	7.00E-04	1
	4	8.45E-08	1	1.83E-02	1	5.43E-13	1	4.75E-11	1	3.06E-02	1	1.83E-07	1	8.45E-08	1
	5	1.11E-06	1	1.50E-03	1	6.49E-13	1	3.81E-10	1	9.67E-01	0	2.58E-09	1	1.11E-06	1
Test 8	**2**	NaN	0	NaN	0	1.93E-13	1	5.80E-03	1	8.17E-02	0	NaN	0	NaN	0
	3	2.00E-04	1	2.07E-01	0	2.23E-13	1	8.16E-05	1	9.48E-01	0	3.42E-01	0	3.42E-01	0
	4	9.30E-11	1	7.09E-01	0	6.09E-13	1	1.45E-10	1	1.00E-03	1	3.83E-06	1	3.83E-06	1
	5	3.36E-08	1	5.64E-01	0	6.49E-13	1	3.11E-12	1	8.19E-01	0	1.55E-11	1	1.55E-11	1
Test 9	**2**	NaN	0	NaN	0	1.86E-09	1	NaN	0	NaN	0	NaN	0	NaN	0
	3	7.61E-01	0	5.90E-03	1	1.07E-13	1	1.25E-09	1	3.87E-06	1	1.46E-05	1	5.90E-03	1
	4	1.00E-04	1	8.43E-05	1	5.82E-13	1	4.45E-12	1	6.83E-02	0	3.94E-07	1	8.43E-05	1
	5	1.35E-02	1	5.80E-03	1	6.52E-13	1	1.56E-11	1	1.00E-03	1	6.51E-09	1	5.80E-03	1
Test 10	**2**	NaN	0	NaN	0	7.99E-12	1	8.17E-02	0	4.23E-02	1	NaN	0	NaN	0
	3	1.60E-01	0	2.64E-01	0	3.01E-14	1	2.18E-10	1	9.65E-01	0	7.33E-05	1	7.33E-05	1
	4	3.77E-06	1	2.53E-02	1	4.63E-13	1	2.25E-10	1	2.90E-01	0	2.02E-10	1	2.02E-10	1
	5	3.37E-02	1	3.13E-06	1	6.45E-13	1	2.51E-12	1	6.00E-09	1	3.51E-12	1	3.51E-12	1

Kapur's method but ranked second in terms of fitness and all other quality measures. Generally, the segmentation effect of TSA-LEO reflects the superiority of the proposed TSA-LEO especially in Kapur's method.

TABLE 20. The convergence curves for the proposed I–EO and the competitor algorithms for multi-threshold image segmentation problems.

Image	Level	Otsu	Kapur
Test 1	3	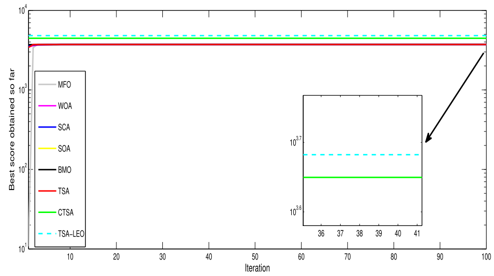	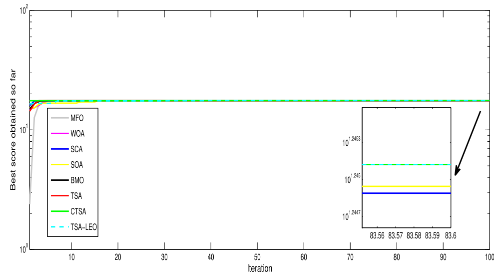
Test 2	4	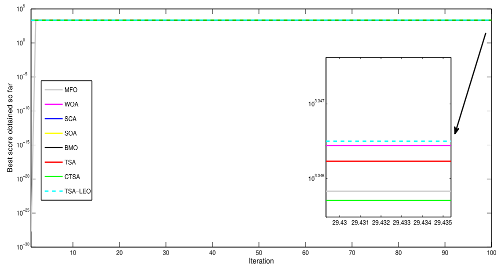	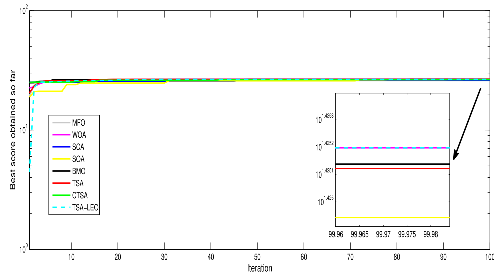
Test 7	5	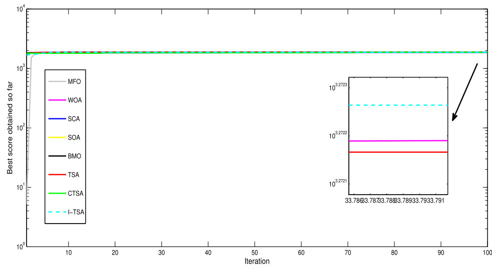	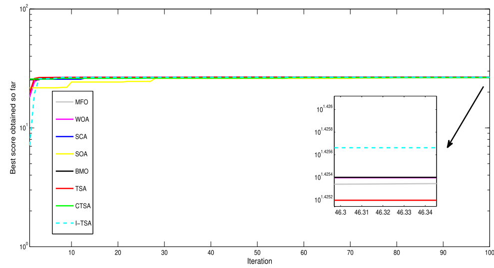
Test 8	4	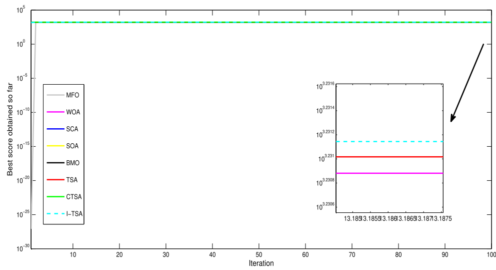	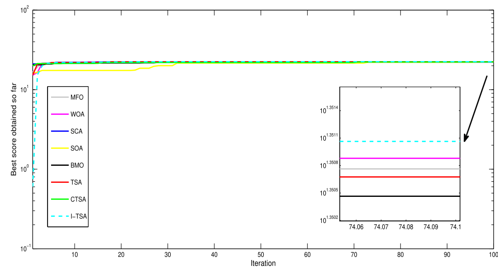
Test 9	5	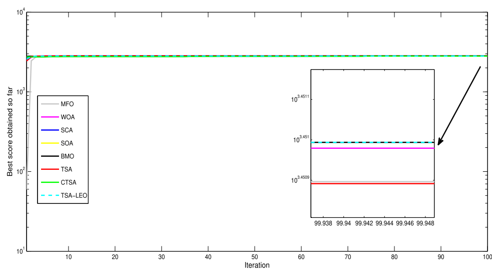	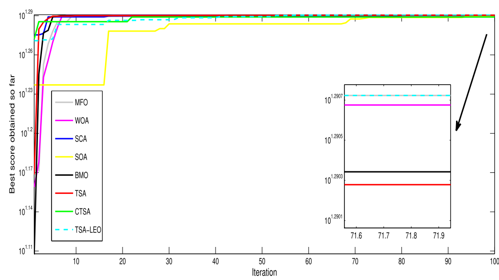

VI. CONCLUSION AND FUTURE WORK

This paper introduced an enhanced variant of a metaheuristic optimization algorithm, named TSA. The TSA was hybridized with an efficient search strategy called LEO, which improves the performance, accuracy, and convergence behavior of TSA. During the solution update process, TSA competes with LEO in the proposed TSA–LEO method. The effectiveness of the proposed TSA–LEO was evaluated using the functions in the CEC'17 benchmark test suite. The proposed method outperformed the competing methods regarding various statistical measures. Moreover, the proposed TSA–LEO can tackle multilevel threshold problems while seeking the optimal thresholds for image separation. Thus, the proposed TSA–LEO method is potentially applicable for solving complicated real-world problems. The proposed method selects the optimal thresholds that intensified the segmentation process in the thresholding experiment.

In future work, we intend to 1) combine two or more objective functions (e.g., Otsu and Kapur) in the proposed TSA–LEO, 2) further evaluate the proposed method on different datasets, and 3) apply the proposed TSA–LEO to other real-world complex problems. Promisingly, the proposed approach can be considered as an efficient and effective strategy for more complex optimization scenarios and the intelligent optimization field's theoretical work as well.

CONFLICT OF INTEREST

The authors declare that there is no conflict of interest.

CREDIT AUTHOR STATEMENT

Essam H. Houssein: Supervision, Methodology, Conceptualization, Software, Formal analysis, Writing - review & editing. Bahaa El-din Helmy: Software, Resources, Writing - original draft. Ahmed A. Elngar: Conceptualization, Formal analysis, Writing - review & editing. Diaa Salama AbdElminaam: Methodology, Conceptualization, Formal analysis, Writing - review & editing. Hassan Shaban: Conceptualization, Formal analysis, Writing - review & editing. All authors read and approved the final paper.

REFERENCES

[1] X.-S. Yang, "Nature-inspired optimization algorithms: Challenges and open problems," *J. Comput. Sci.*, vol. 46, Oct. 2020, Art. no. 101104.

[2] S. Mirjalili, "Moth-flame optimization algorithm: A novel nature-inspired heuristic paradigm," *Knowl.-Based Syst.*, vol. 89, pp. 228–249, Nov. 2015.

[3] S. Mirjalili and A. Lewis, "The whale optimization algorithm," *Adv. Eng. Softw.*, vol. 95, pp. 51–67, May 2016.

[4] S. Mirjalili, "SCA: A sine cosine algorithm for solving optimization problems," *Knowl.-Based Syst.*, vol. 96, pp. 120–133, Mar. 2016.

[5] G. Dhiman and V. Kumar, "Seagull optimization algorithm: Theory and its applications for large-scale industrial engineering problems," *Knowl.-Based Syst.*, vol. 165, pp. 169–196, Feb. 2019.

[6] L. M. Abualigah, A. T. Khader, E. S. Hanandeh, and A. H. Gandomi, "A novel hybridization strategy for krill herd algorithm applied to clustering techniques," *Appl. Soft Comput.*, vol. 60, pp. 423–435, Nov. 2017.

[7] M. H. Sulaiman, Z. Mustaffa, M. M. Saari, and H. Daniyal, "Barnacles mating optimizer: A new bio-inspired algorithm for solving engineering optimization problems," *Eng. Appl. Artif. Intell.*, vol. 87, Jan. 2020, Art. no. 103330.

[8] D. H. Wolpert and W. G. Macready, "No free lunch theorems for optimization," *IEEE Trans. Evol. Comput.*, vol. 1, no. 1, pp. 67–82, Apr. 1997.

[9] A. Mostafa, E. H. Houssein, M. Houseni, A. E. Hassanien, and H. Hefny, "Evaluating swarm optimization algorithms for segmentation of liver images," in *Advances in Soft Computing and Machine Learning in Image Processing*, vol. 730. Cham, Switzerland: Springer, 2018, pp. 41–62.

[10] S. Said, A. Mostafa, E. H. Houssein, A. E. Hassanien, and H. Hefny, "Moth-flame optimization based segmentation for mri liver images," in *Proc. Int. Conf. Adv. Intell. Syst. Inform.*, vol. 639. Cham, Switzerland: Springer, 2017, pp. 320–330.

[11] F. A. Hashim, E. H. Houssein, K. Hussain, M. S. Mabrouk, and W. Al-Atabany, "A modified henry gas solubility optimization for solving motif discovery problem," *Neural Comput. Appl.*, vol. 32, no. 14, pp. 10759–10771, Jul. 2020.

[12] A. E. Hassanien, M. Kilany, E. H. Houssein, and H. AlQaheri, "Intelligent human emotion recognition based on elephant herding optimization tuned support vector regression," *Biomed. Signal Process. Control*, vol. 45, pp. 182–191, Aug. 2018.

[13] E. H. Houssein, M. E. Hosney, D. Oliva, W. M. Mohamed, and M. Hassaballah, "A novel hybrid harris hawks optimization and support vector machines for drug design and discovery," *Comput. Chem. Eng.*, vol. 133, Feb. 2020, Art. no. 106656.

[14] E. H. Houssein, M. E. Hosney, M. Elhoseny, D. Oliva, W. M. Mohamed, and M. Hassaballah, "Hybrid harris hawks optimization with cuckoo search for drug design and discovery in chemoinformatics," *Sci. Rep.*, vol. 10, no. 1, Dec. 2020, Art. no. 14439.

[15] N. Neggaz, E. H. Houssein, and K. Hussain, "An efficient henry gas solubility optimization for feature selection," *Expert Syst. Appl.*, vol. 152, Aug. 2020, Art. no. 113364.

[16] F. A. Hashim, K. Hussain, E. H. Houssein, M. S. Mabrouk, and W. Al-Atabany, "Archimedes optimization algorithm: A new metaheuristic algorithm for solving optimization problems," *Int. J. Speech Technol.*, vol. 51, no. 3, pp. 1531–1551, Mar. 2021.

[17] F. A. Hashim, E. H. Houssein, M. S. Mabrouk, W. Al-Atabany, and S. Mirjalili, "Henry gas solubility optimization: A novel physics-based algorithm," *Future Gener. Comput. Syst.*, vol. 101, pp. 646–667, Dec. 2019.

[18] E. H. Houssein, M. R. Saad, F. A. Hashim, H. Shaban, and M. Hassaballah, "Lévy flight distribution: A new metaheuristic algorithm for solving engineering optimization problems," *Eng. Appl. Artif. Intell.*, vol. 94, Sep. 2020, Art. no. 103731.

[19] D. A. Oliva Navarro, S. Hinojosa, and M. Demeshko, "Engineering applications of metaheuristics: An introduction," *J. Phys., Conf. Ser., Inf. Technol. Bus. Ind.*, Vol. 8032016, Oct. 2017, Art. no. 12111.

[20] L. M. Q. Abualigah, *Feature Selection and Enhanced Krill Herd Algorithm for Text Document Clustering*, vol. 816. Cham, Switzerland: Springer, 2019.

[21] L. M. Abualigah, A. T. Khader, and E. S. Hanandeh, "Hybrid clustering analysis using improved krill herd algorithm," *Int. J. Speech Technol.*, vol. 48, no. 11, pp. 4047–4071, Nov. 2018.

[22] M. M. Ahmed, E. H. Houssein, A. E. Hassanien, A. Taha, and E. Hassanien, "Maximizing lifetime of large-scale wireless sensor networks using multi-objective whale optimization algorithm," *Telecommun. Syst.*, vol. 72, no. 2, pp. 243–259, Oct. 2019.

[23] E. H. Houssein, M. R. Saad, K. Hussain, W. Zhu, H. Shaban, and M. Hassaballah, "Optimal sink node placement in large scale wireless sensor networks based on Harris' hawk optimization algorithm," *IEEE Access*, vol. 8, pp. 19381–19397, 2020.

[24] M. Črepinšek, S.-H. Liu, and M. Mernik, "Exploration and exploitation in evolutionary algorithms: A survey," *ACM Comput. Surv.*, vol. 45, no. 3, pp. 1–33, Jun. 2013.

[25] B. Morales-Castañeda, D. Zaldívar, E. Cuevas, F. Fausto, and A. Rodríguez, "A better balance in Metaheuristic algorithms: Does it exist?" *Swarm Evol. Comput.*, vol. 54, May 2020, Art. no. 100671.

[26] M. H. Nadimi-Shahraki, S. Taghian, and S. Mirjalili, "An improved grey wolf optimizer for solving engineering problems," *Expert Syst. Appl.*, vol. 166, Mar. 2021, Art. no. 113917.

[27] J. Luo, H. Chen, A. A. Heidari, Y. Xu, Q. Zhang, and C. Li, "Multi-strategy boosted mutative whale-inspired optimization approaches," *Appl. Math. Model.*, vol. 73, pp. 109–123, Sep. 2019.

[28] M. Issa, A. E. Hassanien, D. Oliva, A. Helmi, I. Ziedan, and A. Alzohairy, "ASCA-PSO: Adaptive sine cosine optimization algorithm integrated with particle swarm for pairwise local sequence alignment," *Expert Syst. Appl.*, vol. 99, pp. 56–70, Jun. 2018.

[29] M. Abd Elaziz, D. Oliva, and S. Xiong, "An improved opposition-based sine cosine algorithm for global optimization," *Expert Syst. Appl.*, vol. 90, pp. 484–500, Dec. 2017.

[30] H. Zhang, A. A. Heidari, M. Wang, L. Zhang, H. Chen, and C. Li, "Orthogonal nelder-mead moth flame method for parameters identification of photovoltaic modules," *Energy Convers. Manage.*, vol. 211, May 2020, Art. no. 112764.

[31] S.-H. Kim, K.-J. An, S.-W. Jang, and G.-Y. Kim, "Texture feature-based text region segmentation in social multimedia data," *Multimedia Tools Appl.*, vol. 75, no. 20, pp. 12815–12829, Oct. 2016.

[32] Z. Yan, J. Zhang, and J. Tang, "Modified water wave optimization algorithm for underwater multilevel thresholding image segmentation," *Multimedia Tools Appl.*, vol. 79, nos. 43–44, pp. 32415–32448, Nov. 2020.

[33] T. X. Pham, P. Siarry, and H. Oulhadj, "Segmentation of MR brain images through hidden Markov random field and hybrid Metaheuristic algorithm," *IEEE Trans. Image Process.*, vol. 29, pp. 6507–6522, 2020.

[34] S. Ray, A. Das, K. G. Dhal, J. Gálvez, and P. K. Naskar, "Cauchy with whale optimizer based eagle strategy for multi-level color hematology image segmentation," *Neural Comput. Appl.*, vol. 3, pp. 1–33, Oct. 2020.

[35] K. G. Dhal, A. Das, S. Ray, J. Gálvez, and S. Das, "Nature-inspired optimization algorithms and their application in multi-thresholding image segmentation," *Arch. Comput. Methods Eng.*, vol. 27, no. 3, pp. 855–888, Jul. 2020.

[36] E. Abdel-Maksoud, M. Elmogy, and R. Al-Awadi, "Brain tumor segmentation based on a hybrid clustering technique," *Egyptian Informat. J.*, vol. 16, no. 1, pp. 71–81, Mar. 2015.

[37] B. Akay, "A study on particle swarm optimization and artificial bee colony algorithms for multilevel thresholding," *Appl. Soft Comput.*, vol. 13, no. 6, pp. 3066–3091, Jun. 2013.

[38] H. Gao, Z. Fu, C.-M. Pun, H. Hu, and R. Lan, "A multi-level thresholding image segmentation based on an improved artificial bee colony algorithm," *Comput. Electr. Eng.*, vol. 70, pp. 931–938, Aug. 2018.

[39] A. Ben Ishak, "A two-dimensional multilevel thresholding method for image segmentation," *Appl. Soft Comput.*, vol. 52, pp. 306–322, Mar. 2017.

[40] S. Sarkar, S. Das, and S. S. Chaudhuri, "Hyper-spectral image segmentation using Rényi entropy based multi-level thresholding aided with differential evolution," *Expert Syst. Appl.*, vol. 50, pp. 120–129, May 2016.

[41] M. A. Elaziz, A. A. Ewees, and D. Oliva, "Hyper-heuristic method for multilevel thresholding image segmentation," *Expert Syst. Appl.*, vol. 146, May 2020, Art. no. 113201.

[42] N. Otsu, "A threshold selection method from gray-level histograms," *IEEE Trans. Syst., Man, Cybern.*, vol. SMC-9, no. 1, pp. 62–66, Jan. 1979.

[43] J. N. Kapur, P. K. Sahoo, and A. K. C. Wong, "A new method for gray-level picture thresholding using the entropy of the histogram," *Comput. Vis., Graph., Image Process.*, vol. 29, no. 1, p. 140, Jan. 1985.

[44] A. Ben Hamza, "Nonextensive information-theoretic measure for image edge detection," *J. Electron. Imag.*, vol. 15, no. 1, Jan. 2006, Art. no. 013011.

[45] Y. Zhou, X. Yang, Y. Ling, and J. Zhang, "Meta-heuristic moth swarm algorithm for multilevel thresholding image segmentation," *Multimedia Tools Appl.*, vol. 77, no. 18, pp. 23699–23727, Sep. 2018.

[46] Y. Li, X. Bai, L. Jiao, and Y. Xue, "Partitioned-cooperative quantum-behaved particle swarm optimization based on multilevel thresholding applied to medical image segmentation," *Appl. Soft Comput.*, vol. 56, pp. 345–356, Jul. 2017.

[47] E. H. Houssein, B. E.-D. Helmy, D. Oliva, A. A. Elngar, and H. Shaban, "A novel black widow optimization algorithm for multilevel thresholding image segmentation," *Expert Syst. Appl.*, vol. 167, Apr. 2021, Art. no. 114159.

[48] S. Kaur, L. K. Awasthi, A. L. Sangal, and G. Dhiman, "Tunicate swarm algorithm: A new bio-inspired based metaheuristic paradigm for global optimization," *Eng. Appl. Artif. Intell.*, vol. 90, Apr. 2020, Art. no. 103541.

[49] E. Cuevas, A. Echavarría, and M. A. Ramírez-Ortegón, "An optimization algorithm inspired by the states of matter that improves the balance between exploration and exploitation," *Int. J. Speech Technol.*, vol. 40, no. 2, pp. 256–272, Mar. 2014.

[50] I. Ahmadianfar, O. Bozorg-Haddad, and X. Chu, "Gradient-based optimizer: A new metaheuristic optimization algorithm," *Inf. Sci.*, vol. 540, pp. 131–159, Nov. 2020.

[51] N. Awad, M. Ali, J. Liang, B. Qu, and P. Suganthan, "Problem definitions and evaluation criteria for the CEC 2017 special session and competition on single objective real-parameter numerical optimization," Nanyang Technol. Univ., Singapore, Tech. Rep., 2017.

[52] D. Oliva, M. A. Elaziz, and S. Hinojosa, "Multilevel thresholding for image segmentation based on metaheuristic algorithms," in *Metaheuristic Algorithms for Image Segmentation: Theory Application*, vol. 825. Cham, Switzerland: Springer, 2019, pp. 59–69.

[53] P. Upadhyay and J. K. Chhabra, "Kapur's entropy based optimal multilevel image segmentation using crow search algorithm," *Appl. Soft Comput.*, vol. 97, Dec. 2020, Art. no. 105522.

[54] A. K. M. Khairuzzaman and S. Chaudhury, "Multilevel thresholding using grey wolf optimizer for image segmentation," *Expert Syst. Appl.*, vol. 86, pp. 64–76, Nov. 2017.

[55] H. Liang, H. Jia, Z. Xing, J. Ma, and X. Peng, "Modified grasshopper algorithm-based multilevel thresholding for color image segmentation," *IEEE Access*, vol. 7, pp. 11258–11295, 2019.

[56] M. Abdel-Basset, V. Chang, and R. Mohamed, "A novel equilibrium optimization algorithm for multi-thresholding image segmentation problems," *Neural Comput. Appl.*, vol. 16, pp. 1–34, Mar. 2020.

[57] E. Rodríguez-Esparza, L. A. Zanella-Calzada, D. Oliva, A. A. Heidari, D. Zaldivar, M. Pérez-Cisneros, and L. K. Foong, "An efficient harris hawks-inspired image segmentation method," *Expert Syst. Appl.*, vol. 155, Oct. 2020, Art. no. 113428.

[58] M.-A. Díaz-Cortés, N. Ortega-Sánchez, S. Hinojosa, D. Oliva, E. Cuevas, R. Rojas, and A. Demin, "A multi-level thresholding method for breast thermograms analysis using dragonfly algorithm," *Infr. Phys. Technol.*, vol. 93, pp. 346–361, Sep. 2018.

[59] Q. Huynh-Thu and M. Ghanbari, "Scope of validity of PSNR in image/video quality assessment," *Electron. Lett.*, vol. 44, no. 13, p. 800, Mar. 2008.

[60] Z. Wang, A. C. Bovik, H. R. Sheikh, and E. P. Simoncelli, "Image quality assessment: From error visibility to structural similarity," *IEEE Trans. Image Process.*, vol. 13, no. 4, pp. 600–612, Apr. 2004.

[61] U. Sara, M. Akter, and M. S. Uddin, "Image quality assessment through FSIM, SSIM, MSE and PSNR—A comparative study," *J. Comput. Commun.*, vol. 7, no. 3, pp. 8–18, 2019.

[62] C. Liao, S. Li, and Z. Luo, "Gene selection using wilcoxon rank sum test and support vector machine for cancer classification," in *Proc. Int. Conf. Comput. Inf. Sci.*, vol. 4456. Springer, 2006, pp. 57–66.

[63] S. W. Scheff, "Nonparametric statistics," in *Fundamental Statistical Principles for the Neurobiologist*, S. W. Scheff, Ed. New York, NY, USA: Academic, 2016, pp. 157–182.

ESSAM H. HOUSSEIN received the Ph.D. degree in computer science with a focus on wireless networks based on artificial intelligence in 2012. He is currently working as an Associate Professor with the Faculty of Computers and Information, Minia University, Egypt. He is also the Founder of the Computing & Artificial Intelligence Research Group (CAIRG), Egypt. He has more than 80 scientific research articles published in prestigious international journals in the topics of optimization, machine learning, image processing, and the IoT and its applications. His research interests include wireless sensor networks, the IoT, bioinformatics and biomedical, cloud computing, soft computing, image processing, artificial intelligence, data mining, optimization, and metaheuristics techniques. He serves as a reviewer of more than 30 journals, such as Elsevier, Springer, and IEEE.

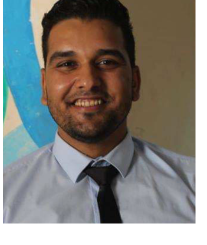

BAHAA EL-DIN HELMY is currently pursuing the M.Sc. degree in computer science with the Faculty of Computers and Information, Minia University, Egypt. He is also working as a Teaching Assistant with the Faculty of Computers and Artificial Intelligence, Beni-Suef University, Egypt. He is also a member of the Computing & Artificial Intelligence Research Group (CAIRG). His research interests include image processing, segmentation, and optimization.

AHMED A. ELNGAR is currently an Assistant Professor with the Department of Computer Science, Faculty of Computers and Artificial Intelligence, Beni-Suef University. His current project is biometrics, AI-based security, image processing, AI-based control, AI-based smart grids, and the Internet of Things Security. He is also the Founder and Chair of the Scientific Innovation Research Group (SIRG). He is also a Managing Editor of *Journal of Cybersecurity and Information Management* (JCIM).

DIAA SALAMA ABDELMINAAM received the Ph.D. degree in information system from the Faculty of Computers and Information, Menofia University, Egypt, in 2015. Since 2011, he has been an Assistance Professor with the Department of Information Systems, Faculty of Computers and Information, Benha University, Egypt. He has worked on several research topics. He has contributed more than 40 technical papers in the areas of wireless networks, wireless network security, information security and Internet applications, cloud computing, mobile cloud computing, the Internet of Things, and machine learning in international journals, international conferences, local journals, and local conferences. He majors in cryptography, network security, the IoT, big data, cloud computing, and deep learning.

HASSAN SHABAN received the Ph.D. degree in computer science. He currently works as a Lecturer with the Department of Computer Science, Faculty of Computers and Information, Minia University, Egypt. His research interests include wireless sensor networks, security, optimization, and metaheuristics.